

325

Low Energy Electron Collisions with some Gaseous
Hydrides and Deuterides.

by

Paul G. Millican.

A thesis submitted in part-fulfilment
of the requirements for the degree of
Doctor of Philosophy of the
University of Stirling

August 1984

Chemistry Department,
University of Stirling

ABSTRACT.

The ratio of lateral diffusion coefficient to electron mobility (D_r/μ) has been measured in several gaseous Hydrides and Deuterides (CH_4 , CD_4 , SiH_4 , SiD_4 , PH_3 , H_2S) using electron swarm techniques. These measured values have been combined with values of the drift velocity under the same conditions, where this is known (all but H_2S), and analysed using a two term Boltzmann Analysis to produce electron - molecule cross sections.

The weaknesses of such an analysis are recognised, so a Monte Carlo simulation of the experiment was developed and tested as an independent means of checking the cross sections so produced. The cross section for methane (at energies less than 5 eV) was fully explored using the simulation, giving a quantitative assessment of the value for the Ramsauer - Townsend minimum in this gas, and establishing the form of the inelastic contributions around the region of the minimum. In the other gases for which two term cross sections were calculated (except phosphine which would stretch the present model beyond its limitations) the Monte Carlo approach has been used qualitatively to indicate the weaknesses of the two term approximation.

CONTENTS

| | Page |
|--|------|
| Chapter 1. INTRODUCTION | 1 |
| 1.1/. Types of Slow Electron - Molecule Collision. | 1 |
| 1.1(a). Elastic Collisions. | 1 |
| 1.1(b). Inelastic Collisions. | 2 |
| 1.2/. Measurement of Cross Sections. | 4 |
| 1.2(a). Beam Techniques | 4 |
| 1.2(b). Swarm Techniques | 8 |
| 1.2(c). Cross Sections From Swarm Data. | 12 |
| Chapter 2. THE BOLTZMANN SOLUTION. | 16 |
| 2.1/. The Two Term Approximation. | 18 |
| 2.2/. The Multi-Term Approach. | 19 |
| Chapter 3. THE MONTE CARLO APPROACH. | 21 |
| 3.1/. Development of The Monte Carlo Approach. | 21 |
| 3.1(a). Time to Next Collision. | 21 |
| 3.1(b). Type of Collision. | 25 |
| 3.1(c). Post - Collision Direction | 26 |
| 3.1(d). Extraction of Swarm Parameters. | 28 |
| 3.2/. Testing The Monte Carlo Approach. | 29 |
| Chapter 4. RELATED WORK. | 36 |
| 4.1/. Non-Polar Targets. | 36 |
| 4.2/. Polar Targets. | 42 |
| Chapter 5. EXPERIMENTAL. | 47 |
| 5.1/. Apparatus. | 47 |
| 5.2/. Primary Data. | 54 |
| 5.2(a). Gas Samples. | 55 |
| 5.3/. Results. | 57 |
| 5.4/. Discussion of Errors. | 72 |
| 5.4(a). Error in E/N. | 72 |
| 5.4(b). Error in D/u. | 73 |
| 5.5/. Discussion of Experimental Results. | 73 |

CONTENTS

| | |
|--|-----|
| Chapter 6. RESULTS OF ANALYSIS AND DISCUSSION. | 75 |
| 6.1/. Introduction. | 75 |
| 6.2/. Methane. | 76 |
| 6.2(a). Experimental Data. | 76 |
| 6.2(b). Choice of Cross Sections. | 76 |
| 6.2(c). Boltzmann Analysis. | 78 |
| 6.2(d). Monte Carlo Analysis. | 80 |
| 6.3/. Perdeuteromethane. | 85 |
| 6.3(a). Experimental Data. | 85 |
| 6.3(b). Choice of Cross Sections. | 86 |
| 6.3(c). Boltzmann Analysis. | 87 |
| 6.3(d). Monte Carlo Analysis. | 87 |
| 6.4/. Silane. | 91 |
| 6.4(a). Experimental Data. | 91 |
| 6.4(b). Choice of Cross Sections. | 95 |
| 6.4(c). Boltzmann Analysis. | 95 |
| 6.4(d). Monte Carlo. | 96 |
| 6.5/. Perdeuterosilane. | |
| 6.5(a). Preliminary Information. | 96 |
| 6.5(b). Boltzmann Analysis. | 100 |
| 6.5(c). Monte Carlo. | 100 |
| 6.6/. Phosphine. | |
| 6.6(a). Preliminary Information. | 101 |
| 6.6(b). Boltzmann Analysis. | 101 |
| 6.7/. Conclusions. | 103 |
| Appendices | 115 |

LIST OF TABLES

| | Page |
|--|------|
| T3.1. Benchmark 1 Comparison of Monte Carlo and Boltzmann Results. | 32 |
| T3.2. Benchmark 2 Comparison of Monte Carlo and Boltzmann Results. | 33 |
| T3.3. Comparison of International Monte Carlo Results, Constant Collision Frequency Model. | 33 |
| | |
| T5.1. Apparatus Dimensions | 49 |
| T5.2. Measured Values of D/μ in Methane. | 60 |
| T5.3. Measured Values of D/μ in Perdeuteromethane. | 62 |
| T5.4. Measured Values of D/μ in Silane. | 64 |
| T5.5. Measured Values of D/μ in Perdeuterosilane. | 66 |
| T5.6. Measured Values of D/μ in Phosphine. | 68 |
| T5.7. Measured Values of D/μ in Hydrogen Sulphide. | 70 |
| | |
| T6.1. Swarm Parameters in CH_4 Using Refined Cross Section | 106 |
| T6.2. Swarm Parameters in CD_4 Using First Trial Cross Section | 106 |
| T6.3. Swarm Parameters in SiH_4 Using Boltzmann Cross Sections | 107 |
| T6.4. Swarm Parameters in SiD_4 Using Boltzmann Cross Sections | 107 |
| T6.5. Methane Boltzmann Output | 108 |
| T6.6. Methane Refined Mont Carlo Cross Section | 109 |
| T6.7. Perdeuteromethane Boltzmann Output | 110 |
| T6.8. Silane Boltzmann Output | 111 |
| T6.9. Perdeuterosilane Boltzmann Output | 112 |
| T6.10. Phosphine Boltzmann Output | 113 |

LIST OF FIGURES

| | Page |
|---|------|
| F1.1. Schematic of Simple Beam Experiment. | 4 |
| F1.2. Schematic of Townsend - Huxley Experiment. | 11 |
| | |
| F3.1. Monte Carlo Overview Flow Diagram. | 22 |
| F3.2. Monte Carlo Collision Decision Flow Diagram. | 27 |
| F3.3. Cross Sections Used in Benchmark 2. | 34 |
| F3.4. Normalised Electron Energy Distribution, Benchmark 1. | 35 |
| | |
| F5.1. Apparatus Used to Measure D/μ . | 48 |
| F5.2. New Cathode Assembly. | 50 |
| F5.3. Gas Handling System. | 53 |

LIST OF GRAPHS

| | Page |
|---|------|
| G4.1. Ramsauer - Townsend Minima in Noble Gases. | 37 |
| G5.1. Measured Values of D/μ vs E/N in Methane. | 59 |
| G5.2. Measured Values of D/μ vs E/N in Perdeuteromethane. | 61 |
| G5.3. Measured Values of D/μ vs E/N in Silane. | 63 |
| G5.4. Measured Values of D/μ vs E/N in Perdeuterosilane. | 65 |
| G5.5. Measured Values of D/μ vs E/N in Phosphine | 67 |
| G5.6. Measured Values of D/μ vs E/N in Hydrogen Sulphide. | 69 |
| G5.7. Comparison of Measured Values of D/u vs E/N . | 71 |
| G6.1. Final Boltzmann Cross Sections For Methane. | 79 |
| G6.2. Final Monte Carlo Cross Sections For Methane. | 81 |
| G6.3. Calculated and Experimental Values of D/μ in Methane. | 82 |
| G6.4. Calculated and Experimental Values of W_d in Methane. | 83 |
| G6.5. Final Boltzmann Cross Sections for Perdeuteromethane. | 88 |
| G6.6. Calculated and Experimental Values of D/μ in Perdeuteromethane. | 89 |
| G6.7. Calculated and Experimental Values of W_d in Perdeuteromethane. | 90 |
| G6.8. Final Boltzmann Cross Sections For Silane. | 92 |
| G6.9. Calculated and Experimental Values of D/μ in Silane. | 93 |
| G6.10. Calculated and Experimental Values of W_d in Silane. | 94 |
| G6.11. Final Boltzmann Cross Sections For Perdeuterosilane. | 97 |
| G6.12. Calculated and Experimental Values of D/μ in Perdeuterosilane. | 98 |
| G6.13. Calculated and Experimental Values of W_d in Perdeuterosilane. | 99 |
| G6.14. Boltzmann Cross Sections For Phosphine. | 102 |

1. INTRODUCTION

CHAPTER 1.

INTRODUCTION

1.1/. Types of Slow Electron - Molecule Collision.

At its simplest, one can consider this field of study in terms of the interaction between a single electron and a single molecule. At low incident electron energies, the type of event which can occur is strongly influenced by both the nature of the target molecule, and the electron energy. This energy and target dependence of the interaction is analogous to the interactions in the more familiar field of optical spectroscopy. The interaction of the incident photon and the target depends on the photon energy (ability to excite a particular transition) and the structure of the target, giving rise to the fruitful field of spectroscopic structural elucidation. For electron - molecule collisions, one can classify the types of collisions which may occur into two groups, elastic and inelastic. Both of these are discussed more fully below.

1.1(a). Elastic Collisions.

Elastic collisions are defined as those in which the internal energy of the molecule is unchanged following a collision. The only energy transfer in the collision is between the kinetic energy of the electron and the translational energy of the

1. INTRODUCTION

molecule. Following simple physics, two colliding bodies of mass m and M result in a fractional energy loss for the lighter particle of

$$\lambda = \frac{2m(1-\cos \theta)}{M} \quad \text{E1.1}$$

θ being the scattering angle of the lighter particle. If all scattering angles are equally probable, $1-\cos \theta = 1$ and the fractional energy loss is $2m/M$. If the lighter particle is an electron and the heavier a molecule, this fraction is usually less than 10^{-4} . For a heavy molecule, this is a very small amount of energy, resulting in a small change in momentum, but for very low energy electrons this type of collision is an important energy loss mechanism.

1.1(b). Inelastic Collisions.

Inelastic collisions are defined as those in which the internal energy of the molecule is changed by the collision. This is a more efficient energy sink for electrons. If an electron excites a process within a molecule, it does so by handing over a quantum of energy sufficient for the excitation. What the molecule does with this energy varies according to the channels open to it. A typical molecule may undergo rotational, vibrational or electronic excitation. It may also form ions, negative by

1. INTRODUCTION

attachment, positive by electron loss. The excited molecule may relax by dissociation, radiation or decay by collision. For very low energy electrons (with which this work is concerned), the most common processes are rotational and vibrational excitation. Some inelastic processes are very efficient near their onset. (For a particular process, the number of collisions exciting that process forms a large proportion of the total number of collisions, i.e., the cross section for that process is a major contributor to the total cross section). This leads to some interesting effects, but also complicates the analysis of collision data.

A special case of the inelastic collision is the superelastic collision. In such a collision the direction of energy transfer is reversed, i.e., the molecule gives up a quantum of energy to an electron. The contribution from such collisions is usually negligible, becoming important only when a significant proportion of the target molecules are not in their ground state. As the reverse of molecular excitation, it is a possible channel for molecules excited by an inelastic collision to relax.

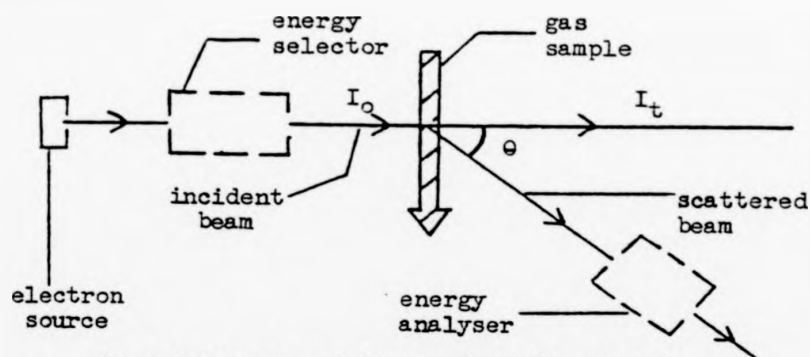
From these possibilities it is readily seen that even the simplest collision system has a range of possible routes through which it may pass. To have some idea as to what processes are actually occurring within a given system, one must be able to differentiate between the observable properties of the possible processes, and be able to quantify the relative probability of each possibility. Experimentally, this is known as measuring the collision cross section for a given process.

1. INTRODUCTION

1.2/. Measurement of Cross Sections.

1.2(a). Beam Techniques.

Conceptually, the simplest way to measure cross sections is to approach the simplest collision system as closely as possible, within the constraints of practical considerations. Experiments which do this are known as beam experiments. A beam of electrons is fired at the target gas and information about the collision gained by observing the properties of the beam before and after collision. A schematic representation of such an experiment is shown in Fl.1.



Fl.1 Schematic of Simple Beam Experiment.

In this simple case, the cross section can be defined in terms of the attenuation of the incident beam I_0 on passing through a length l of gas number density N and cross section Q leaving transmitted current I_t .

$$\frac{I_t}{I_0} = e^{-NQl}$$

El.2

1. INTRODUCTION

This cross section, deriving from all possible scattering processes is termed the total cross section. It is made up of cross sections from individual scattering processes

E1.3

$$Q_t = Q_e + \Sigma Q_i$$
where Q_e is the elastic and Q_i an inelastic cross section.

As implied in the diagram, a further selectivity is offered in analysing the angle through which electrons are scattered. Different types of scattering can often be resolved by observing the variation of the differential cross section with angle. The differential cross section $\sigma(\theta)$ is defined as the probability of scattering through a solid angle $d\Omega$. It follows that the total cross section is the integration of the differential cross section over all solid angles.

$$Q_t = \int_0^\pi \int_0^{2\pi} \sigma(\theta) \sin(\theta) d\theta d\phi \quad \text{E1.4}$$

Experimentally, beam spectrometers are limited at the low energy end of their range by the susceptibility of electrons to stray field effects, and by loss of resolution. The former problem (usually caused by surface imperfections) can give rise to spurious structure in spectra which, if not detected as such, could be wrongly attributed to electron target collision effects. The latter

1. INTRODUCTION

problem is inherent in the use of a low momentum charged particle beam, and effectively sets a lower limit on the usefulness of beam data of around 0.2 eV. A further weakness of beam experiments is that all cross sections derived from them are measured relative to some well explored standard (usually Helium) and are not absolute measurements. The process of normalising the data can introduce normalising errors. It is worth noting here that the cross sections used in the normalisation process are absolute measurements derived from multiple collision (swarm) methods. Such absolute measurements are important in quantifying the processes involved, and as a test of the theory of the collision process.

The first measurements of total cross sections were made by Ramsauer (1921) using this single collision method. The exact techniques used and results obtained are reviewed elsewhere (Massey and Burhop, 1969). The technique has since been refined (e.g. Golden and Bandel, 1965) but, even with refined electron optics giving improved resolution, the information regarding individual scattering processes is not accessible from total cross section measurements. More detailed information can be found by analysing the scattered electron distribution with respect to energy and/or angle of scatter.

A useful technique for examining low energy processes is the use of a potential well within a beam experiment. This electron trap (Schulz, 1958) captures those scattered electrons which have given up their quantum of energy to excite a particular process. At

1. INTRODUCTION

the onset of each excitation, one sees a sharp increase in the trapped electron current which is directly proportional to the magnitude of the cross section for that excitation. This gives a much better picture of near threshold excitation than was available from previous methods. The technique has some drawbacks, and is being superceded as more powerful methods of energy analysis become available.

Much valuable information has been gained from beam experiments, but they all suffer from some serious limitations. The energy spread of the electron beam is difficult to control, particularly at low energies, false structure can be introduced by electron optic effects, and the resultant data must still be normalised to an absolute measurement. Improvements in experimental methods frequently provide ways of improving the energy spread (Allan 1983), nevertheless, electrons are particularly sensitive to surface effects and stray fields, resulting in loss of resolution. (Current techniques give best resolution of 20 meV (160 wavenumbers)). At very low energies (less than 1 eV) these problems, coupled with decreasing signal to noise ratios, effectively sets a lower limit to the energy at which beam experiments can contribute reliable information. To investigate scattering at energies less than this limit, multiple collision techniques are used. The most important contributions in this area come from swarm experiments.

1. INTRODUCTION

1.2(b). Swarm Experiments.

As the name implies, swarm experiments are concerned with the behaviour of a travelling group of electrons. Rather than attempt to constrain the electron energy, one allows the energy of the swarm to equilibrate with the target gas. From measurements made of some parameters of the swarm, one can determine what the energy distribution is, and from this deduce scattering cross sections compatible with the observed behaviour. Swarm experiments are relatively simple experimentally, but the analysis of the results under multiple collision conditions is complicated.

Several macroscopic properties of the swarm are measurable, including the Longitudinal Diffusion Coefficient, D_L , the Drift Velocity, W_d , and the Radial Diffusion Coefficient, D_r . For non-conservative swarms, attachment rates and ionisation coefficients are also measurable. This study is concerned with the measurement of the ratio of D_r to W_d . An outline of the methods of measurement of D_L and W_d (independent of D_r) is included.

The drift velocity of the swarm is measured as the time taken for the centroid of the swarm to cover a known distance through the target gas under the influence of an applied electric field. The measurement can be made in two ways. The most widely used is the shutter technique (Bradbury and Nielsen, 1936). An A.C. Pulse is applied to the shutters which act as gates for the electrons. The maximum current will only be transmitted when the frequency of the pulse is an integer multiple of the drift

1. INTRODUCTION

velocity. This method has produced most of the reliable drift velocity data to date.

The other methods of measurement can be classed as pulsed methods. Using a pulsed source, the drift velocity can be measured as the delay between emission and collection of current (Hurst et al., 1963). On the other hand, using a pulsed field, the measurement of W_d is made by noting the attenuation in collected current as the frequency is increased (Nolan and Phelps 1968). There are experimental difficulties and inaccuracies associated with either method which make them less attractive than the shutter techniques.

A study of the arrival time distribution using the pulsed source method of measuring W_d , yields the Longitudinal Diffusion Coefficient, D_1 . Methods for measuring D_1 are not well advanced. The possibility of anisotropic diffusion ($D_1 \neq D_r$) was not realised until 1967 (Wagner et al.). Swarm theory had developed without considering D_1 , and though its inclusion cleared up some inconsistencies, its measurement is still regarded as relatively unimportant.

The second transport coefficient of the swarm used to deduce cross sections, and the one measured in this work, is the Radial Diffusion Coefficient. This measures the rate of diffusion of the swarm in the plane perpendicular to the applied fields. Some methods measure the parameter directly (Cavalleri, 1969), but the more usual method is to measure the ratio D_r/W_d . This is

1. INTRODUCTION

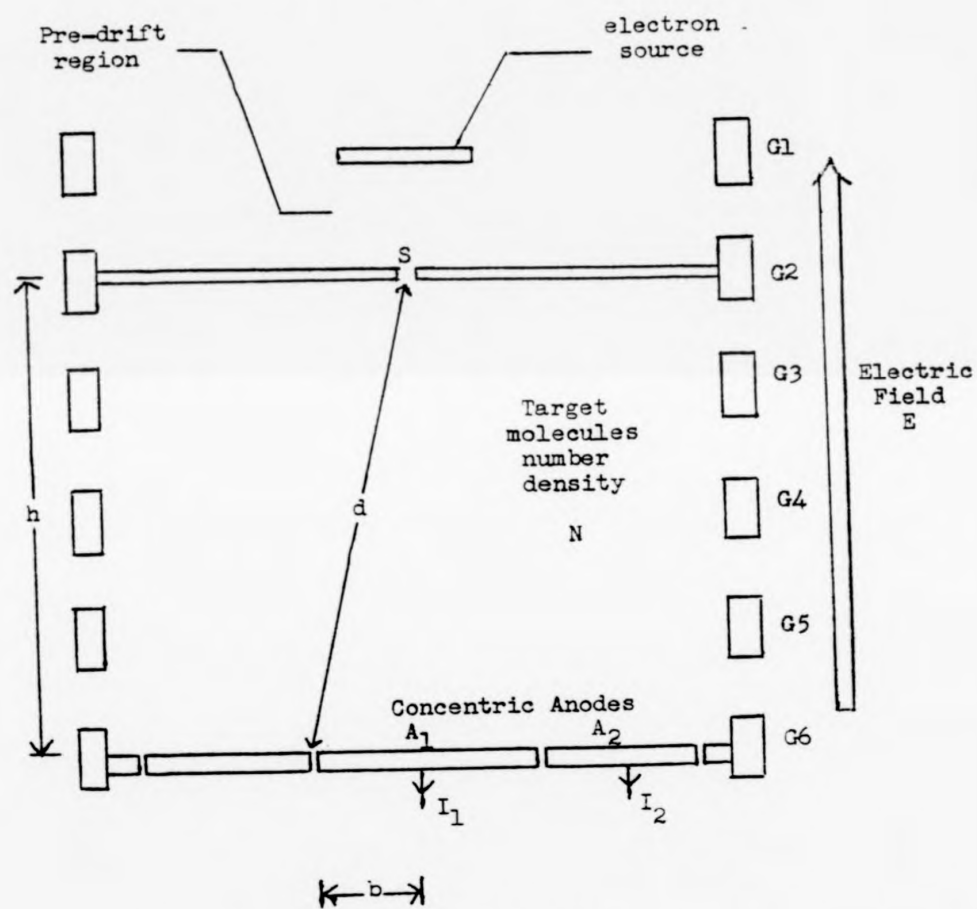
done using the Townsend - Huxley experiment which is represented schematically in Fl.2.

The aim of the experiment is to allow a stream of electrons coming through the source aperture S to drift under the influence of an applied D.C. field towards concentric anodes perpendicular to the field, and at a known distance from the source. The distribution of the electrons over these anodes as measured by current ratios leads to the determination of D_r/W_d . The relationship between the dimension of a particular apparatus as outlined in Fl.2, the current ratios for a given field strength, and the ratio D_r/W_d is complex. An account of the development of a universally applicable equation is given elsewhere (Huxley and Crompton, 1974). By choosing experimental dimensions carefully, approximations to the complete analysis can be made which lead to the relationship used in this work,

$$\frac{E D_r}{W_d} = \frac{-E(d-h)}{2 \ln[(1-R)d/h]} \quad \text{E1.5}$$

The symbols have meanings and values as shown in Fl.2. Expressed in this way, as $D_r/(\text{electron mobility})$, we have an estimate of the energy of the swarm. It is known as the characteristic energy of the swarm and is related to the mean swarm energy. (The exact nature of this relationship depends on the shape of the energy distribution).

1. INTRODUCTION



$$\text{Current Ratio, } R = I_1 / (I_1 + I_2)$$

Fl.2. Schematic of Townsend - Huxley Apparatus.

1. INTRODUCTION

Transport coefficients are measured over a range of electron energies, controlled by changing the strength of the applied field. It is also usual to repeat the measurements at various sample gas pressures, usually between 0.1 and 1000 Torr. This is done to ensure reproducibility of the results, as well as checking for pressure effects. In the present work, the limits to pressures are set at the lower end by the accuracy of pressure measurement and associated problems with gas purity, and at the upper end by surface effects at the photocathode.

Once determined over a range of field strengths and pressures, transport coefficients are plotted as a function of pressure reduced field, at which stage they are amenable to analysis and extraction of cross sections.

1.2(c). Cross Sections From Swarm Data.

The cross section measurable with swarm experiments is the Momentum Transfer Cross Section. This is a total cross section weighted to allow for anisotropic scattering. It is defined in terms of the differential cross section (E1.3) as

$$Q_m = \int_0^\pi \int_0^{2\pi} (1 - \cos\theta) \sigma(\theta) \sin\theta \, d\theta \, d\phi \quad \text{E1.6}$$

For isotropic scattering, the momentum transfer cross section is equivalent to the total cross section. It is easily shown that, considering elastic collisions only, the momentum transfer cross section is related to the total cross section by

1. INTRODUCTION

$$\lambda = \frac{2m}{M} \cdot \frac{Q_M}{Q_t} \quad \text{E1.7}$$

where λ is the mean fractional energy loss per collision. The momentum transfer cross section can thus be described as the probability of transfer of a fraction $2m/M$ of energy to target translational energy, over unit distance, and for unit target density. A very simple analysis will help to clarify the role of transport coefficients in determining cross sections.

The equation of motion of an electron moving in a field E in the z direction can be written

$$Ee = M A \quad \text{E1.8}$$

If scattering is isotropic, the mean velocity in the z direction, W_d , will be

$$W_d = \frac{E \cdot e t}{2M} \quad \text{E1.9}$$

where t is time between collisions. Consider a gas, cross section Q , number density N , wherein the electron has mean free velocity v , and mean free length l . Then

$$t = \frac{l}{v} = \frac{1}{N Q v} \quad \text{E1.10}$$

$$W_d = \frac{E e}{2M N Q v} \quad \text{E1.11}$$

1. INTRODUCTION

This gives W as a function of E/N yielding the product $Q.v$. It is worth noting that if $Q.v$ is constant (Q proportional to $1/v$), the drift velocity is linearly dependent on E/N . To isolate Q , introduce the transverse diffusion coefficient which, by the Einstein relation

$$D_r = \frac{v}{2} \quad \text{E1.12}$$

Using E1.9

Introducing electron mobility ($\mu = W_d/E$)

$$D_r/\mu = \frac{M(v^2)}{e} \quad \text{E1.13}$$

Using this grossly simplified analysis, it is seen that independent measurements of W_d and D_r/μ will yield a value for Q .

Furthermore, under steady state conditions, the energy gained from the field is balanced by the energy lost in collisions,

$$\frac{\lambda M v^2}{2} = \frac{M(2W_d)^2}{2} \quad \text{E1.14}$$

therefore the fractional energy loss per collision is

$$\lambda = \frac{4 W_d^2}{v^2} \quad \text{E1.15}$$

1. INTRODUCTION

As we know that for isotropic elastic collisions

$$\lambda = \frac{2m(1-\cos \theta)}{M} \quad (\text{E1.1})$$

any increase above this value is directly attributable to inelastic encounters, leading to the possibility of discriminating between different scattering processes by analysis of macroscopic properties.

The gross approximations used in this analysis make it unsuitable for quantitative work. More accurate analyses approach the problem by solution of the appropriate transport equation. Such approaches are covered in Chapter 2.

The present study aims to measure D_r/μ as a function of E/N in several gaseous hydrides and deuterides, and to combine these measurements with published measurements of drift velocities in the same gases. Where this is possible, the experimental data will be used to develop electron molecule cross sections using the computational approaches outlined in Chapters 2 and 3.

2. THE BOLTZMANN SOLUTION

CHAPTER 2.

THE BOLTZMANN SOLUTION.

To be able to assess quantitatively the contributions made to the mean swarm energy by various energy loss processes, one needs to have an accurate picture of the electron energy distribution. Ideally, this should be measured directly and the results obtained could be used to calculate cross sections. An energy scan would reveal the energy dependence of the distribution function, giving a unique set of cross sections in favourable circumstances. No experimental technique for direct measurement of the energy distribution of swarms has yet been developed. One must therefore resort to indirect methods of assessing the distribution, and the most common is solving the Boltzmann equation.

Approaching the problem this way immediately jeopardizes the uniqueness of the derived cross sections. One is attempting to determine several independent microscopic variables (the cross sections) by the measurement of two macroscopic quantities (the transport coefficients). However, at intermediate energies where many excitation processes begin, beam experiments provide some information, and this can be used to tie down the known cross sections, reducing the number of variables in the problem.

The expression of the Boltzmann equation appropriate to a hydrodynamic electron swarm was developed initially by Holstein

2. THE BOLTZMANN SOLUTION

(1946). The full development has been covered elsewhere (Huxley and Crompton, 1974), but an outline of the method is included for clarity.

Considering a function describing the population of a shell in six dimensional velocity - position space, one can consider the change in that function with time as being made up of three contributions.

1). Those electrons which will leave the shell by a change in position.

2). Those electrons which will leave the shell by acceleration due to the applied field.

3). Those electrons which will enter the shell following a collision.

$$\left[\frac{\partial f}{\partial t} \right] = -v_z \left[\frac{\partial f}{\partial z} \right] - \frac{E e}{m} \left[\frac{\partial f}{\partial v} \right] + \left[\frac{\partial f}{\partial t} \right]_{\text{coll}} \quad \text{E2.1}$$

This equation (E2.1) is the general form of the Boltzmann equation for a hydrodynamic swarm. This can be further expanded to give a more explicit function of the collision contribution in terms of the individual contributions from each scattering process thus;

$$\begin{aligned} & \frac{(eE)^2}{3} \frac{d}{d\epsilon} \left(\frac{\epsilon}{N Q_m(\epsilon)} \frac{df_0}{d\epsilon} \right) + \frac{2M}{M} \frac{d}{d\epsilon} \left(\epsilon^2 N Q_M(\epsilon) (f_0 + kT \left(\frac{df_0}{d\epsilon} \right)) \right) + \\ & \Sigma \left[(\epsilon + \epsilon_i) f_0(\epsilon + \epsilon_i) N Q_i(\epsilon + \epsilon_i) - f_0(\epsilon) N Q_i(\epsilon) \right] + \\ & \Sigma_{-i}^i \left[(\epsilon - \epsilon_i) f_0(\epsilon - \epsilon_i) N Q_{-i}(\epsilon - \epsilon_i) - f_0(\epsilon) N Q_{-i}(\epsilon) \right] \end{aligned} \quad \text{E2.2}$$

2. THE BOLTZMANN SOLUTION

This is the complete Boltzmann equation for a conservative hydrodynamic swarm (no ionisation or attachment). As a partial differential equation in several variables, this equation is not exactly soluble using currently available methods. Approaches towards the exact solution (Kleban and Davis, 1977, 1978 and Kitamori, 1978) are promising but computationally cumbersome. An alternative approach is to express the equation as a set of coupled ordinary differential equations which are more readily soluble, by applying a Legendre transformation and evaluating the resultant polynomial. One consequence of this approach is that the accuracy of the analysis depends on the number of terms retained in the expansion, i.e. extra accuracy costs computer time. There are two approaches to this problem. The first (the method employed in this work) is to truncate the expression at two terms, then apply an independent test to examine the cross sections. The second (Pitchford, 1981, 1982) is to evaluate the expansion to as many as eight terms, and expect that the accuracy of the calculation is comparable with the accuracy of available experimental data.

2.1/. The Two Term Approximation.

The assumption underlying the truncation at two terms is that the electron distribution function can be considered to be spherical with respect to velocity space under swarm conditions. This is only strictly true at vanishingly small field strengths and diffusion gradients, but is a good approximation for most swarm

2. THE BOLTZMANN SOLUTION

conditions. If the assumption holds, then one can say that the distribution function is angle independent, and terms after the second disappear. At the level of individual collisions, the types of process which will disturb this symmetry are inelastic collisions. One therefore expects the model to be under severe strain when contributions from such processes are relatively high. Such conditions are prevalent in the molecular gases where low energy rotational and vibrational excitation are common. Previous studies have used the two term approximation to evaluate complete energy dependent cross sections, and given a qualitative description of the expected effect on the individual scattering processes of applying the underlying assumptions. With computer time more readily available, it is now possible to use an independent method to probe these approximate cross sections, particularly in areas where the assumption is known to be invalid or suspect. This method is the Monte Carlo method, and is covered in full in Chapter 3.

2.2/. The Multi-Term Approach.

The second method, calculation of the Legendre expansion to several terms is fully described elsewhere (Pitchford *et al.*, 1981). The technique uses vast quantities of computer storage, but has been well adapted to optimum efficiency for use on vector processing machines. A typical calculation to evaluate transport coefficients for a trial cross section takes three seconds of Cray

2. THE BOLTZMANN SOLUTION

time (approximately 5 minutes on a VAX11/780, but the VAX has neither the vector processing or the storage facility to cope with such a problem).

The approach used in this work is to use the two term approximation to get a broad outline of the collision cross sections, and then to refine these using the Monte Carlo approach. To do this an existing two term program (incompatible with current computer facilities) was rewritten. The original program had been extensively tested (Duncan, 1971) and the only test applied to the new version was that it should produce the same results (transport coefficients as $f(E/N)$) for a given input (trial cross section).

The results from the technique have been compared with Monte Carlo results for a model system. Good convergence of the calculated transport coefficients as the number of retained terms is increased is noted, and the agreement of the eight term calculation with an international Monte Carlo benchmark is excellent (T3.1). Monte Carlo calculations are performed on the output cross sections from this method as an independent check of the validity of the calculation.

3. THE MONTE CARLO APPROACH.

CHAPTER 3.

THE MONTE CARLO APPROACH.

3.1/. Development of The Monte Carlo Approach.

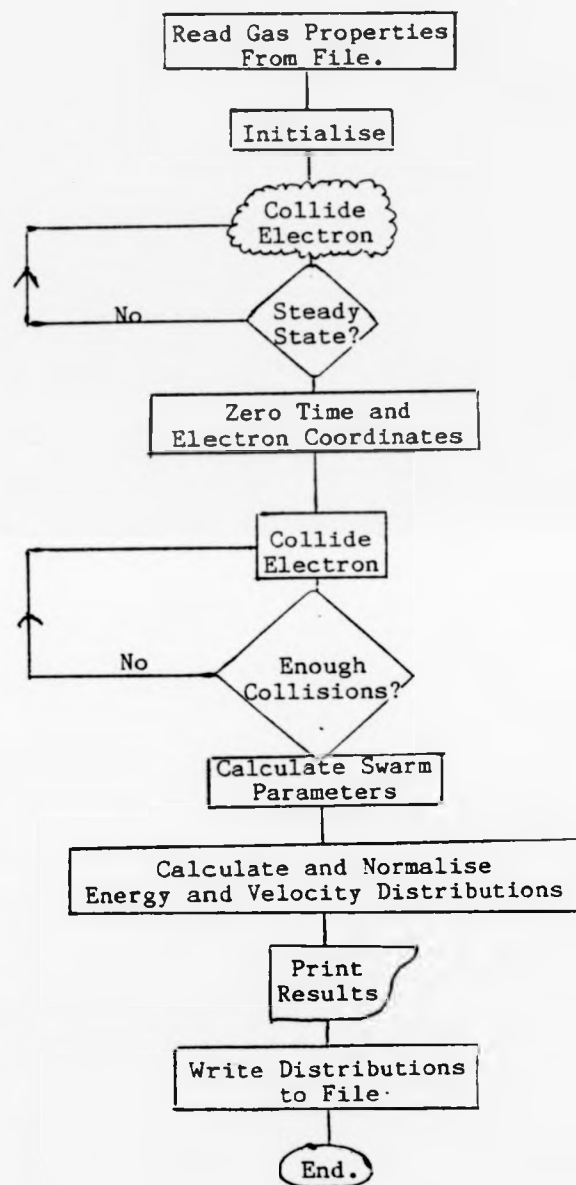
The basis of the Monte Carlo method is to use random numbers to create a statistical model of some system. The history, applications and techniques of the method are well covered elsewhere (Sobol, 1974). For this application, the method used is essentially that of McIntosh (1974).

An electron is sent on a random walk downhill, accelerated by the applied field and scattered by target molecules. Random numbers are used to decide when a collision occurs, what sort of collision has occurred, and the trajectory following the collision. An overview of this sequence is represented in a flow diagram in F3.1.

3.1(a). Time to Next Collision.

The time to the next collision is decided as follows. Let P be the probability of an electron suffering a collision while travelling distance l through a gas (P must lie between 0 and 1). If N'_0 electrons begin such a path, then $N'_0 \cdot P$ will collide, and $N'_0 \cdot (1-P)$ will not. Using E1.2,

3. THE MONTE CARLO APPROACH.



F3.1. Monte Carlo Overview Flow Diagram

3. THE MONTE CARLO APPROACH.

$$1 - P = e^{-N Q t} \quad \text{E3.1}$$

However, for a finite time t the velocity dependent cross section will vary as the electron accelerates in the field, and this expression under swarm conditions is more properly written

$$\ln(1-P) = N \int_0^t Q t(v) \cdot v \cdot dt \quad \text{E3.2}$$

Thus the time to the next collision is a function of the energy dependence of the cross section, and is only easily determinable for simple cases. One model case which is particularly useful is a cross section inversely proportional to velocity.

$$Q = C v^{-1} \quad \text{E3.3}$$

Substitution and evaluation of E3.2 gives

$$\begin{aligned} \ln(1-P) &= -N C t \\ t &= \frac{-\ln(1-P)}{N C} \end{aligned} \quad \text{E3.4}$$

If a model gas has total cross section inversely proportional to electron velocity, E3.4 gives the time to the next collision very simply in terms of a random number P , the gas number density N , and a proportionality constant C . Since, for real gases, the time to the next collision needs to be expressed as a function

3. THE MONTE CARLO APPROACH.

of the velocity dependence of the cross section (E3.2) which is only soluble by time consuming convergence methods, it would be useful to substitute the very simple velocity dependence of E3.4 into the real cross sections for any given real gas. The inclusion of such a cross section with real cross sections as a simplification of choosing the time to the next collision is known as the Null Collision Method (Skullerud, 1968). This adds another type of collision cross section to the more familiar elastic and inelastic, the null cross section. This is defined as the difference between the sum of the real cross sections and the artificial total cross section.

$$\begin{aligned} Q_t &= c v^{-1} \\ &= Q_e + \sum Q_i + Q_n \end{aligned} \tag{E3.5}$$

The null cross section is thus a padding between the total real cross section and a more convenient form of the total cross section. If an electron makes a null collision, its trajectory and energy are undisturbed, and it continues to move under the influence of the field until it encounters a real collision. The null cross section can be considered a convenience for calculating the time to the next collision, and has no physical significance. The only restriction on the null cross section is that it must be greater than 0, that is the total (padded) cross section must always be greater than the sum of the real cross sections in the

3. THE MONTE CARLO APPROACH.

energy region being considered. The ideal null cross section is as small as possible within the bounds of this restriction, so that the electron does not waste time with more null collisions than necessary.

3.1(b). Type of Collision.

Once the time to the next collision has been decided (E3.4), the type of collision must be decided. This is done by finding the energy of the electron at the time of the collision and determining the relative values of the individual cross sections at that energy. A random number R uniformly distributed between 0 and 1 is generated and a collision of type L is deemed to have occurred if

$$\sum_{j=1}^{L-1} Q_j(v) < R Q_t(v) < \sum_{j=1}^L Q_j(v) \quad \text{E3.6}$$

Once the type of collision has been decided, the appropriate action is taken. This is;

- 1). Null - No action, continue trajectory.
- 2). Elastic - Subtract collisional energy loss and develop new trajectory.
- 3). Inelastic - Subtract energy loss for given process and develop new trajectory.

3. THE MONTE CARLO APPROACH.

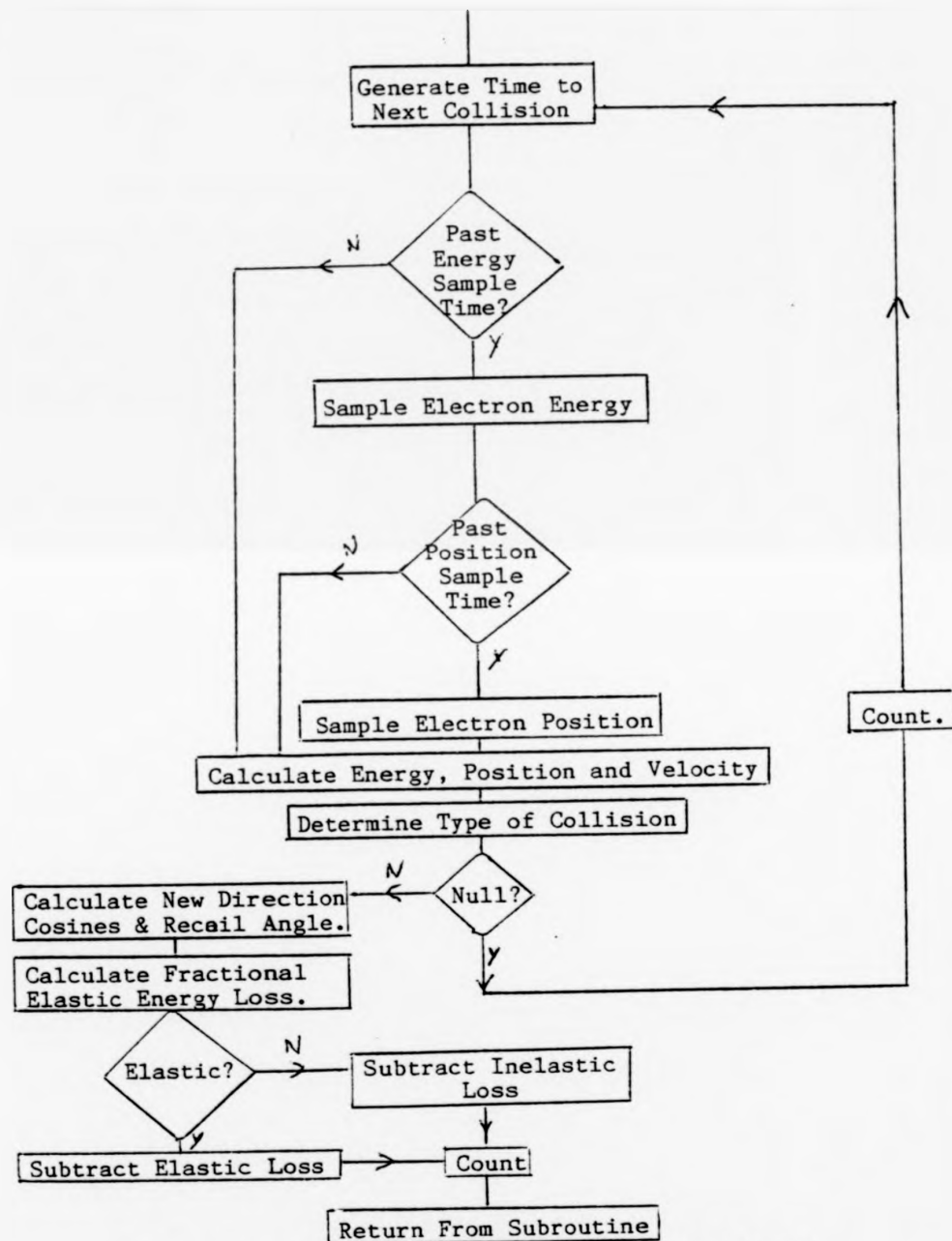
The collisional energy loss for an elastic encounter is dependent on the scattering angle and is given by E1.1. The energy loss for inelastic processes is the excitation energy for that process, so that the energy of the electron before and after the collision is given by

$$E_a = E_b - E_{(\text{excitation})} \quad \text{E3.7}$$

3.1(c). Post - Collision Direction.

After collision, the electron is ejected from the target with energy E_a in a random direction such that the distribution of directions is spherically symmetrical about the target. This model of isotropic scattering is used throughout this work, and is thought to be valid over a wide range of swarm conditions. The symmetry is achieved by distributing $p(\phi)$ uniformly between 0 and $2 * \pi$, and weighting θ such that $p(\theta)$ is given by the arcsine of a uniform distribution between -1 and 1. The reasoning behind this weighting is given elsewhere (Sobol, 1974). Qualitatively, it can be seen as allowing for the greater surface mapped out by the locus of ϕ when θ is fixed at $\pi/2$, over that mapped out when θ approaches either 0 or π . The ejection angle (with respect to the z axis) is used to calculate new direction cosines, which in turn are used to calculate the actual scattering angle and hence the energy loss if the collision is elastic. Following this, the time to the next collision is calculated and the cycle repeated. This collision decision loop is summarised as a flow diagram in F3.2.

3. THE MONTE CARLO APPROACH.



F3.2. Monte Carlo Collision Decision Flow Diagram.

3. THE MONTE CARLO APPROACH.

3.1(d). Extraction of Swarm Parameters.

Assuming that this loop adequately describes the microscopic behaviour of the swarm, one can then analyse the macroscopic behaviour. In this work, this is done by setting a sample time, usually of the order of 100 mean free times, at which to examine the velocity and position of the electron. The sampling was given precedence over collisions, so that the collision loop could be interrupted at any point on the electron trajectory, sample made, then allowed to continue. It is important to choose a sample time long enough to allow appreciable change in the electron properties, such that successive samples are mutually independent. The sample time must also be short enough to allow as many samples as possible within the restriction above so that the statistics are more reliable.

Once the electron has undergone a predetermined number of real collisions, the simulation is terminated and the transport coefficients under the specified conditions are extracted by analysis of the sample data. The final values of the transport coefficients for p simulations are found using

$$W_d = \frac{p}{\sum_{j=1}^p} \left[\frac{Z_f - Z_i}{t} \right] \quad D_r = \frac{p}{\sum_{j=1}^p} \left[\frac{\sum_{i=0}^n (\bar{x}-x')^2 + (\bar{y}-y')^2}{4nt} \right]$$

$$D_z = \frac{p}{\sum_{j=1}^p} \left[\frac{\sum_{i=0}^n (\bar{z}-z')^2}{2nt} \right]$$

3. THE MONTE CARLO APPROACH.

Wherein Δ denotes the change in a value between samples. The equations for D_r and D_1 are modified versions of the Einstein equation for diffusion in two and one dimension respectively.

Other parameters that are traced in the simulation, but are not accessible from experiment are the relative numbers of different types of collision undergone, the maximum and average (as opposed to characteristic) energy. (A comparison of average with characteristic energy gives a coarse guide to the form of the distribution function). Electron energy distribution functions are also available by analysis of the velocity samples. However, to ensure reasonable resolution along the energy scale coupled with low scatter in the frequency, a great many more samples of energy need to be taken than position, and in practise this slows down the simulation unacceptably.

Within the restrictions of the model used, the Monte Carlo method gives a complete and independent measure of the accuracy of proposed cross sections, as gauged by the ability to reproduce the measured macroscopic quantities describing the swarm.

3.2. Testing the Monte Carlo Approach.

To test the validity of the Monte Carlo approach in analysing swarm cross sections, as well as the reliability of individual codes, an international benchmark exercise was set up. Five groups took part from; Parma (Italy), Trondheim (Norway), Canberra (Australia), Pittsburgh (USA), and Stirling. Two sets of

3. THE MONTE CARLO APPROACH.

model cross sections were used, the first for a simple model gas with a large inelastic contribution, designed to test the two term approximation, and the second based on the cross sections of a real gas, those for CO_2 as published by Bulos and Phelps (1976) (see F3.3). The latter benchmark showed up many inadequacies of the Stirling code for use with real gases, and as a consequence of taking part in the exercise successfully, the code was greatly improved. The results of the two tests are given in tables T3.1 and T3.2, and the electron energy distribution for the swarm under the conditions specified for benchmark 1 is shown in F3.4. The accuracy of the swarm parameters is estimated as 1% for W_d and the average energy, and 2% for the diffusion coefficients. A comparison of results for two term and eight term Boltzmann analysis (Pitchford et al, 1981) of the same cross section is included in T3.1 for comparison. It can be seen clearly that the two term truncation is inadequate in cases of high inelastic contributions, as was previously thought. Equally, the eight term Boltzmann solution produces answers in accord with the Monte Carlo results, showing that the two can be used as complementary approaches to the same problem.

In addition to the international benchmarks, a comparison of our code with that of a slightly different approach (Braglia, 1977) using a constant collision frequency model was made. The Boltzmann equation is exactly soluble in this case, and T3.3 summarizes the results. The Braglia method more closely approaches

3. THE MONTE CARLO APPROACH.

the experimental reality of a swarm in that it considers a large number of electrons, each making a relatively small number of collisions during the drift time. Braglia's three results were obtained considering three different starting energy distributions, the one showing the best fit to the Boltzmann result (Braglia3) having started with the swarm in its hydrodynamic state. The present work circumvents this by studying one electron for many collisions, rather than many electrons over fewer collisions, and allows a pre-drift time to allow that electron to reach a steady state. The agreement between the two approaches, and with the exact Boltzmann solution is encouraging.

From the benchmarks, it can be seen that there is general agreement between the groups on the first model, and amongst most of the parameters available for the second model. Only when more results become available will the 12% discrepancy in the results for D_1 for this model be resolved. From this we conclude that our Monte Carlo code is working and is suitable for use on real gases within the restrictions of the model that we have assumed. The agreement with the Parma group's constant collision frequency model confirms this conclusion.

3. THE MONTE CARLO APPROACH.

Benchmark 1.

Gas Properties

| | | |
|---------------------|-----------|---------------------------|
| Molecular Mass | 4 | amu |
| Elastic X-Section | 6 | Angstrom ² |
| Inelastic X-Section | 10(KE-Ei) | Angstrom ² /eV |
| " Onset | 0.2 | eV |
| Temperature | 0 | K |
| E/N | 24 | Townsend |

| SOURCE | W_d/ms^{-1} | D_r/m^2s^{-1} | D_l/m^2s^{-1} | Av.En./eV |
|------------|---------------|-----------------|-----------------|-----------|
| PARMA | 88900 | 11.34 | 4.73 | 0.409 |
| TRONDHEIM | 88700 | 11.31 | 4.54 | 0.407 |
| CANBERRA | 88800 | 11.4 | N/A | 0.408 |
| STIRLING | 88700 | 11.23 | 4.62 | 0.408 |
| PITTSBURGH | 89100 | 11.2 | 4.67 | 0.408 |
| BOLTZ(2) | 91430 | 14.38 | N/A | N/A |
| BOLTZ(8) | 88830 | 11.30 | N/A | N/A |

T3.1 Comparison of Monte Carlo and Boltzmann Calculations.

3. THE MONTE CARLO APPROACH.

Benchmark 2.

Gas Properties

| | |
|----------------|----------|
| Molecular Mass | 4 amu. |
| Cross Sections | see F3.3 |
| Temperature | 0 K. |
| E/N | 40 Td. |

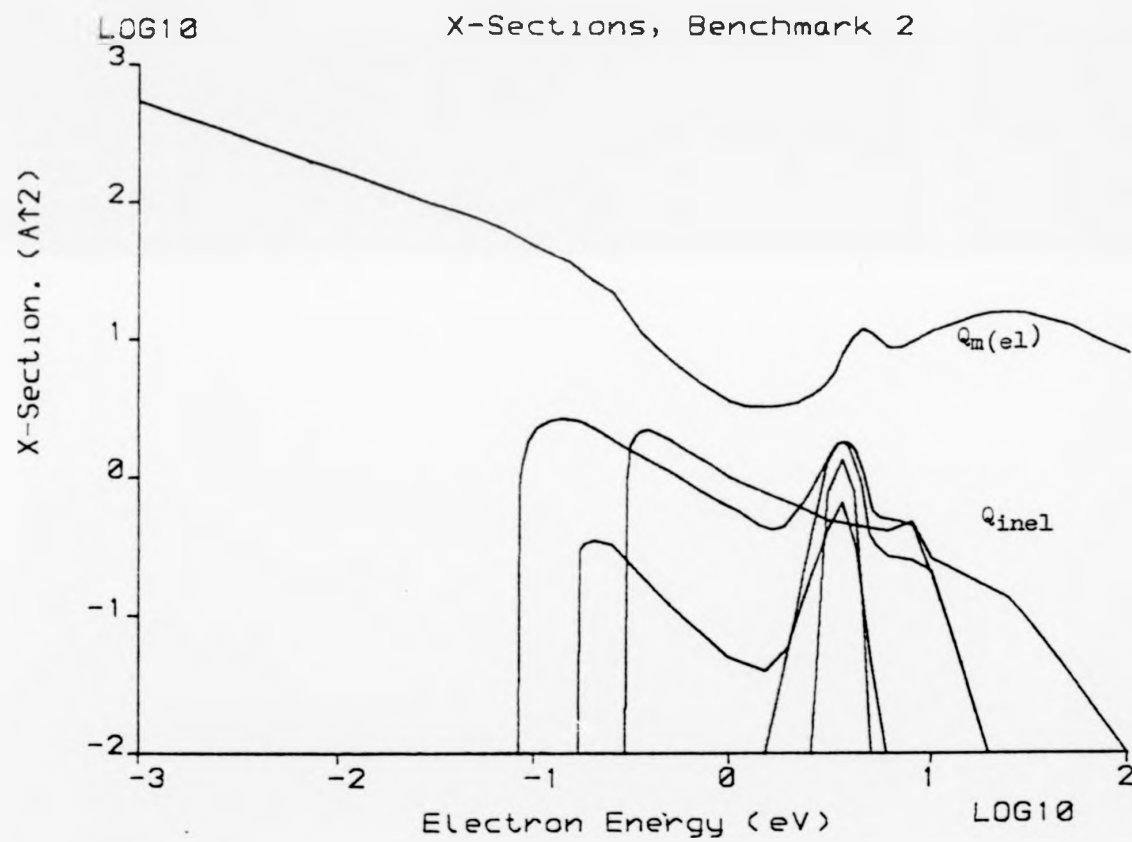
| SOURCE | W_d/ms^{-1} | D_r/m^2s^{-1} | D_l/m^2s^{-1} | Av.En./eV. |
|-----------|---------------|-----------------|-----------------|------------|
| PARMA | 94200 | 35.1 | N/A | 1.84 |
| TRONDHEIM | 94200 | 35.0 | 1.00 | 1.84 |
| STIRLING | 94100 | 35.0 | 1.12 | 1.82 |

T3.2 Comparison of Results, Benchmark 2.

| SOURCE | W_d/ms^{-1} | D_r/m^2s^{-1} | D_l/m^2s^{-1} | Av.En./eV. |
|----------|---------------|-----------------|-----------------|------------|
| BOLTZ | 8570 | 2.90 | 2.90 | 1.522 |
| Braglia1 | 8600 | 3.10 | 2.89 | 1.515 |
| Braglia2 | 8520 | 3.04 | 2.88 | 1.515 |
| Braglia3 | 8600 | 2.89 | 2.89 | 1.515 |
| STIRLING | 8560 | 2.79 | 2.84 | 1.513 |

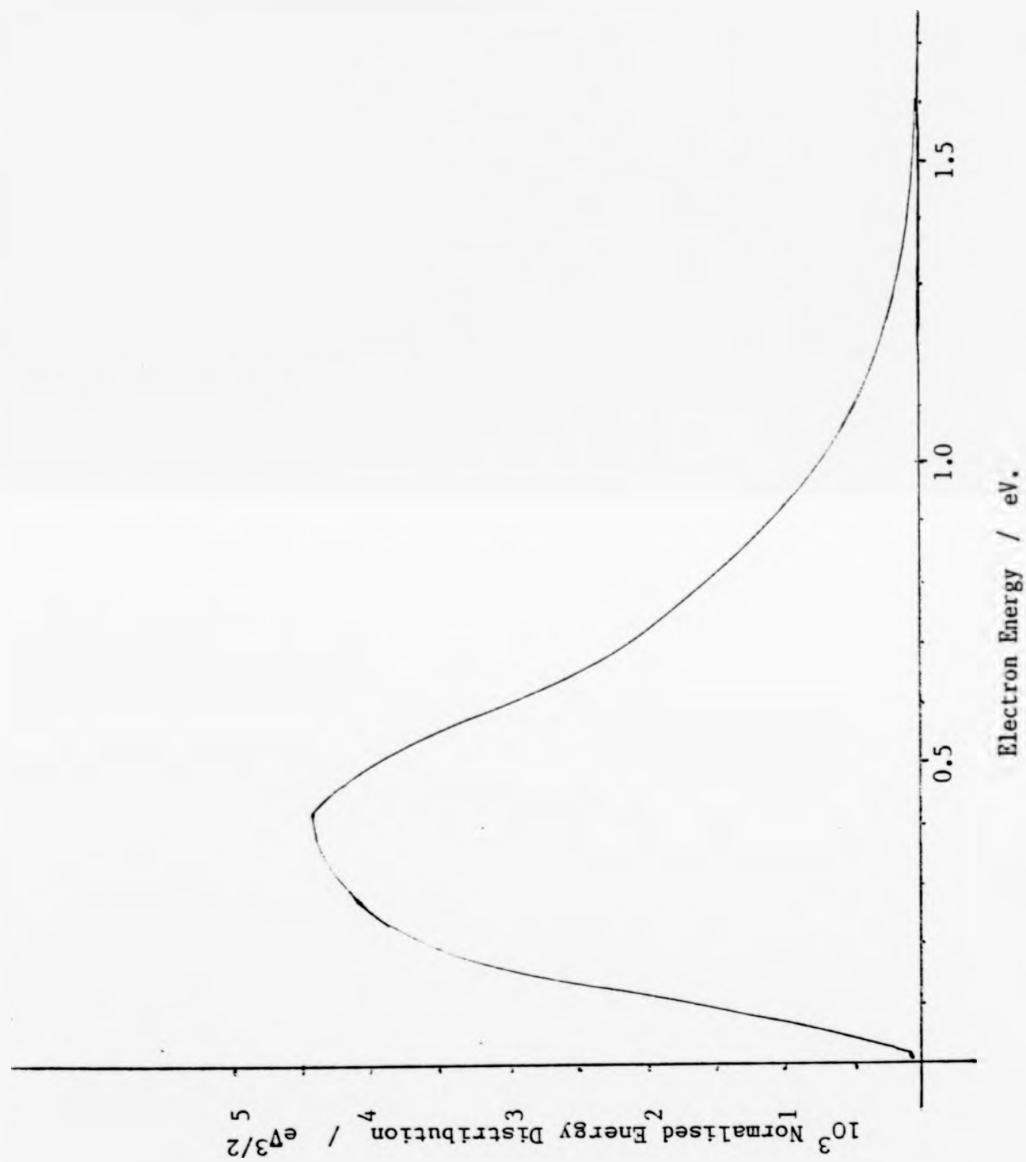
T3.3. Comparison of Results, Constant Coll. Freq. Model.

3. THE MONTE CARLO APPROACH.



F3.3. Cross Sections for Benchmark 2.

3. THE MONTE CARLO APPROACH.



F3.4. Normalised Energy Distribution of Electrons in Benchmark 1.

4. RELATED WORK

CHAPTER 4.

RELATED WORK

Having developed the background to electron molecule scattering, and examined the experimental and analytical methods through which swarm methods contribute to this field, it is pertinent to explain the reasoning behind the choice of molecular targets for this study in the light of other work. For this purpose it is convenient to divide the targets into two categories, polar and non polar.

4.1. Non-Polar Targets.

Early investigations of the motion of low energy electrons in gases were carried out in easily accessible molecular and atomic gases. The noble gases in particular showed interesting features in their low energy electron collision cross sections. The lack of a comparatively strong dipole or quadrupole interaction with electrons means that non-polar molecules do not show any universally applicable velocity dependence in their collision cross sections. However some common features do pertain, particularly the existence of a deep minimum in the total cross section of many non-polar gases. This is known as the Ramsauer Townsend Minimum after it was observed with Argon in beam (Ramsauer, 1921) and swarm (Townsend, 1925) experiments independently. The presence of this minimum in several gases is illustrated in G4.1.

4. RELATED WORK

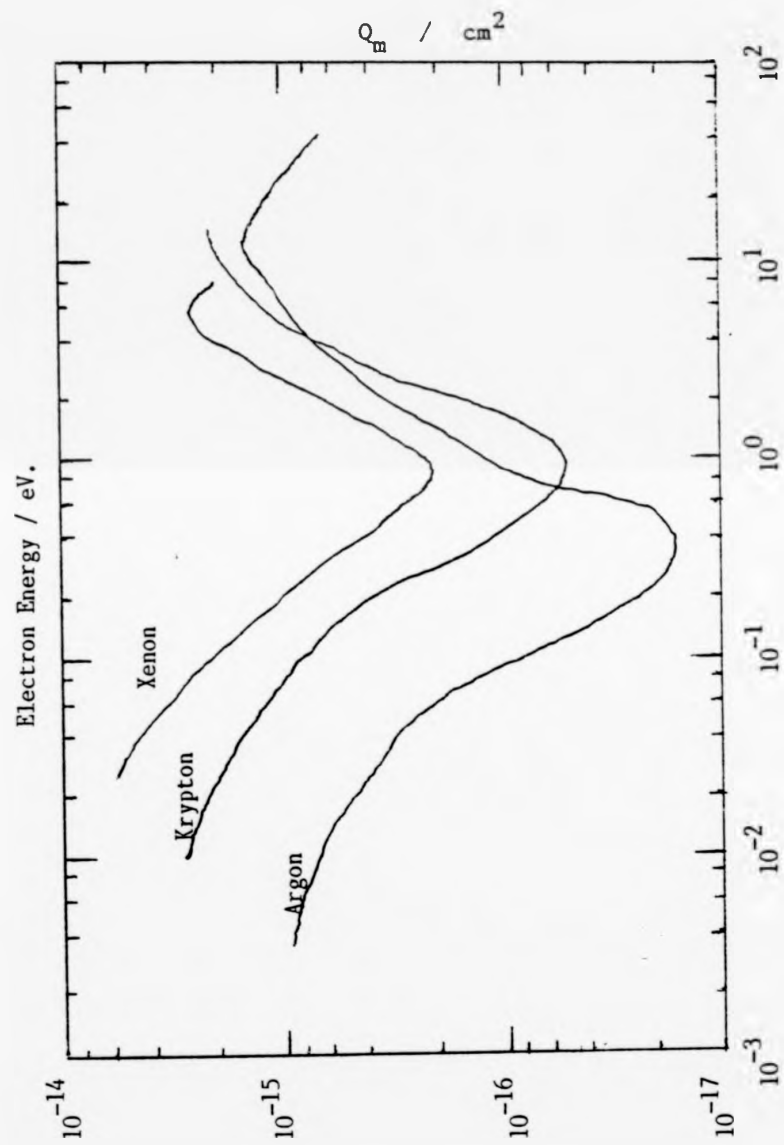
CHAPTER 4. RELATED WORK

Having developed the background to electron molecule scattering, and examined the experimental and analytical methods through which swarm methods contribute to this field, it is pertinent to explain the reasoning behind the choice of molecular targets for this study in the light of other work. For this purpose it is convenient to divide the targets into two categories, polar and non polar.

4.1. Non-Polar Targets.

Early investigations of the motion of low energy electrons in gases were carried out in easily accessible molecular and atomic gases. The noble gases in particular showed interesting features in their low energy electron collision cross sections. The lack of a comparatively strong dipole or quadrupole interaction with electrons means that non-polar molecules do not show any universally applicable velocity dependence in their collision cross sections. However some common features do pertain, particularly the existence of a deep minimum in the total cross section of many non-polar gases. This is known as the Ramsauer Townsend Minimum after it was observed with Argon in beam (Ramsauer, 1921) and swarm (Townsend, 1925) experiments independently. The presence of this minimum in several gases is illustrated in G4.1.

4. RELATED WORK



G4.1. Ramsauer - Townsend Minima in Noble Gases.

4. RELATED WORK

The effect can be explained in terms of the phase change in an incident wave train interacting with a simple potential well of depth D and radius a . The wavelength of the incident electron is given by

$$\lambda = \frac{h}{M V} \quad \text{E4.1}$$

for r greater than a ,

and
$$\lambda = \frac{h}{\sqrt{M^2 V^2 + 2D_M}} \quad \text{E4.2}$$

for r less than a .

The wave train can only retain continuity at $r = a$ by a phase change in the scattered wave. When this interaction is observed by noting the phase shift, it disappears as the phase shift passes through integral multiples of 2π . At such points the observed cross section would be zero.

This simple analysis is physically unrealistic, as it takes account of head on collisions only. It is readily extended to describe the phase shift induced by a simple atomic potential in the (quantised) angular momentum of an approaching electron (Hasted, 1964). For very low energy electrons the summation over all phase shifts used to evaluate the cross section reduces to the zero order phase shift ($l = 0$) and

$$Q_T = \frac{\pi \sin^2 \eta}{k^2} \quad K = \frac{2\pi}{\lambda} \quad \text{E4.3}$$

η is phase shift

4. RELATED WORK

At low incident energies the phase shift tends to $n\pi$ as k tends to zero. For weak fields (e.g. Helium) $n = 0$ and Q remains finite. However for stronger fields, a minimum in the cross section will be observed when the strength of the field can induce a phase change of $n\pi$ in electrons at a particular incident energy. The fields of Argon, Krypton and Xenon fulfil this criterion at the energies shown in G4.1.

The extrapolation of atomic scattering ideas to molecular scattering is complicated in this case by quantisation of the electron angular momentum about the internuclear axes. However, for low energy electrons, the zero order approximation can be applied again, reducing the complexity of the problem. Buckingham *et al* (1941) applied these ideas to Methane, assuming a spherically symmetrical field and concluded that Methane occupies the place of Neon in the Noble Gas Ramsauer-Townsend series.

If a Ramsauer Townsend Minimum in a molecular gas coincides with the onset of a vibrational excitation, the proportion of collisions causing the excitation can be very high, leading to a very efficient channel for vibrational excitation. This is thought to be the case in Methane.

Such processes have important practical implications (Cherrington, 1979) as well as presenting an interesting situation for theoretical analysis. The mechanism of excitation under these conditions is also far from clear, and accurate evaluation of the

4. RELATED WORK

contributory cross sections in the region of their onset ought to provide useful information in this respect. On this basis, it was decided to apply our approach to determine Methane cross sections and to extend this study to other non-polar molecular gases isoelectronic with the Noble Gases, namely Per Deutero Methane, Silane and Per Deutero Silane. A further reason for investigating the behaviour of swarms in Silane is that this gas is used extensively in the semiconductor industry as the deposition precursor for amorphorphous silicon. The deposition process involves passing an electrical discharge through Silane. The inclusion of the deuterated compounds should allow separation of effects due to the potential of the molecule, and those due to the vibrational structure. This approach is not new, but previous studies in the same gases (Cottrell and Walker, 1965, 1967, Pollock, 1968, Duncan and Walker, 1972) have not had the benefit of a Monte Carlo simulation as a check on the validity of the two term truncation of the Boltzmann equation. Recall that it is in the region of high inelastic contributions that this approximation breaks down (see T3.1).

Lucas (Lakshminarasimha and Lucas, 1977) has measured transport coefficients at high E/N in methane and other gases to extract attachment coefficients. Drift velocity measurements in methane have been made by Wagner et al (1967) and by Bowman and Gordon (1967). Lehning (1969) investigated pressure effects on the drift velocity in methane up to 10 atmospheres. Diffusion to

4. RELATED WORK

mobility ratios in methane have been measured by Brose and Keyston (1935), Cochran and Forester (1962), Cottrell and Walker (1967) and Duncan and Walker (1972).

Beam experiments in Methane have been used to probe cross sections at around the energy of the first vibrational excitation (Barbarito *et al.*, 1979, Rohr, 1980, Sohn *et al.*, 1982). Qualitatively, they have confirmed that at around the region of the Ramsauer Townsend Minimum, the momentum transfer cross section is smaller than the value given by the two term Boltzmann solution. They also show very sharp onsets to the vibrational processes, and some structure at these onsets is claimed in one case, although the published spectra do not show such structure clearly. (The presence of structure in a process near onset indicates the presence of a long-lived (on the vibrational time scale) electron-target complex). If verified, this would be an important contribution towards elucidation of the excitation mechanism. Quantitatively there are some discrepancies between the results of separate groups, although all show the same general features. It should be remembered that normalisation techniques in beam experiments can often be a source of error, particularly in the absence of rigorous theoretical solutions. There are no known beam studies in the other non-polar target gases.

In view of the experimental effort being expended on Methane, surprisingly little progress has been made on the theoretical front. The current developments in rigorous

4. RELATED WORK

electron-molecule scattering theory have been reviewed by Burke (1982). Methane is not amenable to study with currently available methods without introduction of some parameterisation, notably a polarization cut off on an interaction potential (Gianturco and Thompson, 1976, 1979). The method is very sensitive to the value of the polarisation cut off, particularly for Methane in the region of the minimum. However, the results taken with cut off at 0.84 au are in better agreement with beam results not then available, than with results from the two term Boltzmann approximation. No contribution to the discussion of vibrational excitation mechanisms is made. The authors extended their approach to some polar molecules, and recently an expansive investigation into the scattering properties of water appeared (Jain and Thompson, 1983). Kleban and Davis (1977) and Kitamori (1978) have approached the problem differently in trying to get an exact solution of the Boltzmann equation without recourse to using coupled ordinary differential equations and the approximations that entails (see Chapter 2). No theoretical work has been done on the other non-polar gases included in this study.

4.2. Polar Targets.

The state of our knowledge of the cross sections for electron interactions with polar gases is rather different from the above. Because of the large electron dipole interaction, these gases show a consistent energy dependence which is well described

4. RELATED WORK

by theory (Lane, 1980, Burke, 1982). Because of this strong interaction, polar molecules tend to attach electrons fairly strongly, making the Townsend - Huxley experiment invalid. A modification to the basic experiment allows measurement of D/μ in the presence of ionisation and attachment (Bailey, 1925). The development of an analytical expression equivalent to E1.5 for this method was not so rigorously developed, limiting its usefulness. Other recent methods have produced more reliable data (Lakshminarasimha and Lucas, 1977, Naidu and Prasad, 1969) with significant changes in method. The measurement of drift velocity in attaching gases is simpler, since the shutter grids can be used to discriminate against negative ions. The body of knowledge for drift velocities therefore extends to rather more gases than that for diffusion coefficients. One further complication with polar gases is the increased importance of intermolecular forces. In some cases these forces are thought to change the nature of the attaching species. Clusters of ammonia molecules solvating electrons have been proposed as responsible for attachment in dense ammonia vapour (Christophoru et al, 1982). The attachment process is often accompanied by compensatory energy loss mechanisms. The channels open for any molecule to relax depend on the relationship of the potential energy surfaces of the initial state of the molecule and the molecule - electron complex. Significant differences in attachment behaviour might therefore be expected between a hydride and the equivalent deuteride if the effects are due to mass or energy levels in a surface, but not if potential effects are dominant. Bearing this in mind, and the fact

4. RELATED WORK

that the present apparatus is inadequate for measurements in attaching gases, it was decided that an exploration of the non-metal Hydrides and Deuterides within the limitations of non-attaching gases and time restrictions may produce some interesting information. Selected polar target gases were NH_3 , PH_3 , PD_3 , H_2O , D_2O and H_2S .

Previous swarm studies have been conducted in these gases. In NH_3 , drift velocities have been measured at room temperature by Nielsen and Bradbury (1937), and at 195, 300 and 381K by Pack et al (1962). Diffusion to mobility ratios were determined by Bailey and Duncanson (1930) using a modified form of the Townsend Huxley apparatus to account for electron attachment. In PH_3 , drift velocities have been measured by Cottrell et al (1968). No known measurements of diffusion to mobility ratio have been made. No measurement of either transport parameter is known in PD_3 . Drift velocities in H_2O have been measured by a number of authors. Pack et al (1962) found no evidence of attachment at elevated temperatures (300 and 443K). At room temperature Lowke and Rees (1963), Ryzko (1966) and Christophoru and Christodoulides (1969) have reported measurements covering overlapping ranges of E/N with agreement to within the quoted errors. Hurst et al (1963) using alpha particle ionisation were able to report drift velocities in isothermal electrons in mixtures of water vapour with ethylene. The ratio of diffusion to mobility has been measured by Bailey and Duncanson (1930) and by Crompton et al (1965). The results do not

4. RELATED WORK

agree, and it has been suggested on the basis of unpublished measurements (Lowke and Parker 1969) that the discrepancy may be due to the high degree of anisotropic diffusion in this gas. In the case of high longitudinal diffusion, some fundamental assumptions made in the derivation of equations describing the swarm's motion break down, and hence the usual analysis is inapplicable. No measurements are known in D_2O . Attachment in Hydrogen Sulphide was studied by Bradbury (1934). Hurst *et al* (1963) measured drift velocities in binary mixtures of Hydrogen Sulphide with Methane, Ethane and Carbon Monoxide, but not in the pure gas. Measurements of D/μ in H_2S (Duncan, 1971) have been made but remain unpublished.

Information from beam experiments is available for H_2S and H_2O . The studies in H_2S carried out so far all indicate a resonant attachment at around 2.3 eV. The transmission experiment of Sanche and Schulz (1973) indicated the presence of such a resonance, but low resolution at this energy prevented elucidation of the nature of the resonance. A more recent study (Rohr, 1979) showed a peaked onset to vibrational excitation followed by a structureless hump in the differential cross section which was interpreted as a short lived resonance. (If the lifetime of the attached state had been comparable with the vibrational period for the molecule, some structure should have been observed.). Evidence for associative detachment as a decay process for the resonant state has been found (Azria *et al*, 1979), but it is likely that only a small proportion

4. RELATED WORK

of the attached species will follow this channel. Beam studies on H_2O have been extensive and have been reviewed elsewhere (Walker, 1974). No other beam studies are known for these molecules.

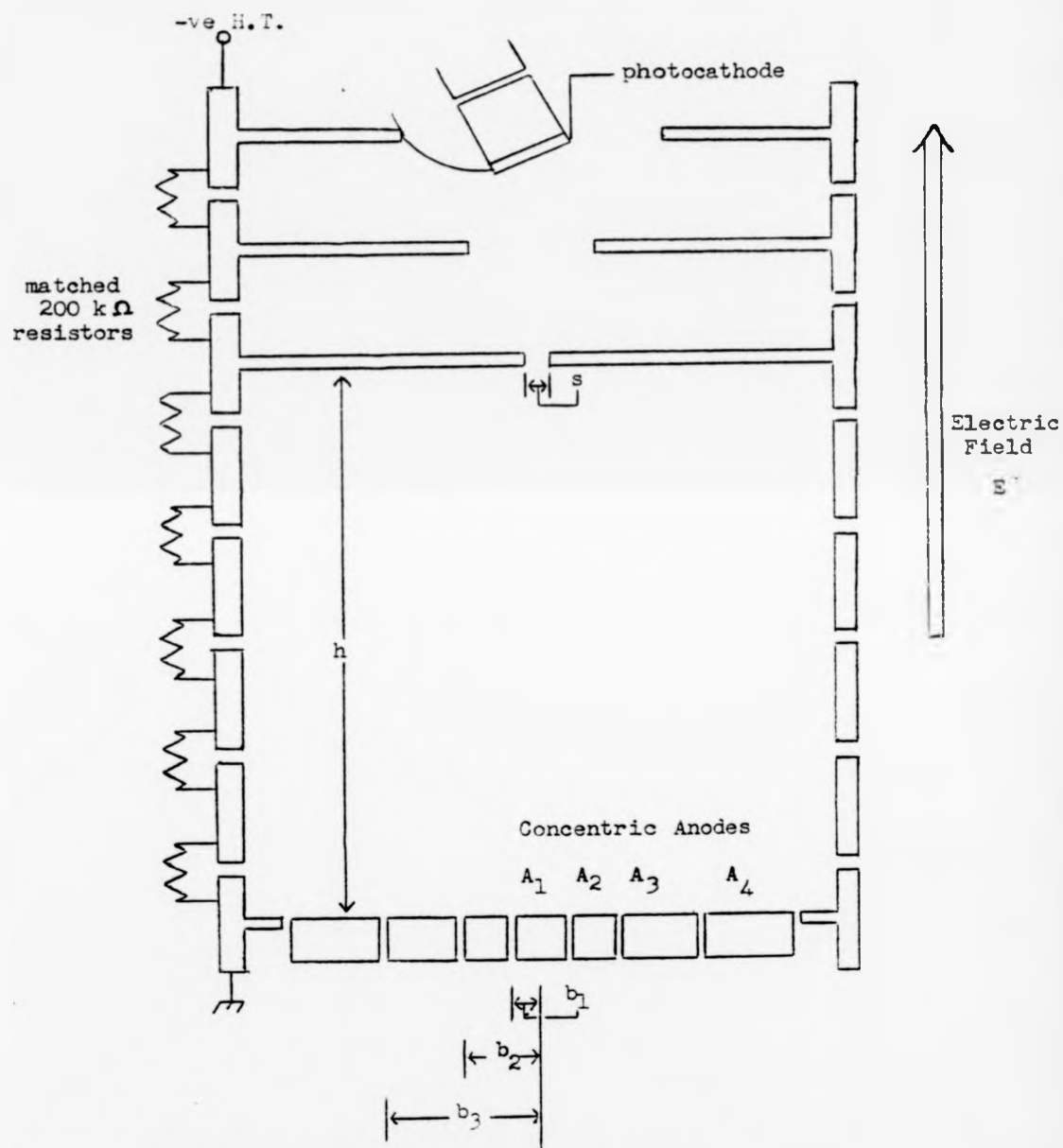
A recent upsurge in theoretical interest in polar molecules has been noted (Lane, 1980). This is due partly to the increasing interest in magnetohydrodynamic power generation, in which plasma conductivity is limited by momentum transfer collisions with polar molecules. A further interest is due to the experimental observation that the momentum transfer cross section for these interactions is often significantly higher than that predicted by theory (Altshuler, 1957). An explanation of this effect could lead to an insight into the nature of the interaction. A rotational resonance was invoked to explain the experimental observations in H_2S (Hurst *et al.* 1963), and the possibility of such a state was confirmed (Turner, 1966) by an extension of the Altshuler theory, although its existence in H_2S seems doubtful (Fox and Turner, 1966). A similar difference between experiment and theory was noted for PH_3 (Cottrell *et al.* 1968). Despite the growth of interest in the lower homologues (H_2O and NH_3) of these two molecules, advanced theory has only been extended to H_2S in one case (Gianturco and Thompson, 1979), utilising a similar approach as in their Methane work, but without developing it to cross section extraction. The quality of the wavefunctions used in the H_2S model was admitted by the authors to be poor, perhaps justifying a reluctance to compare with experiment. No equivalent theoretical approaches have been made for Phosphine.

CHAPTER 5.
EXPERIMENTAL

5.1/. Apparatus

The apparatus used in this work is that described by Duncan (1971). Recall from F1.2 that the experiment consists of measuring the lateral spread of an electron swarm using current ratios on anodes perpendicular to the field and at a known distance from the source. In this case, the electron source is a gold film illuminated through a quartz window by UV light. The cathode is prepared by vacuum evaporation of gold onto a quartz window in an evaporation chamber attached to the vacuum system (see F5.3). A pre-drift region allows the swarm to relax to its hydrodynamic state before passing the source hole S. The current is collected on four concentric anodes mounted on quartz insulating spacer rings. Switching the collected currents allows the radius of the central collector to be varied. This allows the ratio of inner to outer anode current to be kept close to 0.5, reducing the error in applying E1.4. The dimensions of the apparatus for inclusion in E1.4 are given in table T5.1, symbols as in F5.1.

5. EXPERIMENTAL



F5.1. Apparatus Used to Measure D/γ .

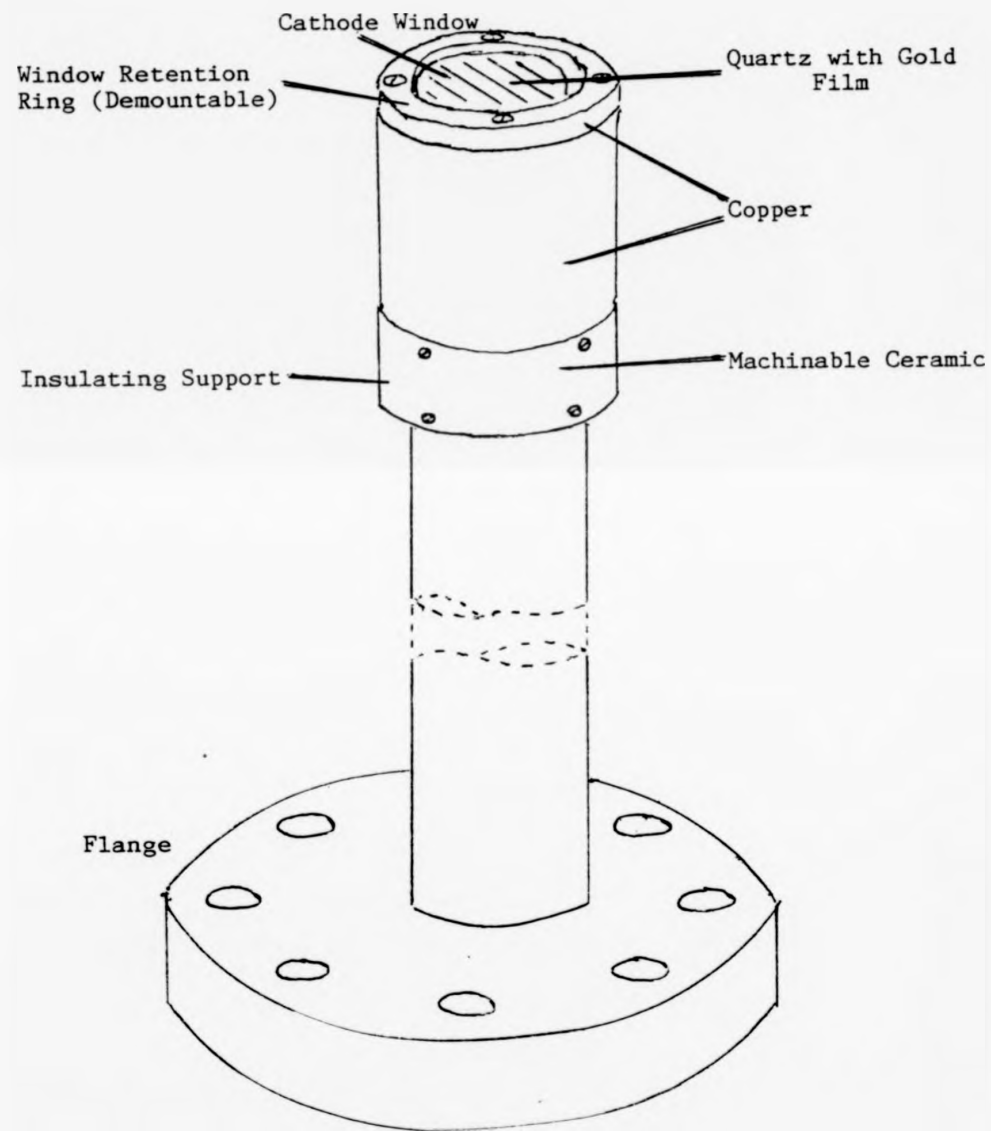
5. EXPERIMENTAL

| | | |
|------|-------------------------------|------------|
| h | - drift distance | 10.073 cm. |
| b(1) | - anode 1 radius | 0.251 cm. |
| b(2) | - anodes 1 + 2 radius | 0.500 cm. |
| b(3) | - anodes 1 + 2 + 3 radius | 1.000 cm. |
| s | - diameter of source aperture | 0.11 cm. |

T5.1. Apparatus Dimensions.

A number of modifications have been made to the apparatus since its original construction. The photocathode support structure was found to be inadequate on two counts. Firstly, the use of bakeable ceramic as the insulation from earth made the support mechanically unsound. As a result, the cathode window was not secure and would often fall out. Secondly, the large bulk of the insulator (needed to improve mechanical integrity) brought the H.T. connector in close proximity to the earthed casing, resulting in sparking at moderate E/N. Both of these problems were solved in the redesigned support. The new structure uses machinable ceramic as an insulating collar which does not need to be dismantled during cathode replacement. Into this is fitted a copper support from which the window can be removed and refitted without deterioration of the support threads. This increases the lifespan of the support beyond the expected one or two cathode lifetimes of the old system. The structure presents no points or sharp edges towards the earthed casing, thereby reducing the sparking problem considerably. The new

5. EXPERIMENTAL



F5.2. The New Cathode Assembly.

5. EXPERIMENTAL

assembly allows significantly higher E/N ranges to be explored and is depicted in F5.2.

A new electrical feedthrough connected to the mid-point of the drift chamber resistor chain allows a check of the chain continuity. This modification was originally included to enable the chain to be floated at a small voltage with respect to earth during speculative experiments on drift velocity measurements. When these early attempts proved unsuccessful, the link was retained as a useful fault diagnoser. In addition, the apparatus has been completely dismantled and electrical surfaces recoated with colloidal graphite (DAG 80). The coating was achieved by spraying a dilute methanol solution of the ethanolic graphite suspension onto the surfaces followed by vacuum furnacing (373 K, 24hrs.). Contact potential behaviour of the new surfaces showed a noticeable improvement over the old (brush, polish) system, justifying the extra care needed with the new method.

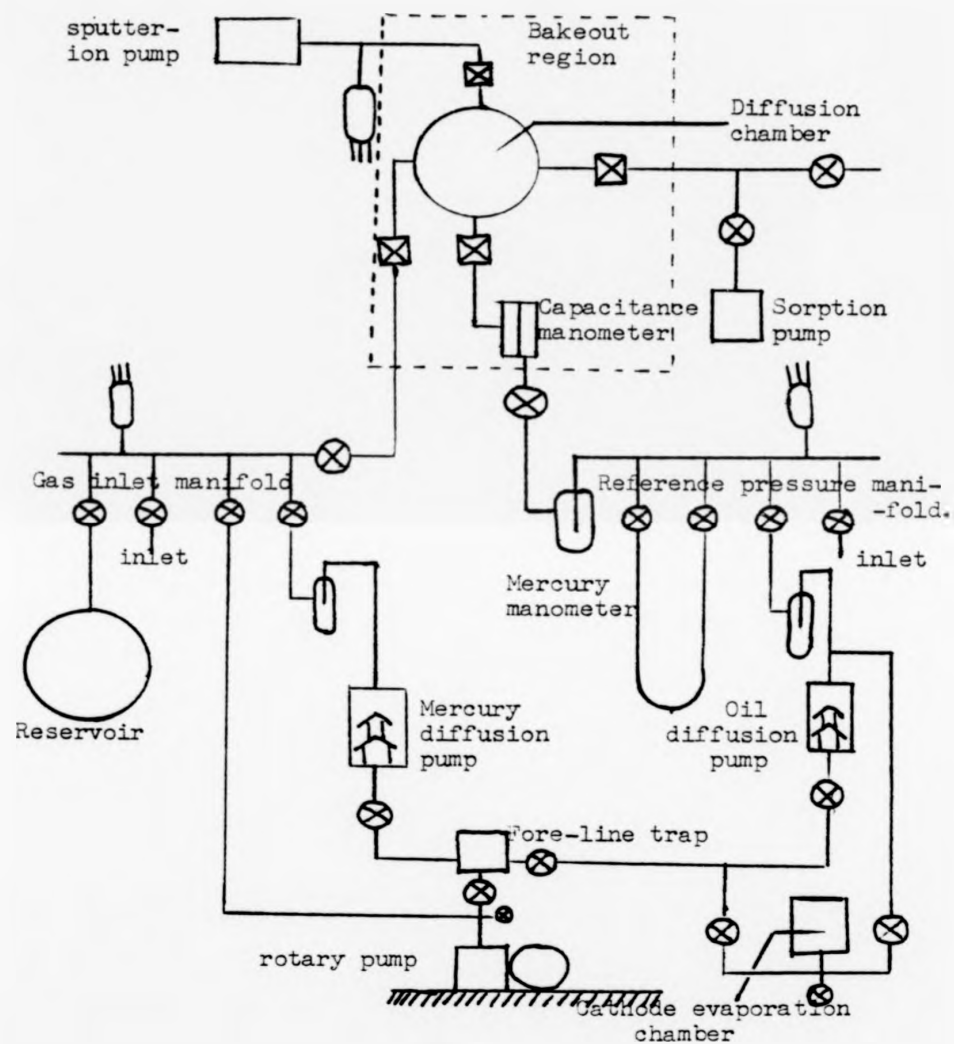
The gas handling system remains largely unchanged. Pressure measurement is indirect, using a reference pressure system in conjunction with a null indicating capacitance manometer, thus maintaining a clean sample gas system. Given the importance of accurate pressure measurement to electron - target collisions generally, and in the determination of absolute cross sections specifically (c.f. Chapter 1), it was decided that the single mercury manometer of the old system should be augmented by two new manometers attached to the reference pressure system, thus

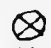


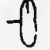
5. EXPERIMENTAL

extending the workable pressure regime. One is a simple oil manometer, and the other is a mercury manometer in which the column heights are determined by micrometer (Thomas and Cross, 1966). The latter instrument was found by calibration to be unreliable at pressures below 2 torr, and may in future be replaced by a micrometer oil manometer. The reference pressure and sample gas systems are represented schematically in F5.3. The bakeout region is bakeable to 500 K, although in practice 400 K produced satisfactory results. Initial pumping of the diffusion chamber is by molecular sorption pump, and below 10^{-4} torr by an ion pump down to 10^{-8} torr.

The data logging system has been replaced by a microcomputer based logger. This is fully described in Appendix 1. The main advantages with the new logging system are associated with the speed of collection, allowing a great deal more data to be observed, and treated. Particularly, much lower currents can be recorded, giving increased accuracy at low E/N where diminishing photocurrent was previously a limiting factor. Typical working currents are around 10^{-11} A, but using the new system, currents as low as 10^{-14} A produced useable data.

5. EXPERIMENTAL



- | | |
|--|--|
|  - Diaphragm Valves |  - All Metal (Bakeable) Valve |
|  - Ionisation Gauge |  - Liquid Nitrogen Trap |

F5.3. Schematic of Gas Handling System.

5. EXPERIMENTAL

5.2/. Primary Data.

The method of measuring D/μ as a function of E/N for any gas is simple.

(1) Admit gas at selected pressure, measured with the appropriate manometer.

(2) Apply voltage as calculated by data logging program to give required E/N value.

(3) Select anode mode such that the currents falling on the inner and outer collectors are approximately the same, giving R values about 0.5 (E1.4).

(4) Measure background currents (UV light off) then photocurrents, obtaining collected currents by difference.

(5) Calculate D/μ , record experimental conditions and repeat from (2).

If there is insufficient photocurrent, the cathode surface may be replaced by the method given in Appendix 2. In practice it was found that the quantity of photocurrent produced was not simply a reflection of cathode quality, but was also dependant on the sample gas. It was found that some gases (e.g. Methane) allow strong electron emission, whereas others (e.g. Hydrogen Sulphide) have to be examined at very low pressures to maintain adequate photocurrent. In this study, it was noted that the trend is for the more polar or polarisable molecules to have the strongest effect in

5. EXPERIMENTAL

suppressing photocurrent. It was found that the photocurrent available at a given pressure varied in the order (from largest available to smallest available photocurrents)



A feasible explanation for this observation is that the increased surface interaction with polar or polarisable molecules in the presence of a strong electric field may lead to a build up of surface layers which attenuate the photocurrent before it leaves the cathode.

5.2/. Gas Samples.

All gas samples were checked for purity on a JEOL 1800 mass spectrometer and on a PERKIN-ELMER 577 infrared grating spectrophotometer. The results of these checks and the sources of the gas samples follow.

Methane CH_4 .

Air Products Methane, stated purity 99%, was used direct from a lecture bottle. Mass spec showed ethane at about 0.5%, but no other impurities. No impurities detectable from I.R.. The gas was frozen (liquid Nitrogen) and briefly pumped to remove volatile contaminants before measurements were made.

Per Deutero Methane CD_4 .

Merck, Sharpe and Dohme CD_4 , stated isotopic purity 99% (atoms D) was found by mass spec to contain a significant (2%) quantity of air. This was removed by distillation through fresh

5. EXPERIMENTAL

Sodium deposited on glass wool (Storch, 1934) and subsequent freezing and pumping. This sample showed no air impurity, some CD_3H (1%) by mass spec, no detectable C-H stretch in I.R.. Gas that was left in the diffusion chamber for 48Hrs showed some signs of Hydrogen exchange.

Silane SiH_4 .

BOC Electra II Silane (Semiconductor Quality) was supplied by Motorola Ltd. of East Kilbride. Stated purity was 99.99% minimum. Mass spec and I.R. showed no detectable impurities. Larger quantities are available through BOC special gases.

Per Deutero Silane SiD_4 .

Prepared from the action of Lithium Aluminium Deuteride on Silicon Tetrachloride in Diethyl Ether (Baudler et al., 1967) Distillation from n-pentane slush (-130) to a liquid nitrogen trap removes solvent. The preparation and collection glassware were allowed to equilibrate with perdeutero water for two hours before preparation began. Analysis showed no detectable chemical or isotopic impurities.

Ammonia NH_3 .

B.O.C. Anhydrous Ammonia, stated minimum purity 99.9% was pumped at liquid nitrogen temperature to remove volatile impurities. No impurities were detected on analysis.

Phosphine PH_3 .

Prepared by the action of water on Calcium Phosphide (Baudler et al, 1967). Purified by repeated distillation over Potassium

5. EXPERIMENTAL

Hydroxide. Analysis showed no detectable impurities.

Per Deutero Phosphine PD_3 .

Prepared by the action of perdeutero water on Calcium Phosphide (Baudler et al., 1967). The preparation and collection glassware were allowed to equilibrate with perdeutero water for two hours before preparation began. Analysis showed no detectable chemical or isotopic impurities.

Water H_2O

Triple distilled under vacuum. No analysis was performed.

Per Deutero Water D_2O

Merck, Sharpe & Dohme 'gold' Analar quality (99.8% stated isotopic purity) was distilled under vacuum. No analysis was performed.

Hydrogen Sulphide H_2S

Matheson C.P. grade Hydrogen Sulphide, minimum stated purity 99.5% showed no detectable impurity.

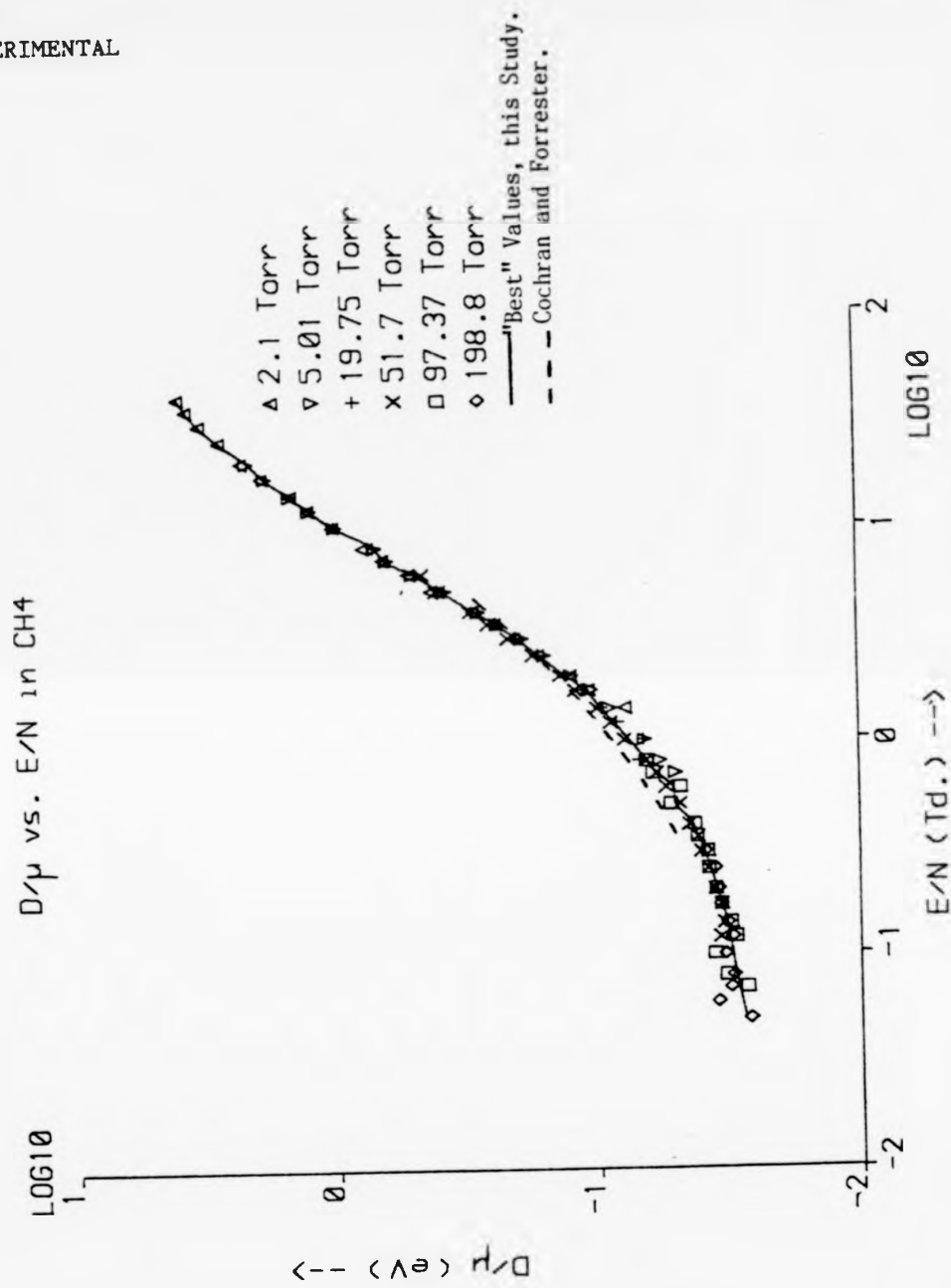
5.3/. Results.

D/μ as a function of E/N in each of the above gases for which consistent and reliable data were obtained is tabulated and plotted over. Several of the gases produced data inconsistent with simple conservative swarm behaviour and their detailed behaviour is not recorded here. The gases which showed inconsistencies were NH_3 , PD_3 , H_2O and D_2O . In all of these gases the behaviour shown was symptomatic of electron attachment. This is observed as a very

5. EXPERIMENTAL

strong current on the innermost collector relative to the outer concentric anodes, leading to gross inconsistencies in the observed D/μ values, for a given E/N , using different collector modes. The behaviour can be rationalised as being due to the attached species gaining a great deal of momentum in the field and accelerating from the source electrode to the central anode with little collisional lateral spread. This inconsistencies between modes check, once diagnosed, can be used as an early check as to the suitability of gases for extended study. The attachment of electrons to NH_3 , H_2O and D_2O has been observed before, particularly when the state of the gas is such that intermolecular interactions become significant (for review see Hatano & Shimamori, 1981). This is not the case for PD_3 , however, and the attaching behaviour in this gas is probably due to a conataminant (probably D_2O) at concentrations low enough to avoid detection by our methods, but high enough to affect the results.

5. EXPERIMENTAL



G5.1. Measured Values of D/μ vs E/N in Methane.

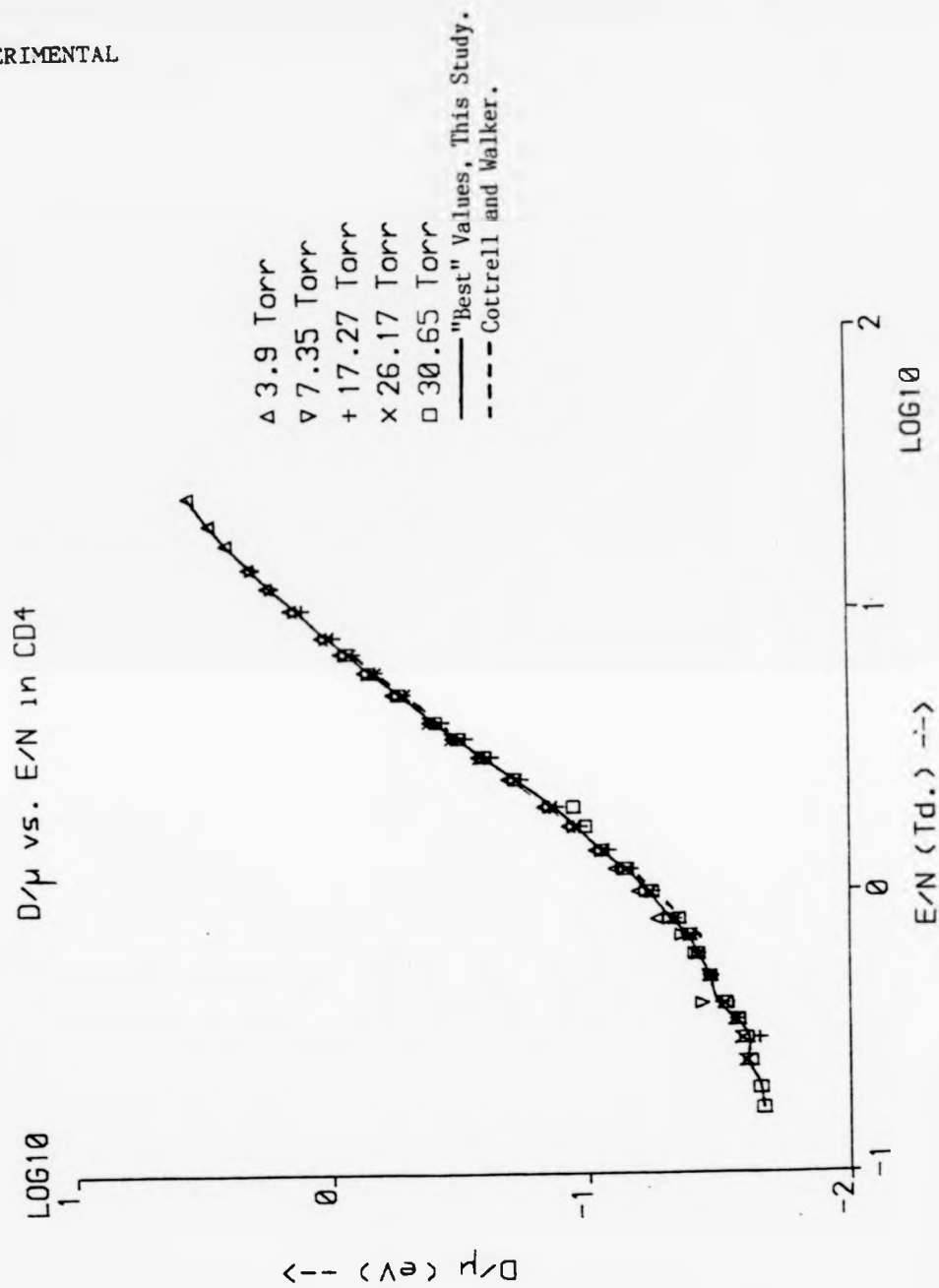
5. EXPERIMENTAL

Experimental Values of D/μ in Methane.

| E/N (Td.) | Pressure (Torr) | | | | | | |
|--------------|--------------------|--------|--------|--------|--------|--------|--------|
| | 2.1 | 5.01 | 19.75 | 51.7 | 97.37 | 198.8 | "BEST" |
| 40 | 3.775 | | | | | | 3.77 |
| 35 | 3.521 | | | | | | 3.52 |
| 30 | 3.142 | | | | | | 3.14 |
| 25 | 2.652 | | | | | | 2.65 |
| 20 | 2.190 | 2.086 | | | | | 2.05 |
| 17 | 1.826 | 1.774 | | | | | 1.79 |
| 14 | 1.423 | 1.424 | | | | | 1.42 |
| 12 | 1.218 | 1.209 | | | | | 1.21 |
| 10 | 0.983 | 0.965 | 0.969 | | | | 0.974 |
| 8 | 0.756 | 0.683 | 0.687 | | | | 0.685 |
| 7 | 0.635 | 0.615 | 0.615 | | | | 0.620 |
| 6 | 0.512 | 0.495 | 0.488 | 0.459 | | | 0.490 |
| 5 | 0.425 | 0.384 | 0.376 | 0.409 | | | 0.390 |
| 4 | 0.295 | 0.282 | 0.281 | 0.304 | | | 0.290 |
| 3.5 | 0.242 | 0.238 | 0.238 | 0.260 | | | 0.243 |
| 3 | 0.204 | 0.191 | 0.199 | 0.216 | | | 0.202 |
| 2.5 | 0.165 | 0.158 | 0.164 | 0.174 | | | 0.165 |
| 2 | 0.125 | 0.124 | 0.131 | 0.137 | | | 0.131 |
| 1.7 | 0.106 | 0.105 | 0.112 | 0.120 | | | 0.110 |
| 1.4 | 0.0767 | 0.0881 | 0.0949 | 0.0991 | | | 0.0953 |
| 1.2 | | 0.0835 | 0.0824 | 0.0880 | | | 0.0850 |
| 1 | | 0.0648 | 0.0653 | 0.0774 | 0.1125 | | 0.0756 |
| 0.8 | | 0.0566 | 0.0682 | 0.0638 | 0.0633 | | 0.0642 |
| 0.7 | | 0.0495 | | 0.0585 | 0.0603 | | 0.0595 |
| 0.6 | | | | 0.0542 | 0.0472 | | 0.0507 |
| 0.5 | | | | 0.0478 | 0.0514 | | 0.0496 |
| 0.4 | | | | 0.0437 | 0.0416 | | 0.0422 |
| 0.35 | | | | 0.0406 | 0.0408 | | 0.0407 |
| 0.3 | | | | 0.0395 | 0.0370 | 0.0380 | 0.0382 |
| 0.25 | | | | 0.0371 | 0.0368 | 0.0349 | 0.0363 |
| 0.2 | | | | 0.0349 | 0.0347 | 0.0338 | 0.0343 |
| 0.17 | | | | 0.0330 | 0.0330 | 0.0333 | 0.0331 |
| 0.14 | | | | 0.0322 | 0.0303 | 0.0313 | 0.0313 |
| 0.12 | | | | 0.0334 | 0.0292 | 0.0301 | 0.0308 |
| 0.1 | | | | | 0.0350 | 0.0320 | 0.0335 |
| 0.08 | | | | | 0.0316 | 0.0298 | 0.0309 |
| 0.07 | | | | | 0.0264 | 0.0305 | 0.0285 |
| 0.06 | | | | | | 0.0342 | 0.0342 |
| 0.05 | | | | | | 0.0259 | 0.0259 |

T5.2. Measured Values of D/μ vs E/N in Methane.

5. EXPERIMENTAL



G5.2. Measured Values of D/μ vs E/N in Perdeuteromethane.

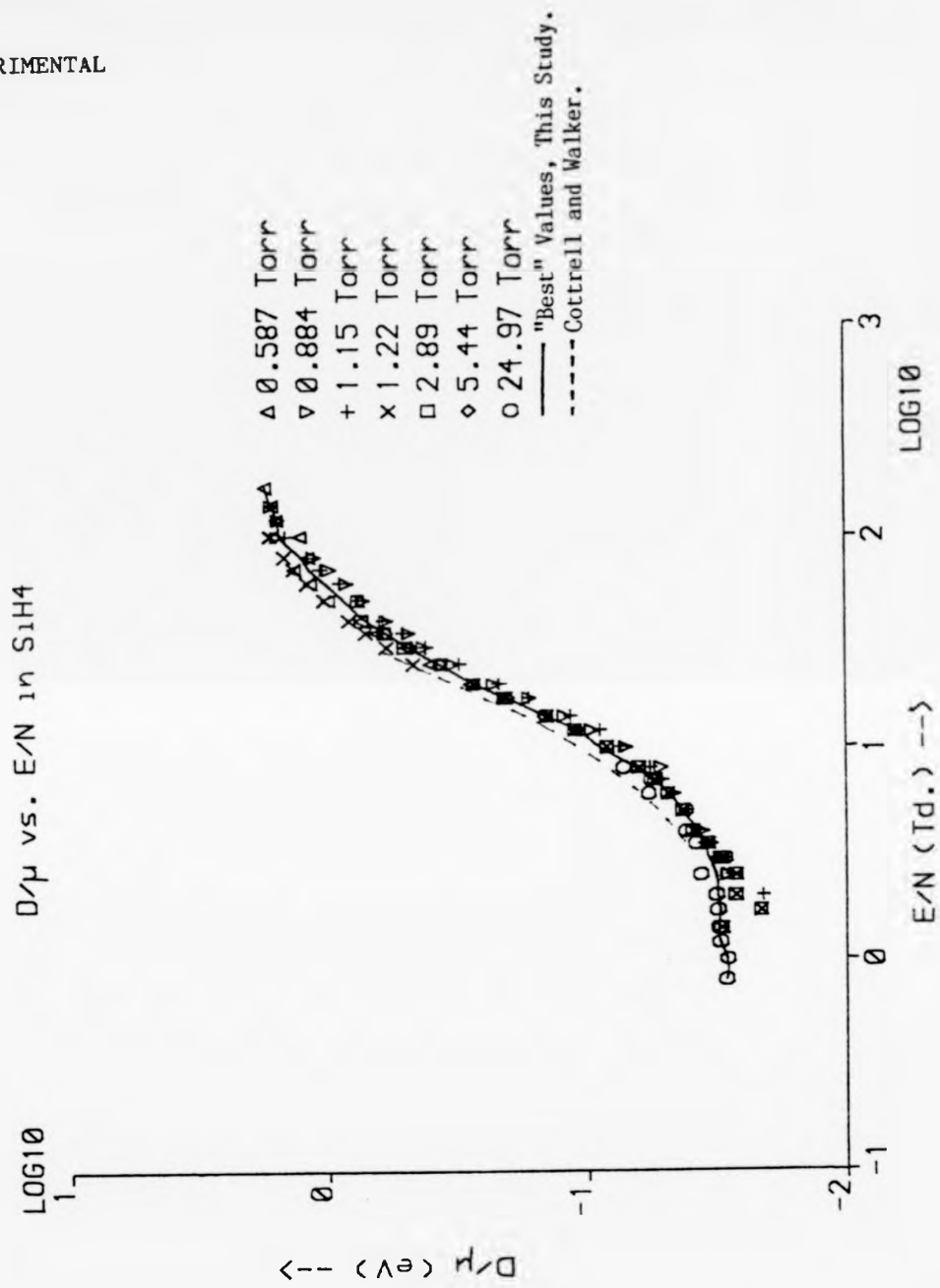
5. EXPERIMENTAL

Experimental Values of D/μ in Per Deutero Methane.

| Pressure (Torr) E/N (Td.) | 3.9 | 7.35 | 17.27 | 26.17 | 30.65 | "BEST" |
|------------------------------------|---------|---------|---------|---------|---------|--------|
| 25 | 3.428 | | | | | 3.42 |
| 20 | 2.844 | | | | | 2.84 |
| 17 | 2.449 | | | | | 2.45 |
| 14 | 2.021 | 1.936 | | | | 1.98 |
| 12 | 1.718 | 1.636 | | | | 1.68 |
| 10 | 1.404 | 1.333 | 1.256 | | | 1.33 |
| 8 | 1.075 | 1.028 | 1.016 | 1.021 | | 1.02 |
| 7 | 0.9078 | 0.8656 | 0.8045 | 0.8345 | 0.8556 | 0.854 |
| 6 | 0.7376 | 0.7023 | 0.6570 | 0.6643 | 0.7048 | 0.693 |
| 5 | 0.5713 | 0.5438 | 0.5057 | 0.5136 | 0.5348 | 0.534 |
| 4 | 0.4140 | 0.3905 | 0.3652 | 0.4127 | 0.3874 | 0.394 |
| 3.5 | 0.3386 | 0.3200 | 0.2962 | 0.3369 | 0.3175 | 0.322 |
| 3 | 0.2680 | 0.2544 | 0.2354 | 0.2627 | 0.2526 | 0.254 |
| 2.5 | 0.2047 | 0.1938 | 0.1814 | 0.1925 | 0.1921 | 0.193 |
| 2 | 0.1489 | 0.1414 | 0.1321 | 0.1406 | 0.1138 | 0.135 |
| 1.7 | 0.1197 | 0.1138 | 0.1069 | 0.1132 | 0.1021 | 0.111 |
| 1.4 | 0.09418 | 0.08930 | 0.08395 | 0.08825 | 0.08858 | 0.0889 |
| 1.2 | 0.07922 | 0.07489 | 0.07010 | 0.07216 | 0.07318 | 0.0741 |
| 1 | 0.06594 | 0.06170 | 0.05781 | 0.05940 | 0.05795 | 0.0606 |
| 0.8 | 0.05586 | 0.05000 | 0.04744 | 0.04743 | 0.04568 | 0.0493 |
| 0.7 | | 0.04470 | 0.04226 | 0.04131 | 0.04164 | 0.0425 |
| 0.6 | | 0.03973 | 0.03813 | 0.03856 | 0.03843 | 0.0387 |
| 0.5 | | 0.03398 | 0.03480 | 0.03500 | 0.03456 | 0.0346 |
| 0.4 | | 0.03733 | 0.03121 | 0.03061 | 0.03002 | 0.0323 |
| 0.35 | | | 0.02758 | 0.02795 | 0.02717 | 0.0276 |
| 0.3 | | | 0.2275 | 0.02635 | 0.02534 | 0.0248 |
| 0.25 | | | | 0.02535 | 0.02458 | 0.0250 |
| 0.2 | | | | | 0.02260 | 0.025 |

T5.3. Measured Values of D/μ vs E/N in Perdeuteromethane.

5. EXPERIMENTAL



G5.3. Measured Values of D/μ vs E/N in Silane.

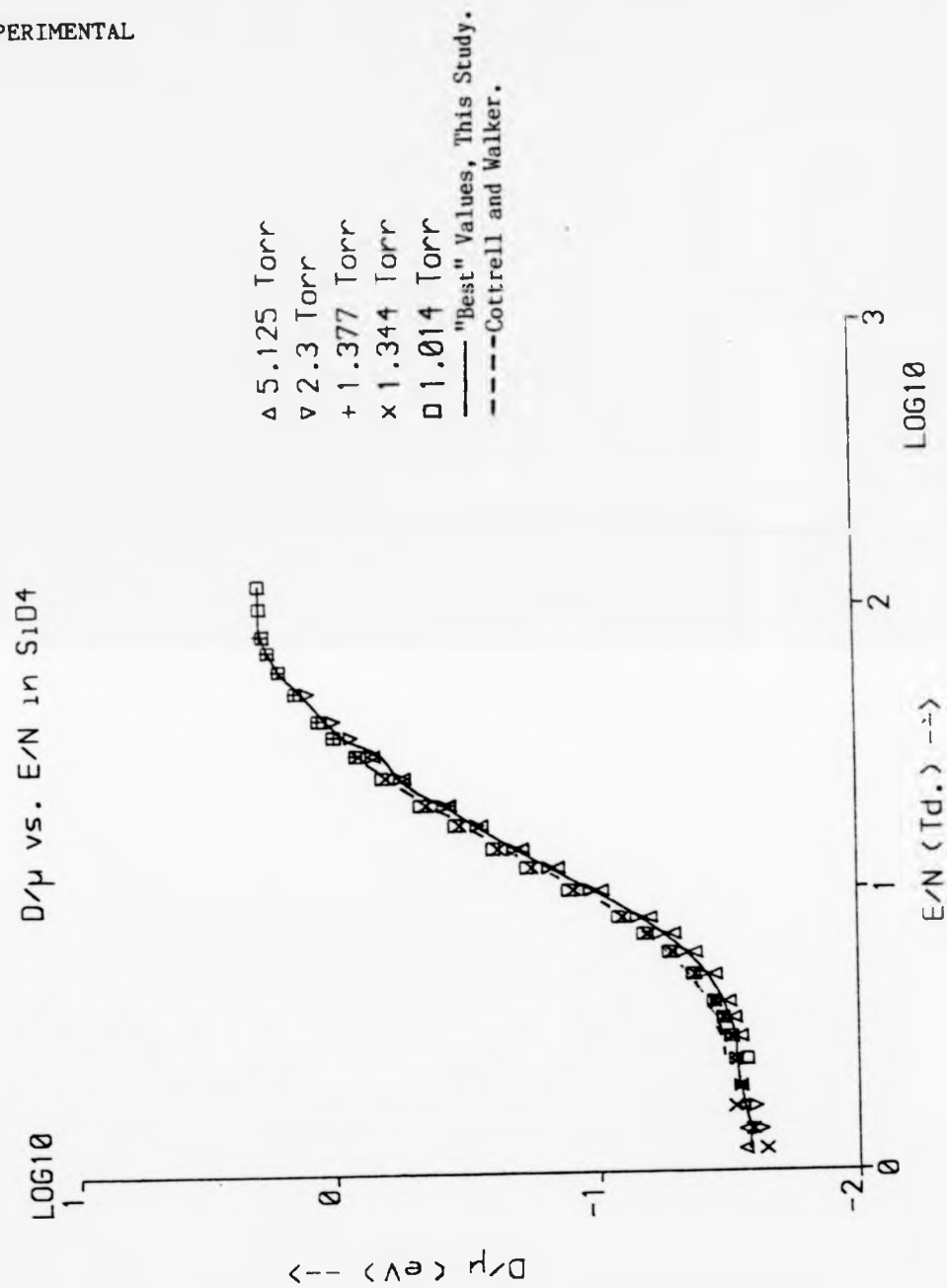
5. EXPERIMENTAL

Experimental Values of D/μ in Silane.

| Pressure (Torr) E/N (Td.) | 0.587 | 0.884 | 1.15 | 1.22 | 2.89 | 5.44 | 24.97 | "BEST" |
|------------------------------------|--------|---------|---------|---------|---------|--------|---------|--------|
| 170 | 1.710 | | | | | | | 1.71 |
| 140 | 1.615 | 1.622 | | | | | | 1.62 |
| 120 | 1.540 | 1.525 | | | | | | 1.53 |
| 100 | 1.255 | 1.532 | 1.417 | 1.639 | | | | 1.49 |
| 80 | 1.167 | 1.111 | 1.173 | 1.448 | | | | 1.25 |
| 70 | 1.322 | 1.022 | 1.045 | 1.331 | | | | 1.16 |
| 60 | 1.143 | 0.8331 | 0.8771 | 1.180 | | | | 1.01 |
| 50 | 0.9811 | 0.7192 | 0.7434 | 1.014 | 0.7504 | | | 0.853 |
| 40 | 0.7288 | 0.5843 | 0.5964 | 0.8147 | 0.7229 | | | 0.700 |
| 35 | 0.6349 | 0.4787 | 0.5001 | 0.7037 | 0.5952 | 0.5868 | | 0.587 |
| 30 | 0.4870 | 0.4172 | 0.4058 | 0.5836 | 0.4973 | 0.4768 | | 0.482 |
| 25 | 0.3919 | 0.3223 | 0.3034 | 0.4584 | 0.3584 | 0.3607 | | 0.363 |
| 20 | 0.2757 | 0.2232 | 0.2134 | 0.3300 | 0.2670 | 0.2679 | | 0.266 |
| 17 | | 0.1677 | 0.1669 | 0.2450 | 0.2048 | 0.2021 | | 0.201 |
| 14 | | 0.1216 | 0.1147 | 0.1840 | 0.1431 | 0.1468 | | 0.145 |
| 12 | | 0.09499 | 0.08850 | 0.1402 | 0.1115 | 0.1086 | | 0.109 |
| 10 | | 0.07024 | 0.07348 | 0.1059 | 0.08345 | | | 0.0888 |
| 8 | | 0.05416 | 0.05658 | 0.07576 | 0.06293 | | 0.07212 | 0.0657 |
| 7 | | 0.05272 | 0.05086 | 0.06166 | 0.05477 | | 0.05682 | 0.0565 |
| 6 | | 0.04621 | 0.04578 | 0.05210 | 0.04864 | | 0.05773 | 0.0482 |
| 5 | | | 0.04087 | 0.04440 | 0.04256 | | 0.04137 | 0.0431 |
| 4 | | 0.03594 | 0.03712 | 0.03917 | 0.03876 | | 0.04152 | 0.0375 |
| 3.5 | | 0.03362 | 0.03512 | 0.03661 | 0.03432 | | 0.03805 | 0.0348 |
| 3 | | 0.03053 | 0.03155 | 0.03478 | 0.03079 | | 0.02981 | 0.0337 |
| 2.5 | | 0.02889 | 0.02788 | 0.03373 | 0.02724 | | 0.03636 | 0.0323 |
| 2 | | | 0.02133 | 0.03500 | 0.02726 | | 0.03215 | 0.0317 |
| 1.7 | | | | 0.03521 | 0.02175 | | 0.03176 | 0.0312 |
| 1.4 | | | | 0.03286 | 0.03067 | | 0.03152 | 0.0311 |
| 1.2 | | | | | | | 0.03115 | 0.0311 |
| 1 | | | | | | | 0.02983 | 0.0298 |
| 0.8 | | | | | | | 0.02970 | 0.0297 |

T5.4. Measured Values of D/μ vs E/N in Silane.

5. EXPERIMENTAL



G5.4. Measured Values of D/μ vs E/N in Perdeuterosilane.

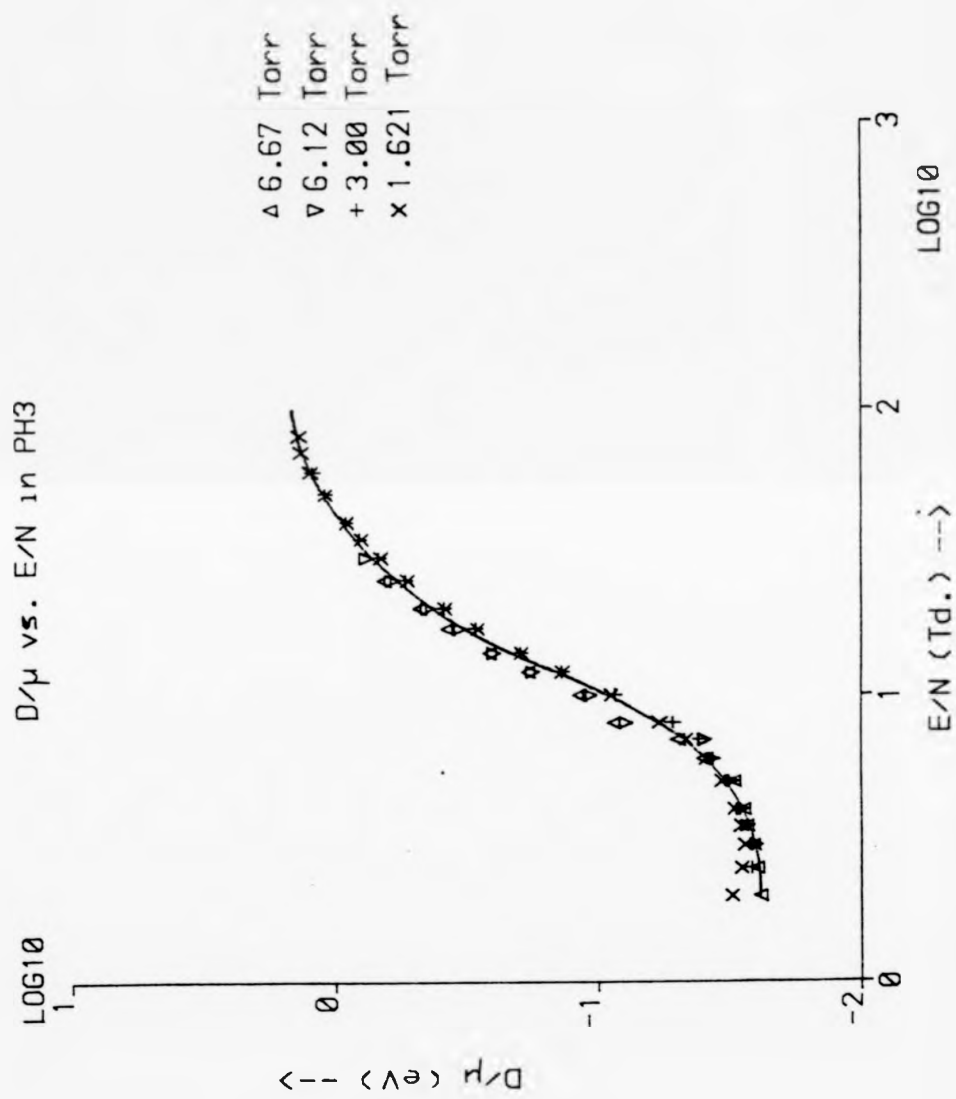
5. EXPERIMENTAL

Experimental Values of D/μ in Per Deutero Silane.

| Pressure (Torr) E/N (Td.) | 1.014 | 1.344 | 1.377 | 2.30 | 5.125 | "BEST" |
|------------------------------------|---------|---------|--------|---------|---------|--------|
| 120 | 1.883 | | | | | 1.88 |
| 100 | 1.868 | | | | | 1.87 |
| 80 | 1.827 | | 1.866 | | | 1.85 |
| 70 | 1.741 | | 1.762 | | | 1.75 |
| 60 | 1.584 | | 1.592 | | | 1.59 |
| 50 | 1.373 | | 1.379 | 1.228 | | 1.30 |
| 40 | 1.116 | | 1.120 | 0.9777 | | 1.05 |
| 35 | 0.9785 | | 0.9706 | 0.8386 | | 0.908 |
| 30 | 0.8047 | 0.7870 | 0.8081 | 0.6904 | 0.6303 | 0.723 |
| 25 | 0.6345 | 0.6170 | | 0.5355 | 0.5227 | 0.550 |
| 20 | 0.4559 | 0.4388 | | 0.3780 | 0.3652 | 0.388 |
| 17 | 0.3488 | 0.3356 | | 0.2859 | 0.2740 | 0.293 |
| 14 | 0.2467 | 0.2367 | | 0.2050 | 0.1900 | 0.206 |
| 12 | 0.1828 | 0.1762 | | 0.1515 | 0.1393 | 0.152 |
| 10 | 0.1278 | 0.1230 | | 0.1059 | 0.09626 | 0.105 |
| 8 | 0.08385 | 0.08066 | | 0.07052 | 0.06276 | 0.0692 |
| 7 | 0.06683 | 0.06469 | | 0.05761 | 0.05137 | 0.0563 |
| 6 | 0.05344 | 0.05215 | | 0.04773 | 0.04274 | 0.0463 |
| 5 | 0.04358 | 0.04338 | | 0.04057 | 0.03600 | 0.0389 |
| 4 | 0.03655 | 0.03627 | | 0.03545 | 0.03159 | 0.0336 |
| 3.5 | 0.03357 | 0.03361 | | 0.03348 | 0.03018 | 0.0318 |
| 3 | 0.03104 | 0.03151 | | 0.03177 | 0.02869 | 0.0300 |
| 2.5 | 0.02729 | 0.02970 | | 0.03024 | 0.03006 | 0.0298 |
| 2 | | 0.02892 | | 0.02889 | 0.02882 | 0.0289 |
| 1.7 | | 0.03035 | | 0.02531 | 0.02828 | 0.0278 |
| 1.4 | | 0.02600 | | 0.02413 | 0.02767 | 0.0265 |
| 1.2 | | 0.02309 | | | 0.02779 | 0.0268 |

T5.5. Measured Values of D/μ vs E/N in Perdeuterosilane.

5. EXPERIMENTAL



G5.5. Measured Values of D/μ vs E/N in Phosphine.

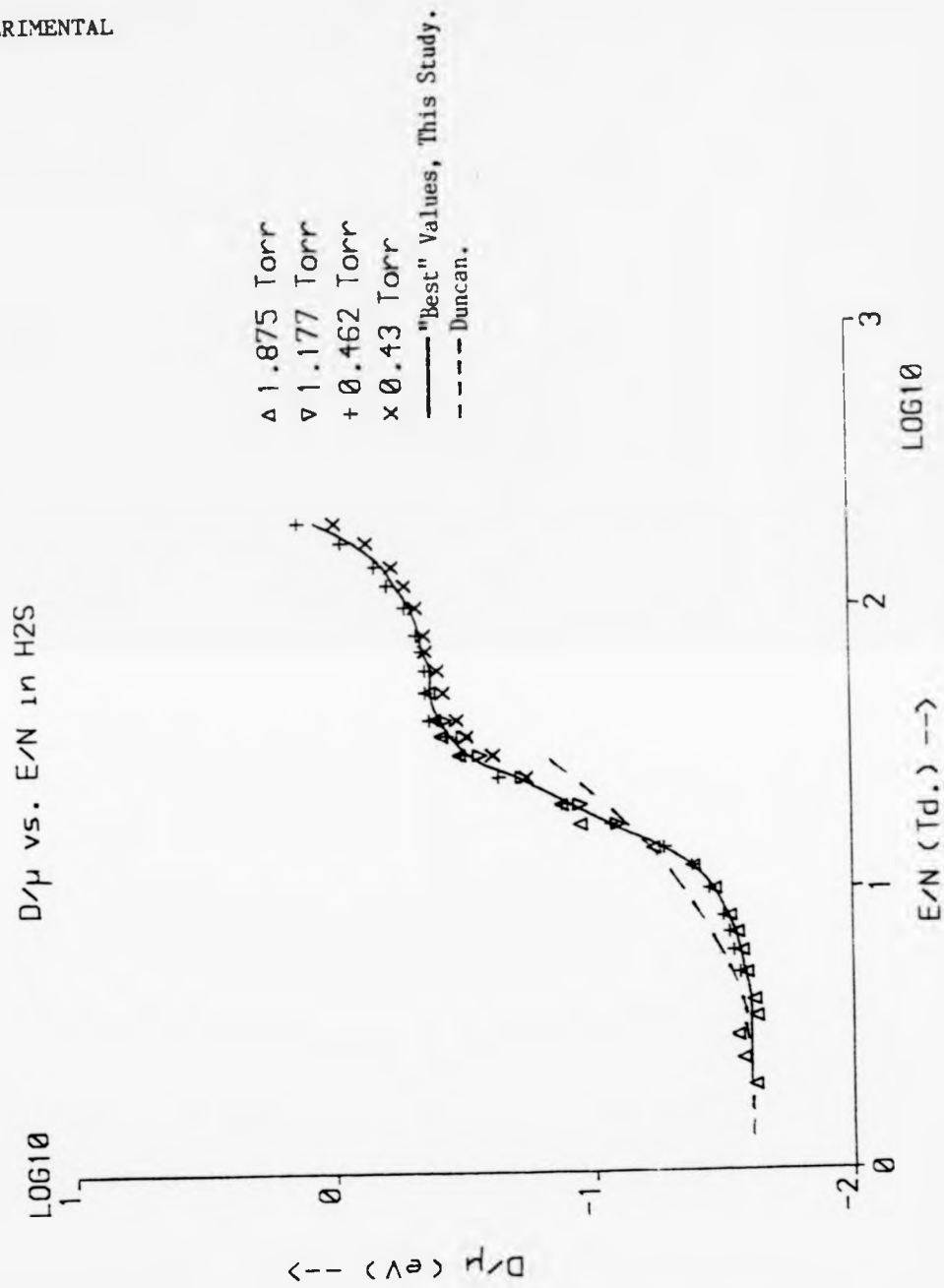
5. EXPERIMENTAL

Experimental Values of D/μ in Phosphine.

| Pressure (Torr) E/N (Td.) | 1.621 | 3.00 | 6.12 | 6.67 | "BEST" |
|------------------------------------|---------|---------|---------|---------|--------|
| 80 | 1.331 | | | | 1.33 |
| 70 | 1.310 | | | | 1.31 |
| 60 | 1.220 | 1.203 | | | 1.21 |
| 50 | 1.081 | 1.085 | | | 1.08 |
| 40 | 0.9017 | 0.8999 | | | 0.901 |
| 35 | 0.7898 | 0.7966 | | | 0.796 |
| 30 | 0.6673 | 0.6733 | 0.7546 | | 0.719 |
| 25 | 0.5298 | 0.5380 | 0.6042 | 0.6478 | 0.603 |
| 20 | 0.3813 | 0.3835 | 0.4414 | 0.4763 | 0.439 |
| 17 | 0.2869 | 0.2910 | 0.3378 | 0.3715 | 0.338 |
| 14 | 0.1947 | 0.1939 | 0.2489 | 0.2584 | 0.238 |
| 12 | 0.1375 | 0.1376 | 0.1765 | 0.1833 | 0.169 |
| 10 | 0.08927 | 0.08611 | 0.1082 | 0.1182 | 0.106 |
| 8 | 0.05351 | 0.05291 | 0.07303 | 0.08673 | 0.0653 |
| 7 | 0.04761 | 0.04240 | 0.04040 | 0.05091 | 0.0454 |
| 6 | 0.03977 | 0.03730 | 0.03751 | 0.04070 | 0.0370 |
| 5 | 0.03468 | 0.03272 | 0.03194 | 0.03094 | 0.0319 |
| 4 | 0.03100 | 0.02972 | 0.02873 | 0.02823 | 0.0289 |
| 3.5 | 0.02917 | 0.02727 | 0.02758 | 0.02738 | 0.0276 |
| 3 | 0.02806 | 0.02600 | 0.02532 | 0.02584 | 0.0259 |
| 2.5 | 0.02888 | 0.02631 | | 0.02508 | 0.0259 |
| 2 | 0.03158 | | | 0.02427 | 0.0257 |

T5.6. Measured Values of D/μ vs E/N in Phosphine.

5. EXPERIMENTAL



G5.6. Measured Values of D/μ vs E/N in Hydrogen Sulphide.

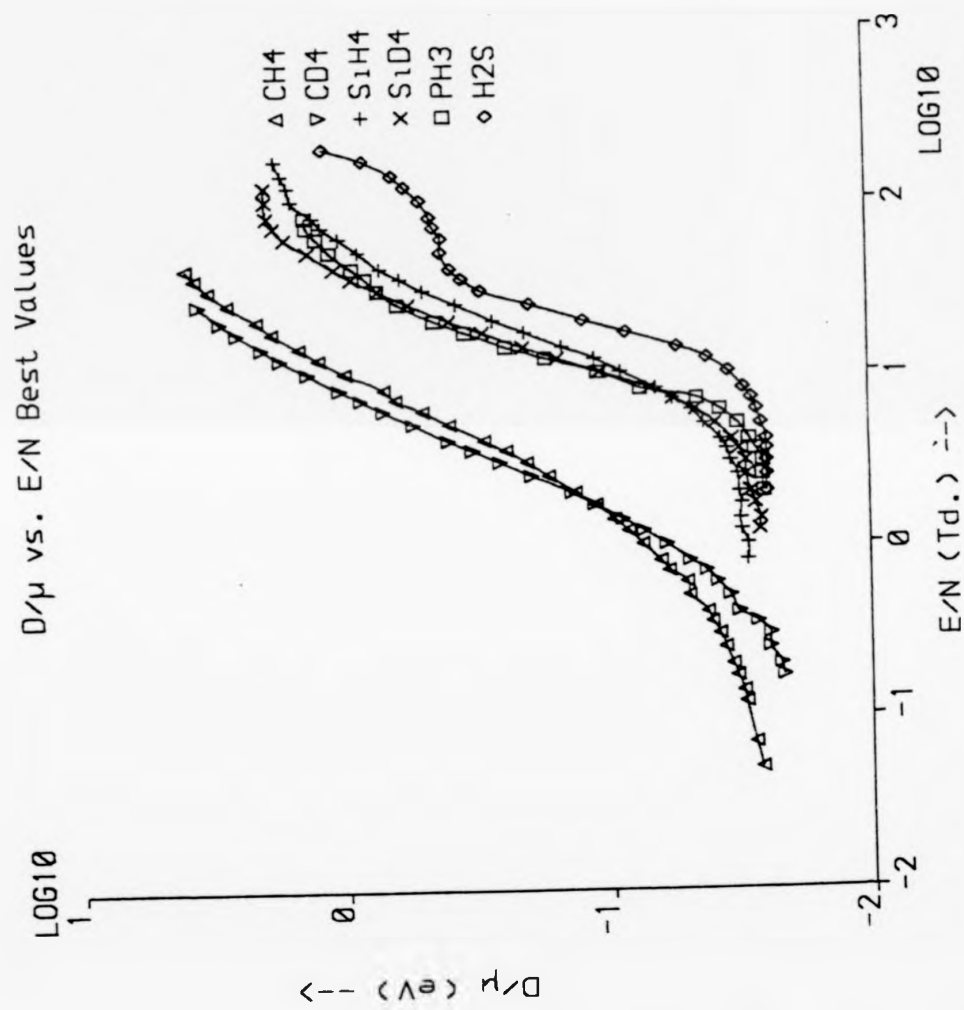
5. EXPERIMENTAL

Experimental Values of D/μ in Hydrogen Sulphide.

| Pressure (Torr) E/N (Td.) | 0.43 | 0.462 | 1.177 | 1.875 | "BEST" |
|------------------------------------|--------|---------|---------|---------|--------|
| 200 | 0.9540 | 1.305 | | | 1.14 |
| 170 | 0.7212 | 0.8998 | | | 0.814 |
| 140 | 0.5762 | 0.6705 | | | 0.625 |
| 120 | 0.5156 | 0.5980 | | | 0.558 |
| 100 | 0.4663 | 0.5152 | | | 0.492 |
| 80 | 0.4349 | 0.4651 | | | 0.451 |
| 70 | 0.4294 | 0.4449 | | | 0.437 |
| 60 | 0.3884 | 0.4295 | | | 0.410 |
| 50 | 0.3703 | 0.4284 | | 0.4179 | 0.412 |
| 40 | 0.3273 | 0.4155 | 0.3654 | 0.3961 | 0.382 |
| 35 | 0.3020 | 0.3577 | 0.3084 | 0.3768 | 0.346 |
| 30 | 0.2396 | 0.3163 | 0.2692 | 0.3212 | 0.296 |
| 25 | 0.1788 | 0.2284 | 0.1849 | | 0.193 |
| 20 | | 0.1307 | 0.1109 | 0.1317 | 0.120 |
| 17 | | 0.08497 | 0.07950 | 0.1109 | 0.0853 |
| 14 | | 0.05368 | | 0.05922 | 0.0541 |
| 12 | | 0.04185 | | 0.04133 | 0.0414 |
| 10 | | 0.03600 | | 0.03421 | 0.0346 |
| 8 | | 0.03166 | | 0.02999 | 0.0303 |
| 7 | | 0.02988 | | 0.02803 | 0.0284 |
| 6 | | 0.02904 | | 0.02608 | 0.0273 |
| 5 | | 0.02739 | | 0.02595 | 0.0262 |

T5.7. Measured Values of D/μ vs E/N in Hydrogen Sulphide.

5. EXPERIMENTAL



G5.7. Comparison of Measured Values of D/μ vs E/N .

5. EXPERIMENTAL

5.4/. Discussion of Errors.

5.4(a). Error in E/N.

The measurable quantities here are the applied voltage, the field distance and the gas temperature and pressure. The voltage from a Fluke 412B has a stated accuracy of 0.25% and is applied over matched 200k resistors and a measured distance of 10.073 cm. The resultant field is thought to be uniform and accurate to within 0.5%. Three mutually perpendicular Helmholtz coils are used to cancel the effect of the Earth's magnetic field, and the accuracy of the cancellation is always less than 0.1% of the applied field. The gas pressure is measurable to within 0.1 torr using the mercury manometer (10 - 1000 torr) and to within 0.01 torr using the oil manometer (0.4 - 20 torr), resulting in errors no greater than 3%. The gas temperature is measurable to 1 K using a thermocouple. This produces an error of 0.3% in E/N at 293 K. The resultant random error in the determination of E/N is at its largest at low pressures, and is nowhere greater than 3%. At low E/N the error is less than 1%. As far as we are aware, there are no significant systematic errors in the determination of E/N, however, it should be noted that a random error in pressure measurement results in a systematic displacement of all results at that pressure along the E/N axis.

5. EXPERIMENTAL

5.4(b). Error in D/μ .

Measurable quantities this time are those outlined in E1.4.. The field strength error is discussed above, the distances d and h are reported in T5.1. Errors in their measurement produce a maximum error in D/μ of 1% (largest for mode 1, smallest for mode 3). The largest error comes from the measurement of current ratios, and may produce an error in D/μ as large as 10% at low photocurrents (low E/N). As measurements are made at more than one pressure, the values can be averaged and a best value taken. This does not reduce the error, but gives confidence that the final value is close to the mean of all values. At high photocurrents, the error from this source is negligible.

5.5/. Discussion of Experimental Results.

For methane, the agreement with previous measurements is good. Only those of Cochran and Forrester have been represented on the graph as the other measurements (Cottrell and Walker, 1967, and Duncan and Walker, 1972) are so close as to be indistinguishable on the graph. The present study does extend the range of the other studies significantly at high values of E/N . For perdeuteromethane, the agreement is again very close, the previous results (Cottrell and Walker, 1967) being in agreement with the present to within experimental error. Where any differences are seen, the present results give slightly higher values of D/μ at a given E/N . The present study extends the range of data at high E/N .

5. EXPERIMENTAL

In silane the present results lie just below previous results (Cottrell and Walker, 1967). Over most of the range the difference is greater than that expected from experimental error, although the previous results converge well with the readings reported here for 1.22 torr. A similar situation is seen with the results for perdeuteriosilane where the present results are always lower than in the previous study and the previous measurements converge well with the new measurements made at low pressures.

No measurements of D/μ as a function of E/N in phosphine other than the present study are known. The fit of the Hydrogen Sulphide data with the previous study (Duncan, 1971) is very poor. Emission from the photocathode in this gas is very poor, leading to the measurements being made at low gas densities. It is thought that with the data logging system now used leading to better monitoring of small currents, the present data is the more reliable of the two sets.

In comparing all the values (G5.7), it can be seen that in both cases where a hydride can be compared with the corresponding deuteride, the values of D/μ in the latter start off low, but then overtake the values for the hydride. Further, the energy of the electron swarm is always much less at a given E/N in the gases with the most massive central atom.

6. RESULTS OF ANALYSIS AND DISCUSSION

CHAPTER 6.

RESULTS OF ANALYSIS AND DISCUSSION.

6.1/. INTRODUCTION.

In practice, the accurate matching of cross sections with experimental data using the Monte Carlo method was found to be time consuming. The refinement of cross sections can be done automatically (as with the present Boltzmann analysis programme) using effective cross sections (Crompton *et al.*, 1969). However, as the calculated transport coefficients approach the measured ones, the cross section adjustments become very minor, and the major amount of computer time is used on increasing the number of collisions suffered by the electron. The refinement of cross sections for the Monte Carlo code was therefore left as a manual adjustment. This allows easier inclusion of features known from beam experiments and finer sculpting around regions in which the transport coefficients are sensitive to change. Because of the time required to achieve statistically reliable data over a range of energies, only methane has been given a full quantitative Monte Carlo treatment. Perdeuteromethane was analysed using the final methane Monte Carlo cross sections, with the magnitude of the inelastic cross sections being multiplied by the square root of two. Further refinement of these cross sections is still being

6. RESULTS OF ANALYSIS AND DISCUSSION

carried out. The other gases are analysed using the two term Boltzmann analysis. All of the cross section data presented graphically in the following sections appears in tabular form, alongside calculated (Monte Carlo) transport coefficients, at the end of the chapter.

6.2/. Methane.

6.2(a). Experimental Data.

The experimental data used for methane are the D/μ values reported in Chapter 5 and the drift velocity data of Crompton (1982). The latter was reported over a range of E/N between 0.046 and 1.98 Townsend. This restricts the wider range (0.04 - 40 Td.) of D/μ data, but still allows good coverage of the energy region below the onset of electronic excitation. Both sets of data show good agreement with previous studies.

6.2(b). Choice of Cross Sections.

The molecules of the type XY_4 studied here all have nine normal vibrational modes. Degeneracy reduces these to four fundamental frequencies (Herzberg, 1945). In methane, these frequencies are:

| | | | |
|---------|-----------------------|------------|--------------------|
| ν_4 | 1306 cm^{-1} | (0.162 eV) | asymmetric bend |
| ν_2 | 1526 cm^{-1} | (0.189 eV) | symmetric bend |
| ν_1 | 2914 cm^{-1} | (0.361 eV) | symmetric stretch |
| ν_3 | 3020 cm^{-1} | (0.374 eV) | asymmetric stretch |

6. RESULTS OF ANALYSIS AND DISCUSSION

The Monte Carlo and Boltzmann techniques are able to distinguish contributions from elastic and inelastic processes, but the complexity of the analysis and the difficulty of refinement both increase with the number of independent variables (cross sections) affecting macroscopic properties (transport coefficients). For this reason, a compromise must be struck between computational complexity and physical reality with regard to the number of inelastic processes used.

If we recall that swarm techniques are rather a blunt tool for probing collision processes, it becomes apparent that the separation of effects due to excitation of closely spaced onsets is difficult. Further, evidence from theory (Claydon *et al.*, 1970) and from beam studies (Stamatovic and Schulz, 1969) suggests that the strongest electron - molecule interaction for targets of this type will be through transient dipoles. This implies that the highest contribution will come from the infrared active modes, the asymmetric bend and stretch. However, if the excitation is resonance enhanced, the symmetry of the vibrational excitation which occurs must match the symmetry of the resonance. Thus a resonance of A_1 symmetry could lead to excitation of the ν_1 (symmetric stretch (a_1 symmetry)) mode only. However, from early explorations of the cross sections, it was apparent that the fit of measured with calculated transport coefficients was always very poor unless either the lowest energy (ν_2 (e symmetry)) mode or the

6. RESULTS OF ANALYSIS AND DISCUSSION

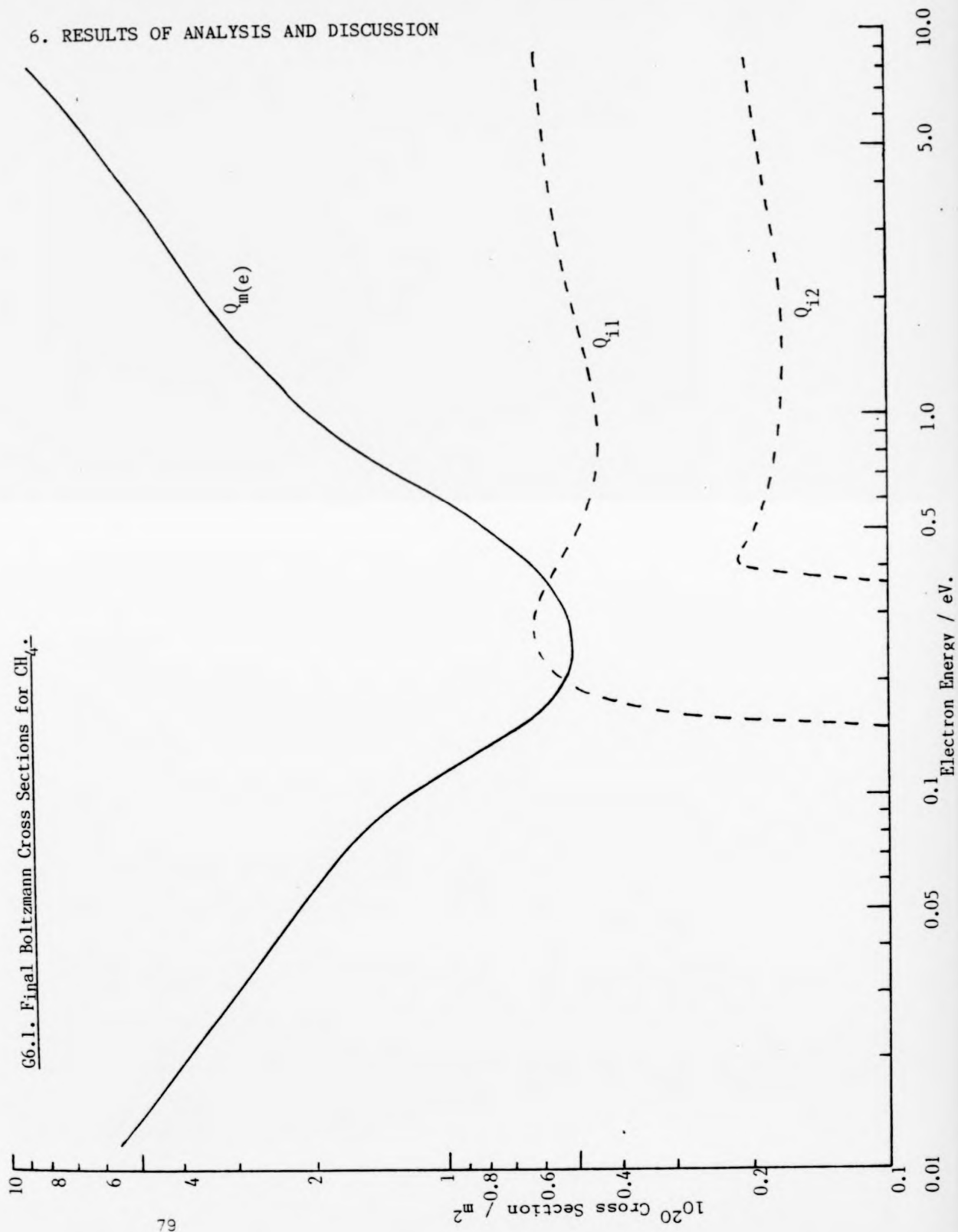
v_4 (t_2 symmetry) was included. The present work confirms this as a probable excitation mechanism. The grouping of the onsets into two pairs makes it convenient to choose the second process from one of the pair at higher energy. For these reasons two vibrational cross sections were used for both the Boltzmann and the Monte Carlo analysis, having onsets of 0.162 and 0.361 eV.

6.2(c). Boltzmann Analysis.

The cross sections produced by the Boltzmann analysis for methane are presented on G6.1, and the fit of the transport coefficients using the two term analysis on these cross sections is shown in G6.3, and G6.4. The cross sections were produced after 200 iterations of the refinement, from starting cross sections which were energy independent. (The momentum transfer was started at a constant $5 \cdot 10^{-20} \text{ m}^2$, and the two inelastics started as box cross sections of equal size $1 \cdot 10^{-20} \text{ m}^2$). The refined cross sections are similar to an earlier two term analysis (Duncan and Walker, 1972). The vibrational excitation of the asymmetric bend mode shows a steeper onset in the present analysis, but otherwise the results are in close agreement. The elastic cross section reaches a minimum of $0.4 \cdot 10^{-20} \text{ m}^2$ at 0.25 eV, which is smaller both in magnitude and energy than Ramsauer's original (total cross section) measurements indicated. Recall that it is in the region of the minimum in the elastic cross section, and the onset of inelastic processes, that the two term analysis is thought to be suspect. An insight into the

6. RESULTS OF ANALYSIS AND DISCUSSION

G6.1.1. Final Boltzmann Cross Sections for CH_4^-



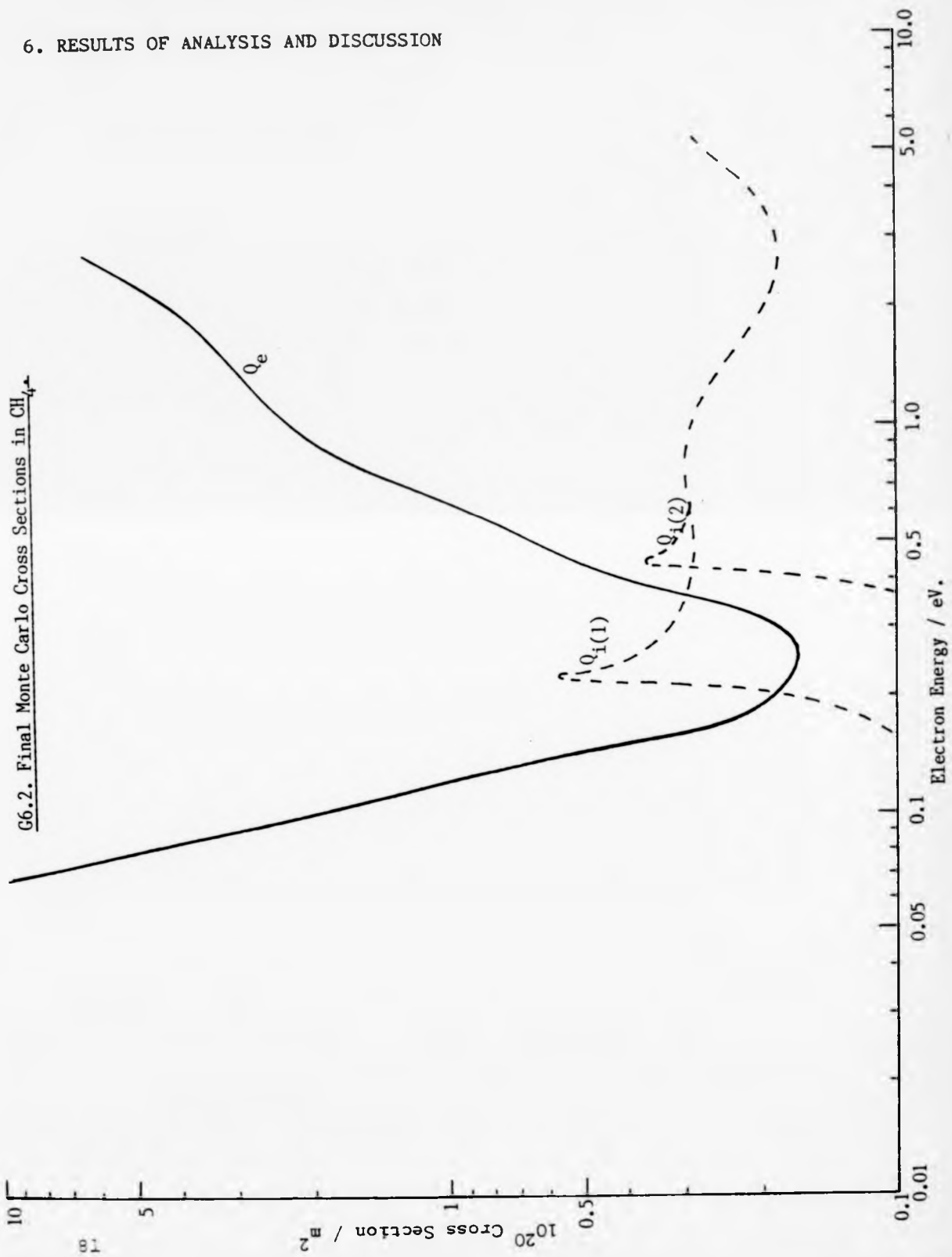
6. RESULTS OF ANALYSIS AND DISCUSSION

extent of the discrepancy between the two term approximation and the real situation may be provided by the Monte Carlo technique.

6.2(e). Monte Carlo Analysis.

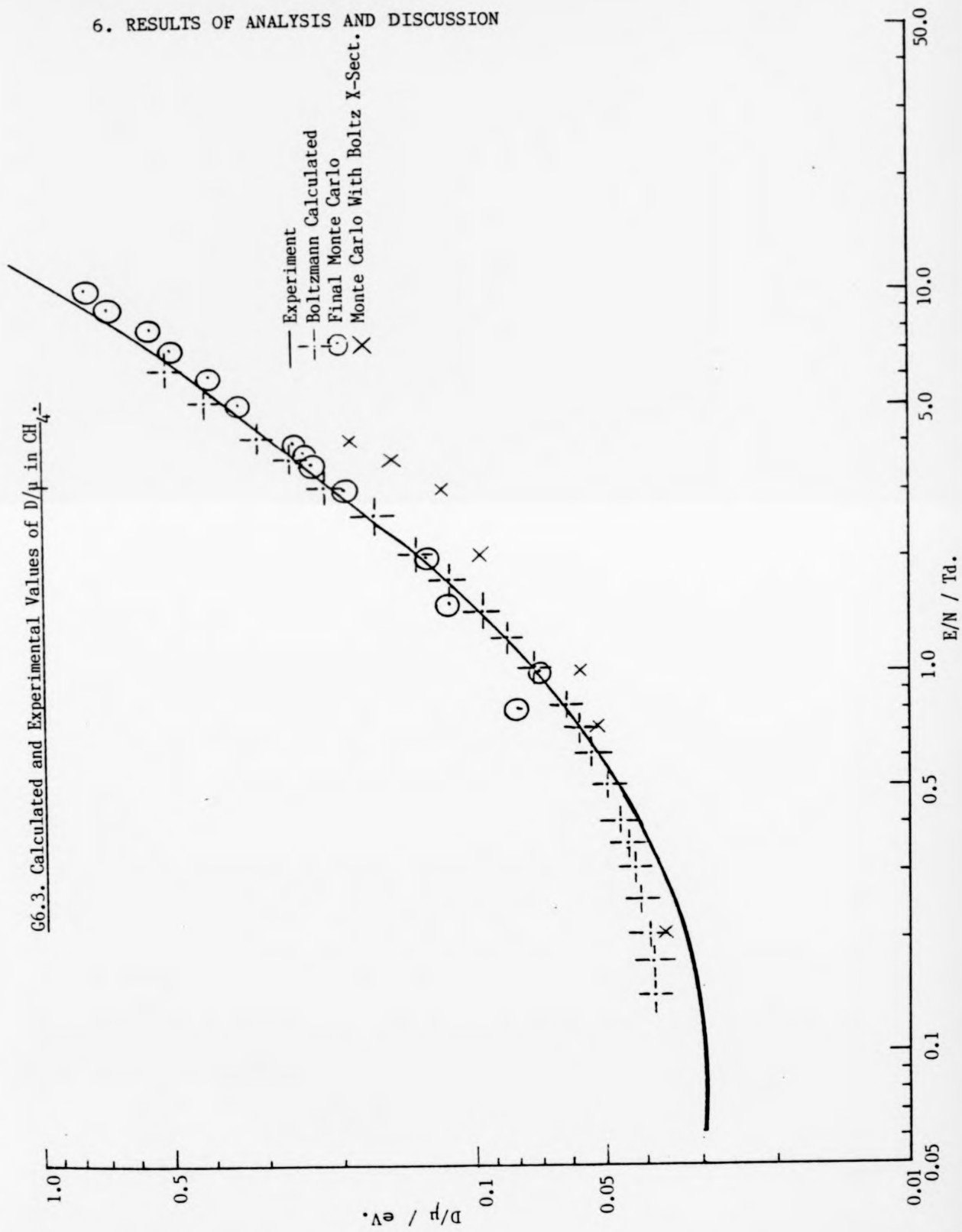
The refined Monte Carlo cross sections are presented in G6.2, and the fit of the calculated transport data with both experiment and the two term analysis is shown in G6.3, and G6.4. As a comparison of the Boltzmann and Monte Carlo approaches, the transport data calculated by the Monte Carlo method, using the Boltzmann cross sections are included in the graphs G6.3 and G6.4. It can be seen that the fit is very poor, indicating that a great deal of refinement to the Boltzmann cross sections is needed to produce an acceptable fit using Monte Carlo. The refinement process uses the effective cross sections technique of Crompton et al, (1969). The method used was to retain all the features of the Boltzmann cross sections which have been established as reliable, and to attempt to fit the data by changing those sections known to be suspect (regions of high inelastic contributions). By varying the cross sections around the region of the minimum in the momentum transfer cross section, it became apparent that the factors which most greatly affected the fit of the data were the energy position and magnitude of the minimum, and the shape of the onset of the first inelastic process. The sensitivity of the drift velocity, in the region of its maximum, to changes in the vibrational cross sections at onset was initially a difficulty. Very small changes in

6. RESULTS OF ANALYSIS AND DISCUSSION

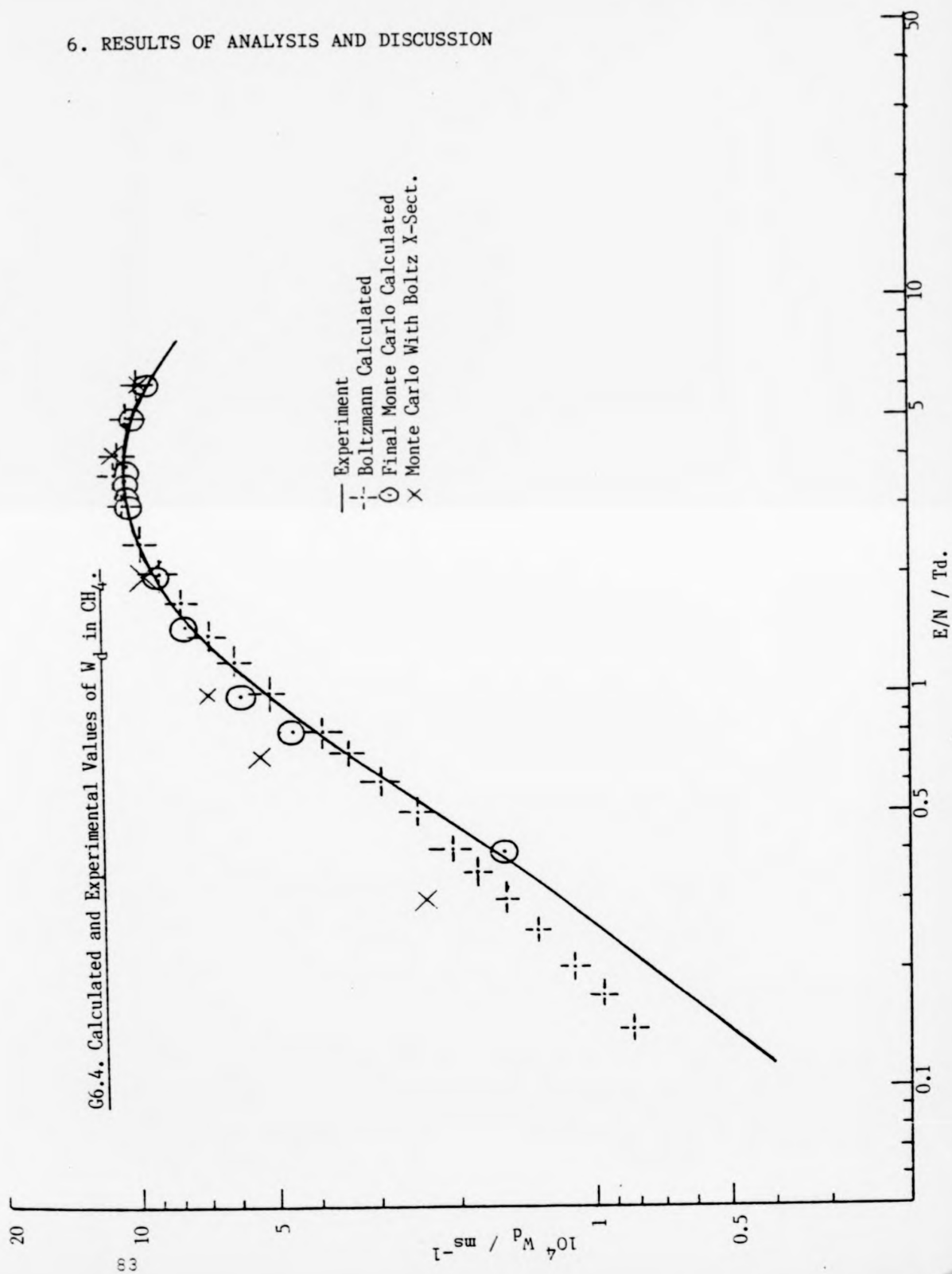


6. RESULTS OF ANALYSIS AND DISCUSSION

G6.3. Calculated and Experimental Values of D/μ in CH_4 .



6. RESULTS OF ANALYSIS AND DISCUSSION



6. RESULTS OF ANALYSIS AND DISCUSSION

cross sections gave large variations in the drift velocity. Eventually this sensitivity was a useful indicator as to those features of the cross section which appeared necessary to achieve a suitable fit, and those which did not. The 'desirable' cross section properties are firstly, a peaked onset to vibrational excitation followed by a decrease, and secondly a very deep minimum ($0.17 \cdot 10^{20} \text{ m}^2$ at 0.25 eV.) in the elastic cross section preceded by a very sharp energy dependence. Using the refined Monte Carlo cross sections the fit of calculated with experimental transport coefficients is very good for both D/μ and W_d .

The observation of peaks at the onset of vibrational excitation in methane has been noted before in swarm work (Pollock, 1968, Duncan and Walker, 1972), and the present work supports these findings. More recently, beam studies (Rohr, 1980) have shown the presence of peaks, and even some structure in the peaks, implying a long lived (i.e. on the vibrational period time-scale) electron - molecule complex. The present work appears to reinforce these conclusions in that, if the peaks are removed from the onsets, no other changes to the cross sections can be made which give such good agreement of calculated and experimental transport coefficients. Beyond onset, the vibrational cross sections fall, as they do in the two term analysis, implying that the two approaches are consistent. This observation suggests that single mode excitation is predominant, giving further credence to the criteria used in selecting which inelastic processes would be considered.

6. RESULTS OF ANALYSIS AND DISCUSSION

The very deep minimum in the elastic cross section has not been observed through swarm work before. Recent beam studies (Barbarito *et al.*, 1979, Rohr, 1980, Sohn *et al.*, 1983) have shown that the cross section is smaller than previously thought, the most recent giving a value of $0.17 \cdot 10^{-20} \text{ m}^2$ at 0.18 eV (c.f. $0.17 \cdot 10^{-20} \text{ m}^2$ at 0.25 eV, this study). The absolute value of the cross section at the minimum is of considerable interest to those exploring the theory of the collision process. The small value relative to the competing inelastic process implies a very efficient vibrational excitation channel for electrons of this particular energy. The other feature of interest on the elastic cross section is the very sharp energy dependence of the cross section below the minimum. This has not yet been investigated by beam techniques. It is suspected that this dependence is a consequence of over extending the Monte Carlo model to energies below that of the thermal swarm. A full investigation of the swarm behaviour at such low energies must include an experimental determination of transport parameters at low temperature. These final cross sections may not be fully reliable at energies below 0.1 eV.

6.3/. Perdeuteromethane.

6.3(a). Experimental Data.

The experimental data used are the D/μ values reported in

6. RESULTS OF ANALYSIS AND DISCUSSION

Chapter 5, and the drift velocity data of Pollock (1968). No beam studies have yet been performed in perdeuteromethane.

6.3(b). Choice of Cross Sections.

The choice of cross sections in this gas was influenced by the same considerations as in methane (6.2(b)). Two different sets of cross sections were used in the analysis, one for the Boltzmann, and another for the Monte Carlo. Due to the difficulty in distinguishing effects from competing inelastic processes and the arbitrary nature of any relationship assumed between such processes, it was decided that the vibrational excitation for this gas would be represented by a single inelastic cross section for the two term analysis. The onset for this process was chosen to be the lowest energy infrared active mode (asymmetric bend) at 0.1234 eV (1002 cm^{-1}). Any contributions from higher energy processes should show up as humps in this single cross section. For the Monte Carlo simulation, only an initial guess at the cross sections was used. Work on the refinement of this initial guess has been initiated. The cross sections used were similar to the refined (Monte Carlo) methane cross sections, but with the magnitude of the vibrational contribution multiplied by the square root of two (this being the ratio of the vibrational frequencies for the two gases), and the onsets changed to 0.123 and 0.2585 eV, corresponding to the infrared active modes used in methane.

6. RESULTS OF ANALYSIS AND DISCUSSION

6.3(c). Boltzmann Analysis.

The cross sections produced by the Boltzmann analysis are presented on G6.5, and in T6.7. The fit of the transport coefficients using the two term analysis on these cross sections is shown in G6.6, and G6.7, and in T6.2. The analysis was allowed to go through 200 iterations of the refinement procedure, starting from cross sections similar to those outlined for methane. The differences were the use of only one inelastic process and the value of the onset energy of that process.

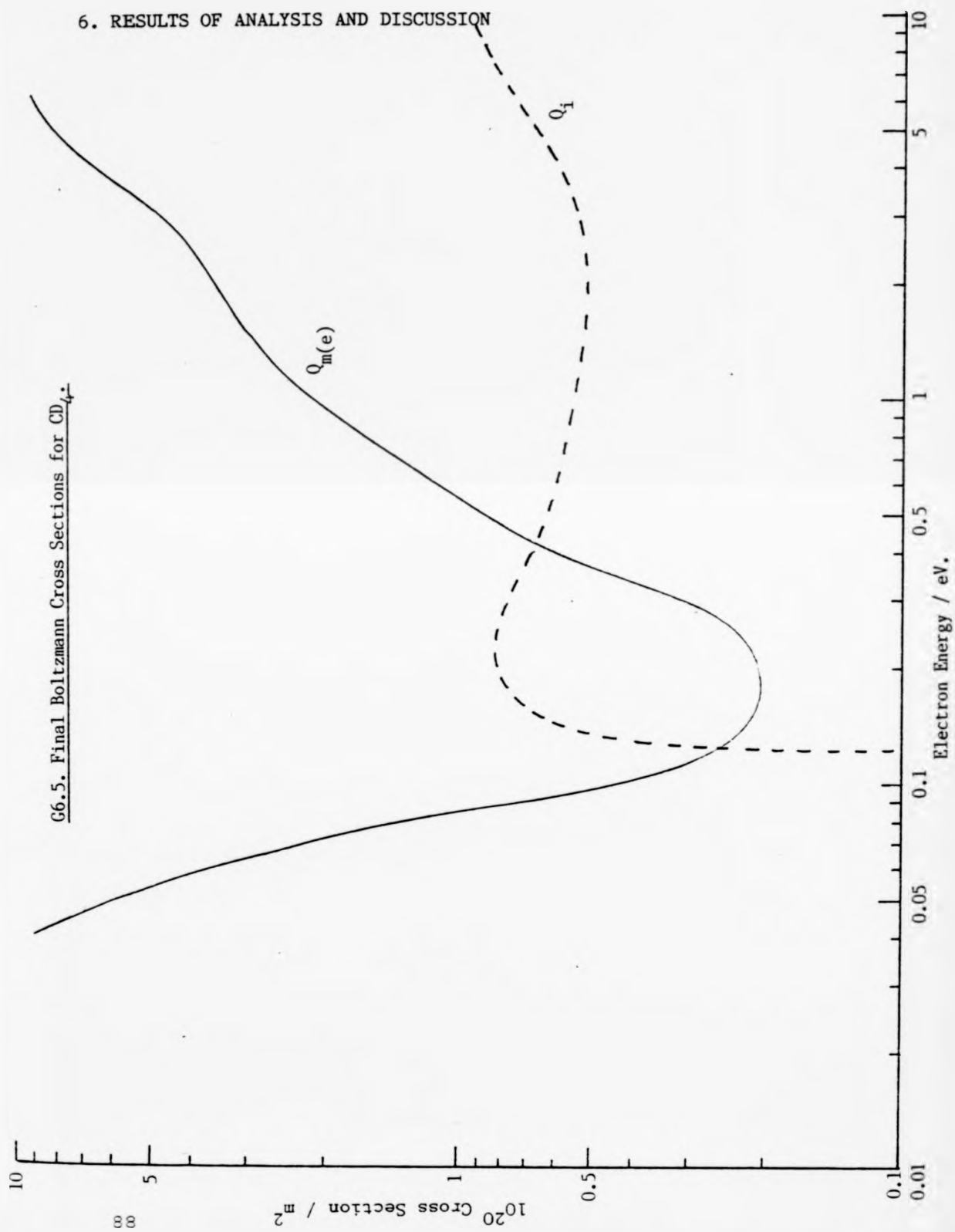
The most striking feature of the elastic cross section is the minimum ($0.21 \cdot 10^{-20} \text{ m}^2$ at 0.17 eV). This is much deeper than the minimum produced by the two term analysis in methane. If we can interpolate the data for the two gases, this implies that the Monte Carlo model will require a still deeper minimum. If verified, this will indicate that the channel for vibrational excitation by electrons of this energy is even more efficient in the perdeutero compound. The inelastic cross section shows a steep onset as in methane, followed by a slow decay, and then an increase which is probably due to the onset of higher inelastic processes.

6.3(d). Monte Carlo Analysis.

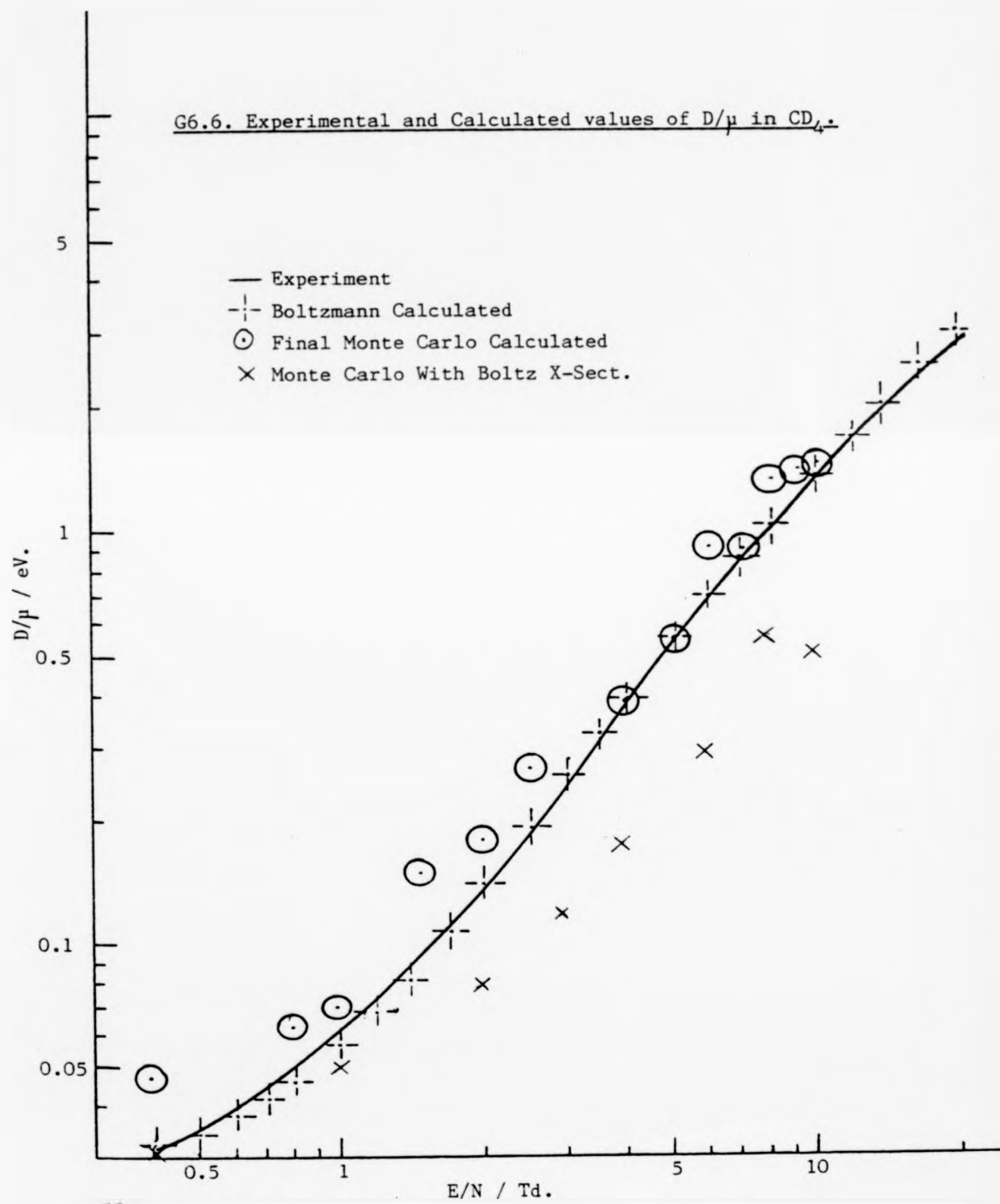
The cross sections used in this simulation are described in 6.3(a), and the fit with experimental data is shown in G6.6 and G6.7, and in T6.2.

6. RESULTS OF ANALYSIS AND DISCUSSION

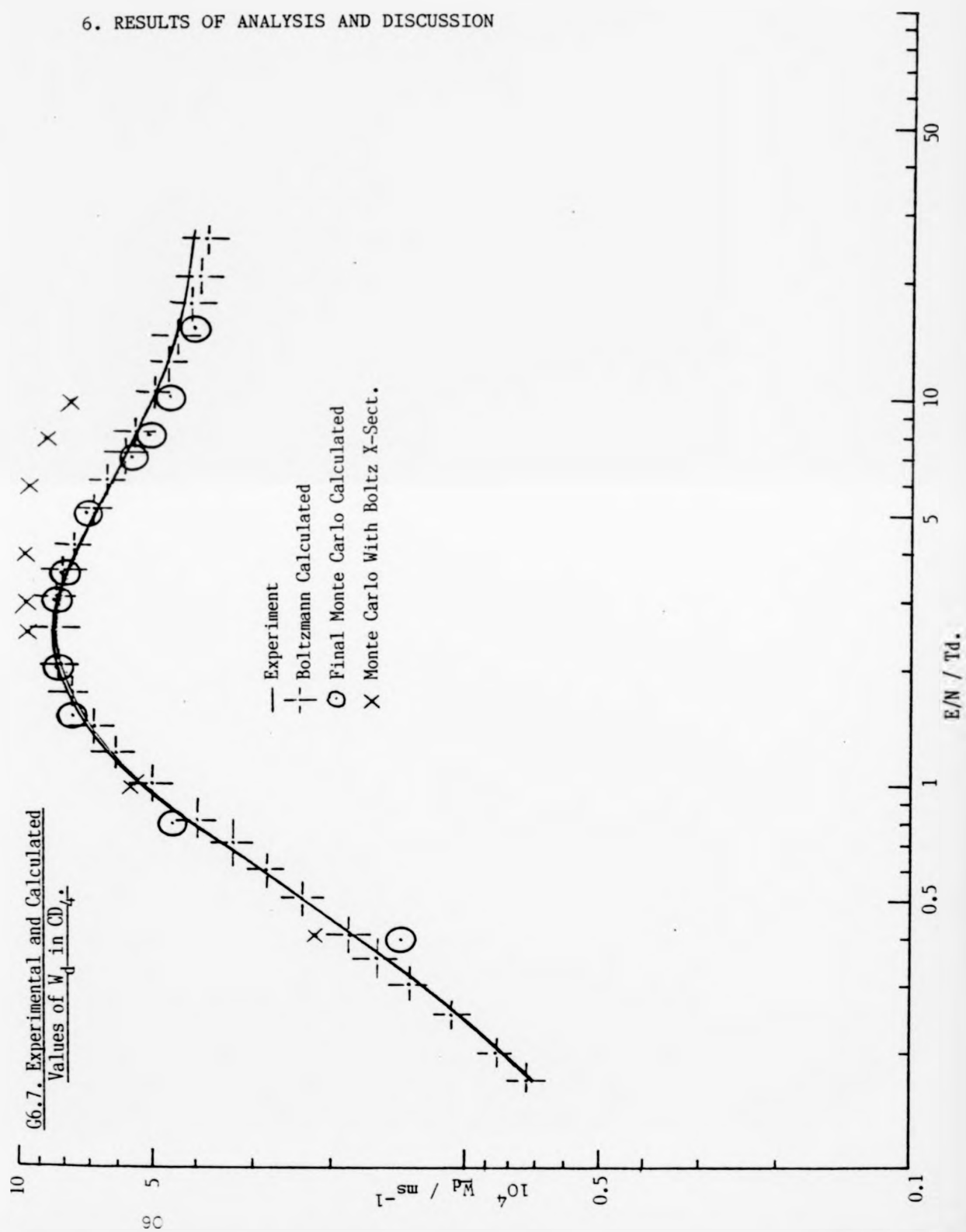
G6.5. Final Boltzmann Cross Sections for CD_4 .



6. RESULTS OF ANALYSIS AND DISCUSSION



6. RESULTS OF ANALYSIS AND DISCUSSION



6. RESULTS OF ANALYSIS AND DISCUSSION

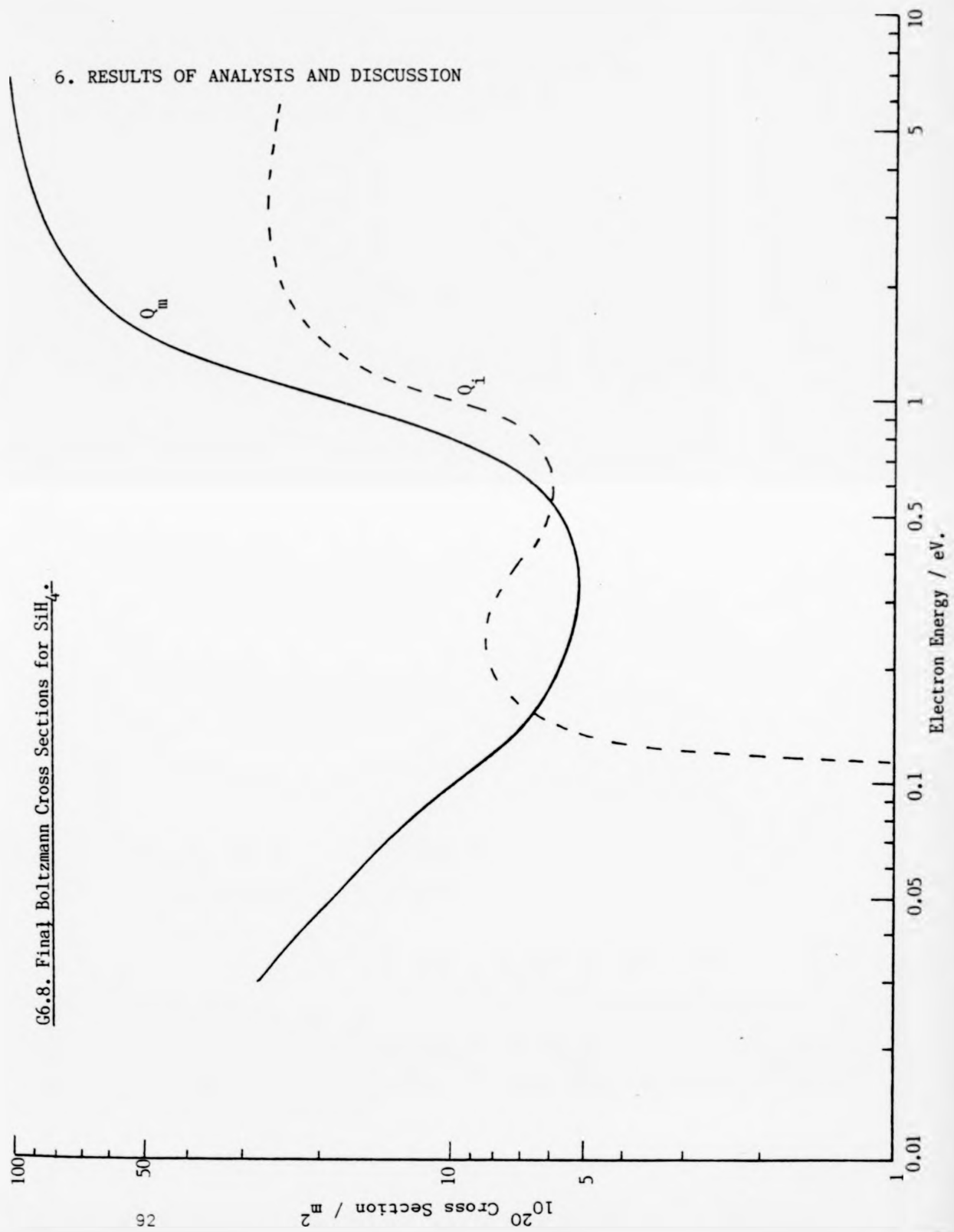
The fit is poor, especially for D/μ , the low energy values of which lie above the experimental data. For the Monte Carlo model ($T_g = 0$ K) the thermal energy of the swarm should always be below the room temperature thermal energy of the gas. It is encouraging that the drift velocity values show good agreement, particularly in the region of the maximum. The scatter of the data, particularly for D/μ shows one of the greatest difficulties of implementing a Monte Carlo simulation. To get a rough idea of the data fit one uses few electron collisions which leads to large amounts of scatter in the results. As the fit is improved, so must be the resolution of the analysis, so larger numbers of collisions are used. This slows down the process a great deal. Due to the length of time needed to refine cross sections, no further refinement was attempted for this work, although the refinement is to be continued using the techniques outlined previously.

6.4/. Silane.

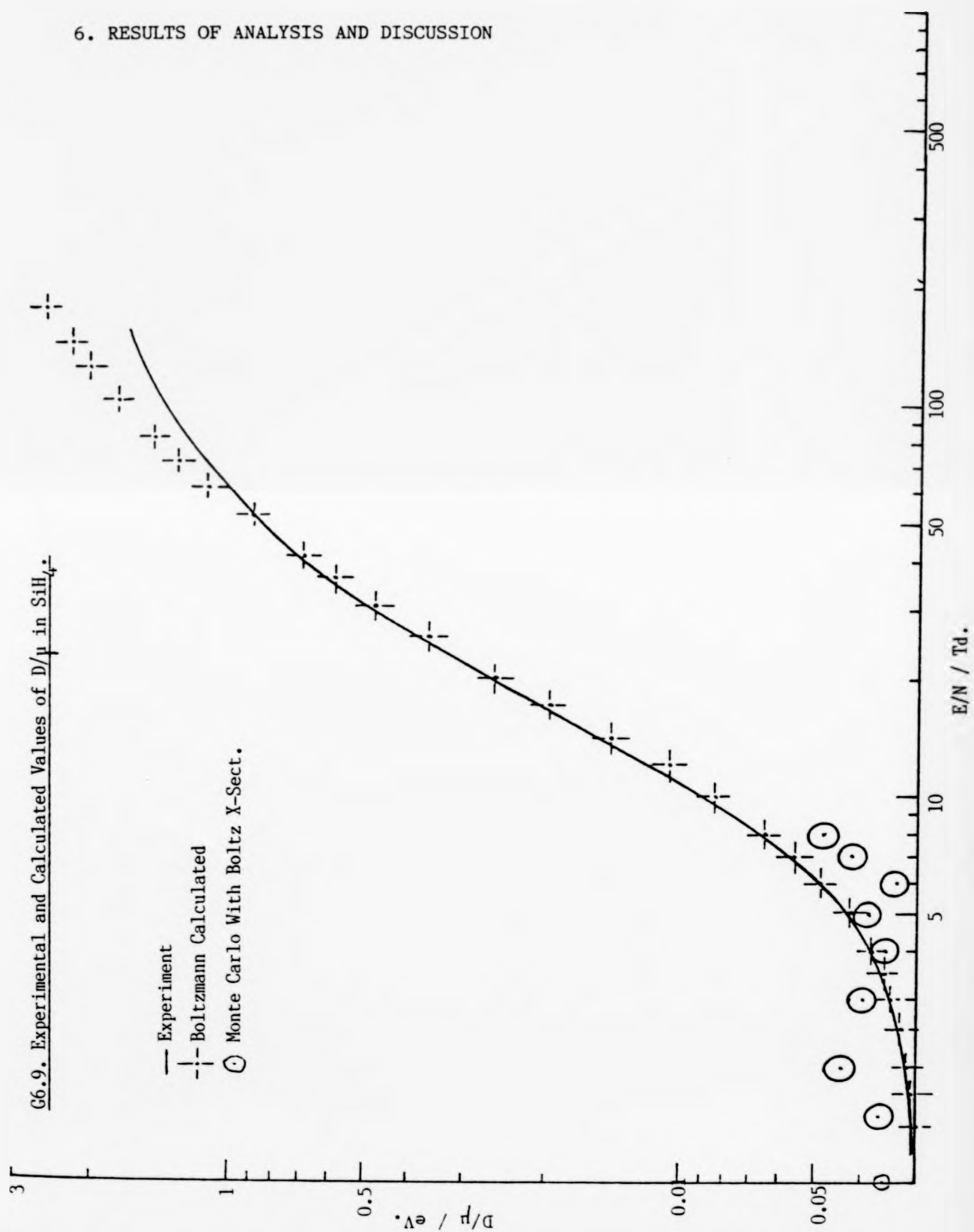
6.4(a). Experimental Data.

The experimental data used are the D/μ values reported in Chapter 5 and the drift velocity data of Pollock (1968). Pollock also used a two term analysis to deduce cross sections in this gas. No beam studies have yet been reported.

G6.8. Final Boltzmann Cross Sections for SiH_4^+

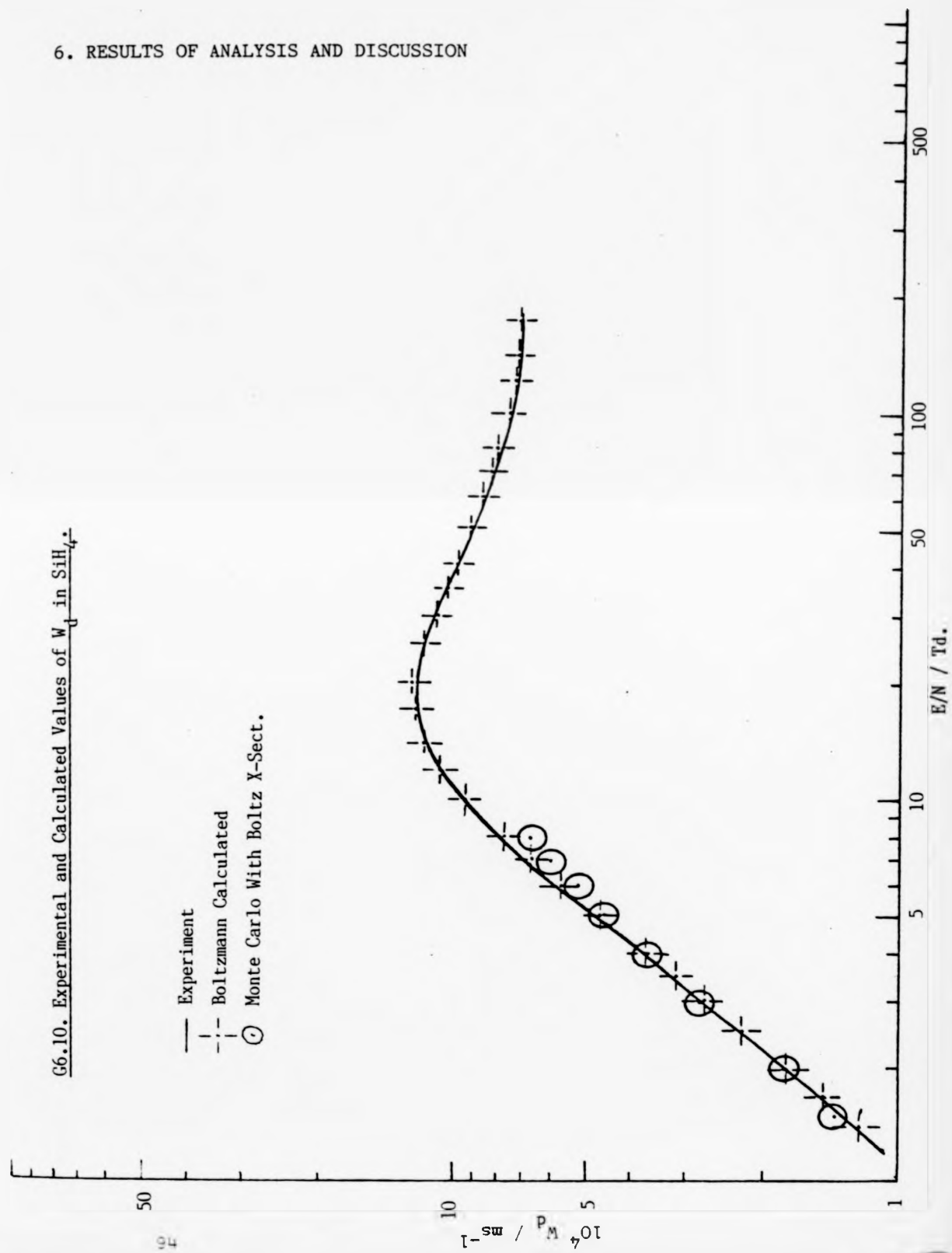


6. RESULTS OF ANALYSIS AND DISCUSSION



6. RESULTS OF ANALYSIS AND DISCUSSION

G6.10. Experimental and Calculated Values of W_d in SiH_4 .



6. RESULTS OF ANALYSIS AND DISCUSSION

6.4(b). Choice of Cross Sections.

One set of cross sections was used, as no attempt was made to refine the Monte Carlo model, and no useful starting cross sections were available. The choice was influenced by the same factors that influenced the choice in methane (6.2(b).), and limited to one inelastic process for the reasons outlined for perdeuteromethane (6.3(b).). The onset for the single inelastic process was chosen as 0.120 eV (968 cm^{-1}), the asymmetric bend energy.

6.4(c). Boltzmann Analysis.

The cross sections produced by the Boltzmann analysis are represented in G6.8 and in T6.8. The fit of calculated and experimental data is shown in G6.9 and G6.10, and in T6.3. The analysis was allowed to go through 22 iterations of the refinement procedure, starting from cross sections similar to those used for perdeuteromethane (6.3(b).), but with the magnitudes increased by a factor of five, and inelastic onset as outlined above. The output cross section shows gross differences from the earlier analysis by Pollock, and some inconsistencies with physical reality. In comparison with the the earlier analysis, the inelastic cross section shows a similar sharp onset and peak of $9 \cdot 10^{-20} \text{ m}^2$ at 0.3 eV. Beyond the initial decay it rises steeply indicating a large inelastic process at higher energy. This was not observed in the previous analysis. Further, the momentum transfer cross section falls below the inelastic cross section over a limited energy

6. RESULTS OF ANALYSIS AND DISCUSSION

range. This is clearly unrealistic, and is an indication of the difficulty involved in fitting the observed data using this analysis. The data fit achieved is good except for D/μ at high values of E/N , where the calculated results are consistently too large.

6.4(d). Monte Carlo.

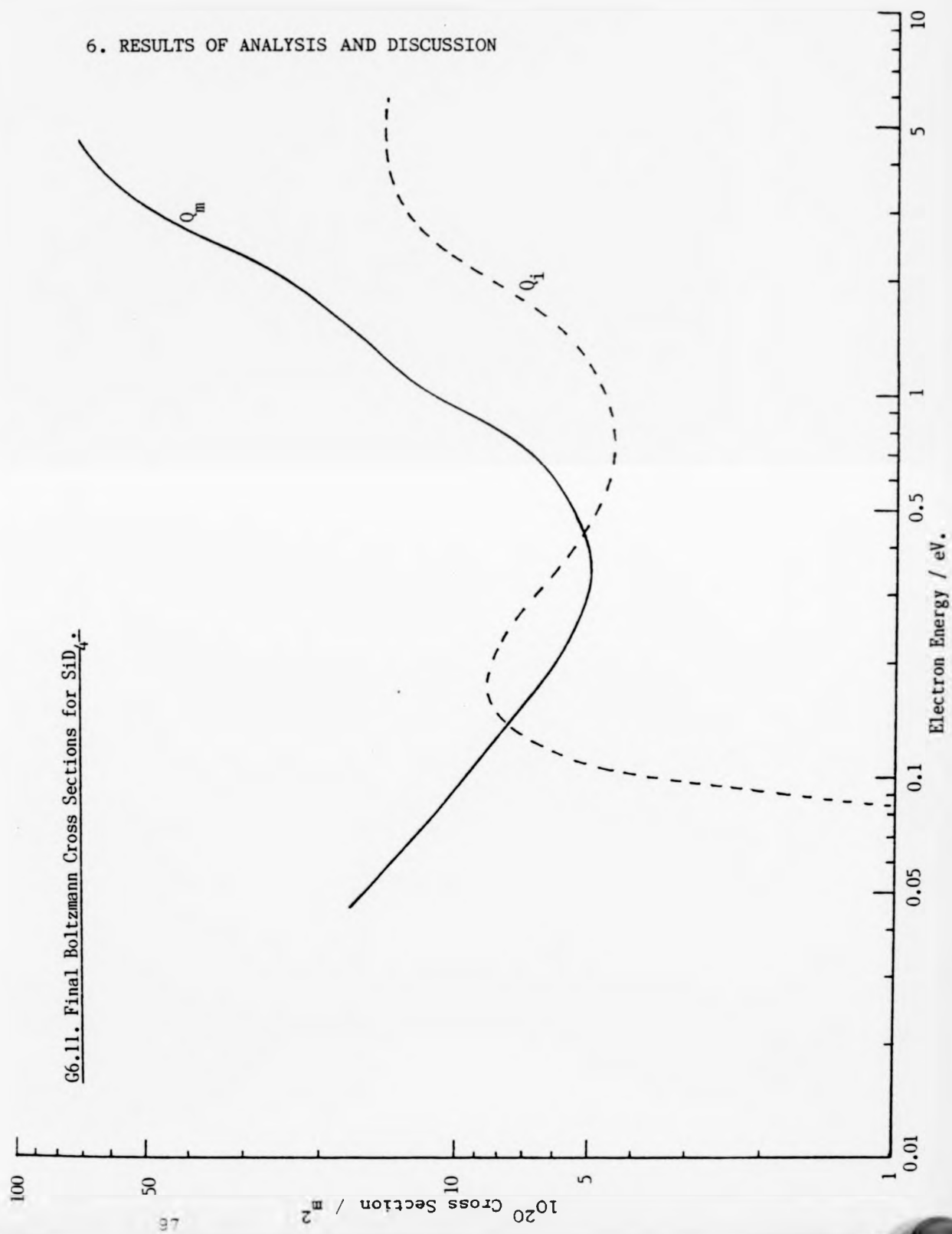
The cross sections produced by the two term analysis (modified to avoid negative elastic contributions) were used as starter cross sections for a Monte Carlo study. The data fit was very poor (G6.9, G6.10, T6.3) and no refinement was attempted.

6.5/. Perdeuterosilane.

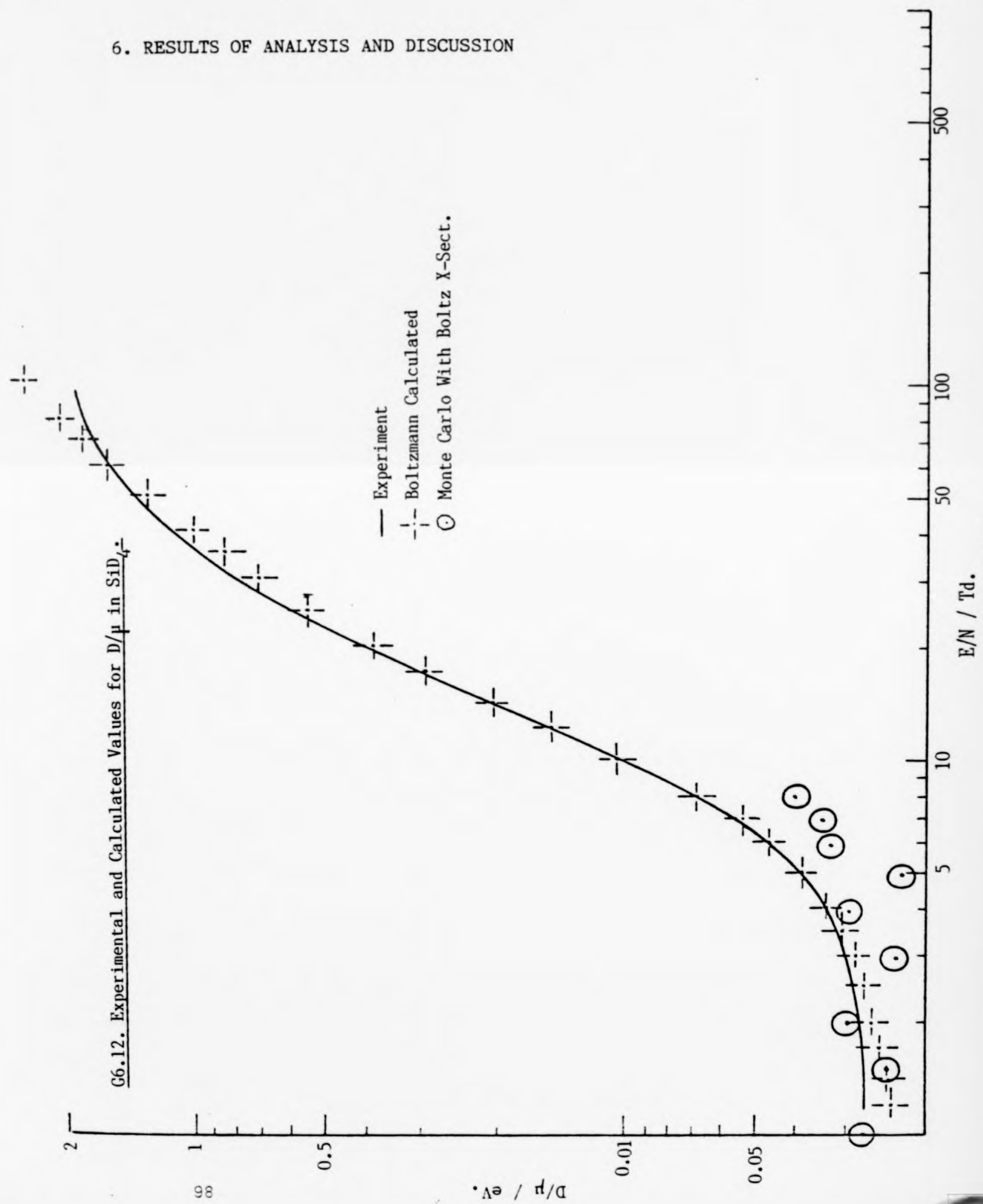
6.5(a). Preliminary Information.

The experimental data used are the D/μ values reported in Chapter 5 and the drift velocity data of Pollock (1968). No cross sections have been derived for this gas previously, and no beam studies reported. One inelastic process with onset 0.100 eV was used.

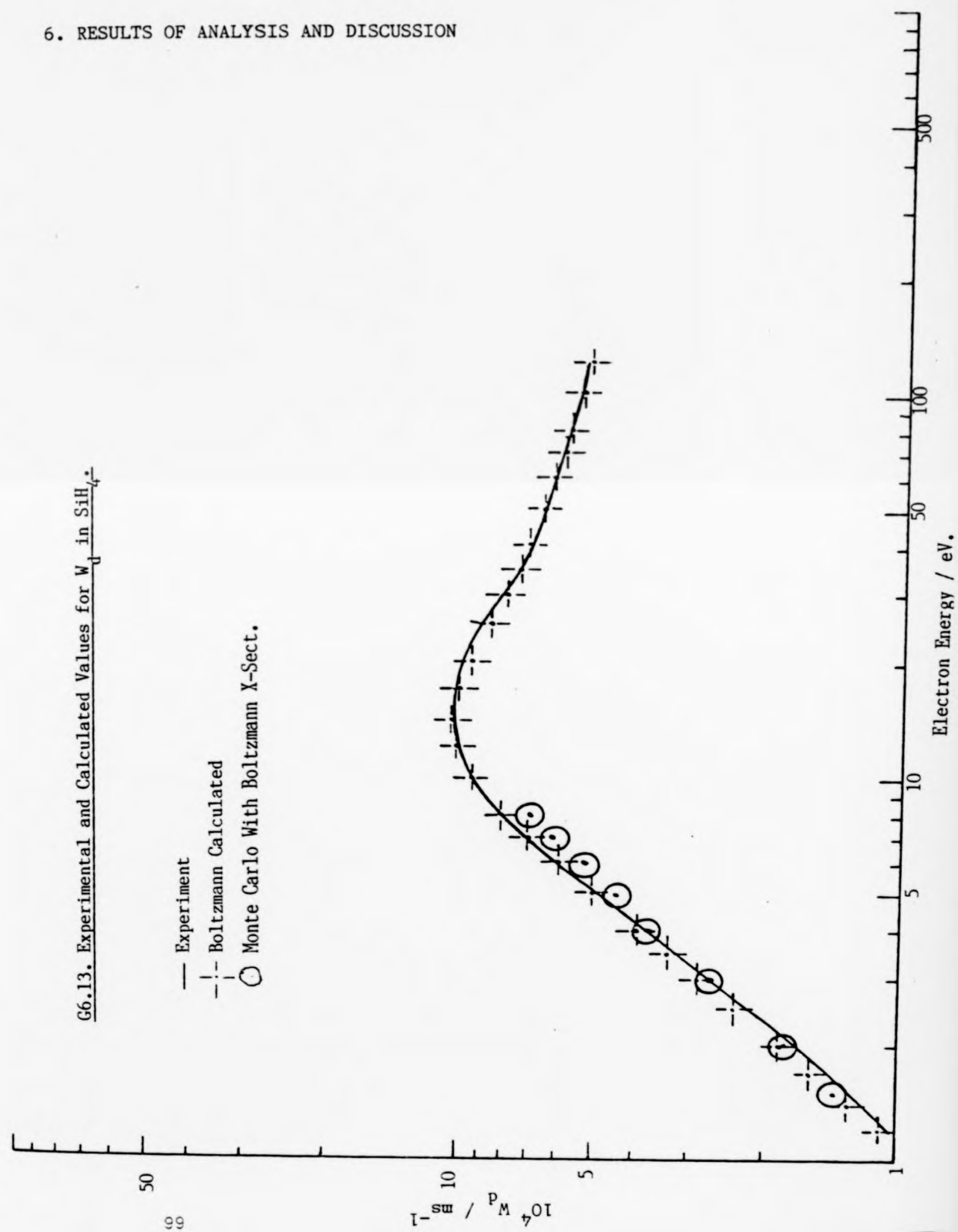
6. RESULTS OF ANALYSIS AND DISCUSSION



6. RESULTS OF ANALYSIS AND DISCUSSION



6. RESULTS OF ANALYSIS AND DISCUSSION



6. RESULTS OF ANALYSIS AND DISCUSSION

6.5(b). Boltzmann Analysis.

The cross sections produced by the Boltzmann analysis are represented in G6.11 and in T6.9. The fit of calculated and experimental data is shown in G6.12 and G6.13, and in T6.4. The starting cross sections were the same as those used for silane, but with onset as described above. The calculation was performed over 22 iterations. As with silane, the derived cross sections have an energy region in which the momentum transfer falls below the inelastic contribution. There are many other similarities between the cross sections of the two gases. Firstly, the momentum transfer contribution is almost identical up to 0.5 eV, at which point the silane cross section rises more steeply. Secondly, the rise of the inelastic process beyond onset is not so marked in the deuterio compound. These similarities are hardly surprising if one considers the difference that such a small change in the mass of a ligand makes to the whole molecule when the central atom is so massive as silicon. The more pronounced changes seen between methane and perdeuteromethane are not observed as the change in ligand mass becomes less significant.

6.5(c). Monte Carlo.

The cross sections produced by the two term analysis (modified to avoid negative inelastic contributions) were used as starter cross sections for a Monte Carlo study. The data fit was very poor (G6.12, G6.13, T6.4) and no refinement was attempted.

6. RESULTS OF ANALYSIS AND DISCUSSION

6.6/. Phosphine.

6.6(a). Preliminary Information.

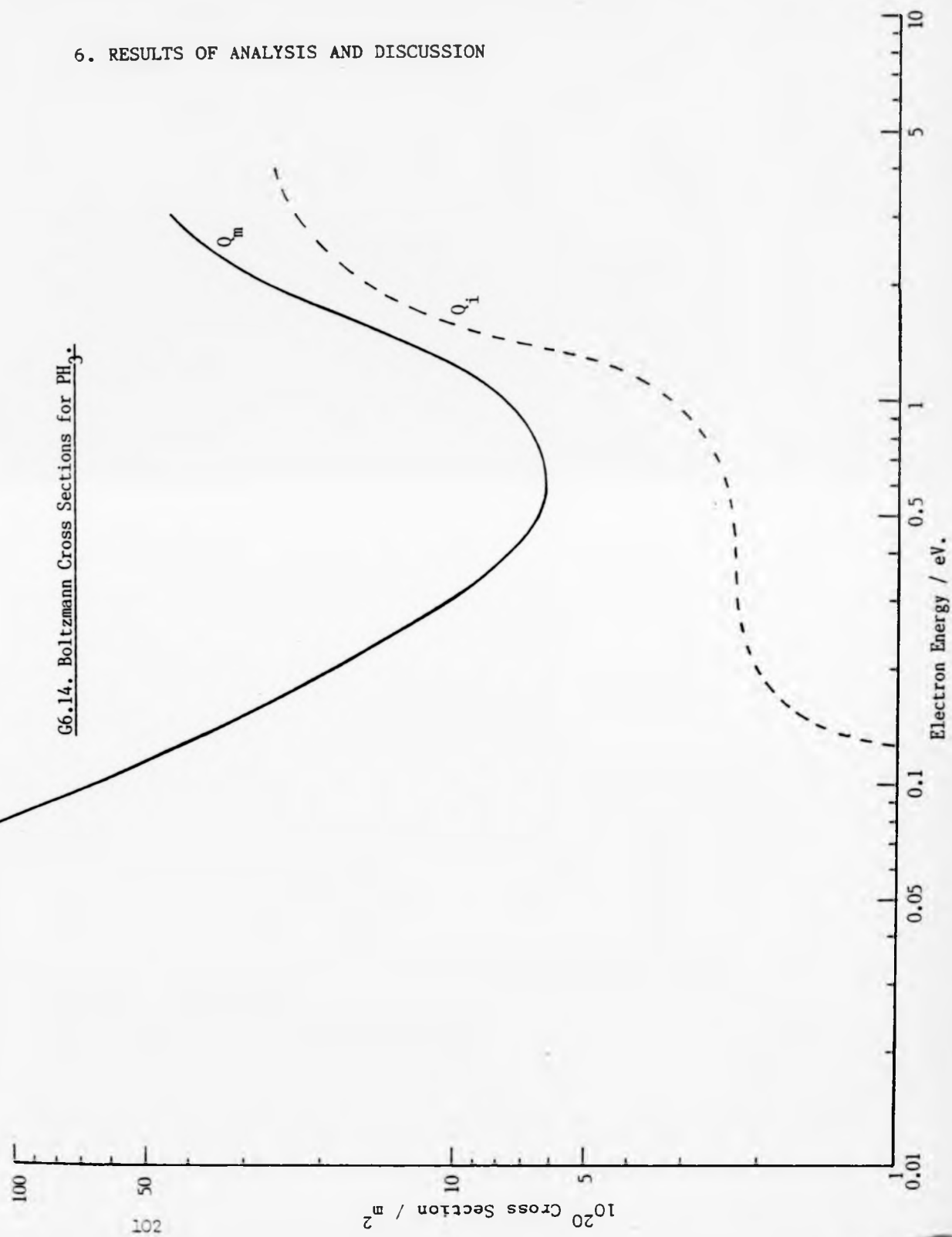
The experimental data used are the D/μ values reported in Chapter 5 and the drift velocity data of Pollock (1968). No beam studies have yet been reported in this gas. One inelastic process was used with onset 0.123 eV. No attempt was made to account for rotational excitation. A Monte Carlo Simulation was not used for this gas.

6.6(b). Boltzmann Analysis.

The cross sections produced by the Boltzmann analysis are represented in G6.14 and T6.10. It was expected that the neglect of rotational contributions to the inelastic cross section at low energies would induce a peaked onset to the vibrational cross section. As this is not the case, it seems that rotational energy transfer is not an important energy loss channel for electrons in this gas. However, the Boltzmann analysis was unable to match calculated and experimental transport coefficients to within 20% over most of the energy range covered, so these cross sections must not be regarded as final, even within the restrictions of the two term approximation. At low energies, where the data fit is best, the momentum transfer cross section levels off at a value of $189 \cdot 10^{-20} \text{ m}^2$ below 0.05 eV.

6. RESULTS OF ANALYSIS AND DISCUSSION

G6.14. Boltzmann Cross Sections for PH_3 .



6. RESULTS OF ANALYSIS AND DISCUSSION

Theory predicts (Altshuler, 1957) that this gas will have a slightly lower cross section than this ($170 \cdot 10^{-20} \text{ m}^2$) but the point dipole model on which the theory is based has been called into question for molecules with a small dipole moment such as this one (Crawford *et al.*, 1967). Other inorganic hydrides show cross section values consistently higher than theory predicts (Cottrell *et al.*, 1968), Christophoru and Christodoulides, 1969).

6.7/. Conclusions.

The aim of this work was to test the validity of the two term Boltzmann analysis in the derivation of electron molecule cross sections and to investigate the cross sections of selected gases in the light of the findings of that test. In attempting to fulfill this aim a number of achievements have been made.

A Monte Carlo simulation of electron motion in gases has been developed and tested. In the course of this testing using model gases, the validity of the two term analysis was shown to be suspect in regions of high inelastic contributions (Benchmark 1). The simulation technique has been used in conjunction with the two term analysis, and in the light of the exploration of the invalidity of the latter approach over restricted regions, to probe a real gas (methane). The investigation of methane produced some valuable information.

6. RESULTS OF ANALYSIS AND DISCUSSION

Firstly, the two term approximation gives a quantitative indication of the final cross sections in all energy regions except those of high inelastic contributions. It outlines qualitatively the presence of a Ramsauer Townsend minimum, and the coincidence of that minimum with a large vibrational contribution.

Secondly, during the quantitative analysis (using Monte Carlo) of the region of the Ramsauer Townsend minimum, an absolute value of that minimum in methane has been obtained. This should be useful both as a test for theory and for comparison with the results of beam experiments. Quantitatively, the value obtained agrees very well with the most recent beam studies.

Thirdly, it has been established that one of the necessary features of the inelastic cross sections (if a good fit is to be obtained) is a very sharp, peaked onset. This finding is supported by recent evidence from differential cross sections in beam work, and is an important indicator of the type of energy transfer involved.

In other gases, the general shape of the cross section has been explored using the two term analysis, verifying the presence of a Ramsauer Townsend minimum in the gases of type XY_4 , and a preliminary Monte Carlo investigation of CD_4 shows that a great deal of refinement to the two term cross sections needs to be done to improve the data fit.

The aim of the work has only partly been fulfilled, in that only one gas was fully explored. The major reason for this was the

6. RESULTS OF ANALYSIS AND DISCUSSION

amount of time taken to refine cross sections and test them using the Monte Carlo model. Because of the large amounts of computer time that a single simulation consumes, the method is not suited to refinement procedures. A more suitable approach would be to calculate probable cross sections using an eight term Boltzmann code, and then use Monte Carlo to check those cross sections independently.

The present Monte Carlo model has two restrictions which could be removed to improve the model. Firstly, the scattering from the target is isotropic. Under swarm conditions in the gases studied here, this is a good approximation, but to extend the range of gases amenable to study using this method, some means of giving directional bias (probably energy dependent) in the scattering must be included. Secondly, the temperature of the gas should be taken into account. This would allow the low energy region to be investigated thoroughly, and would encourage quantitative comparisons of the temperature dependence of the transport data.

Future studies may include the above ideas as a complete investigation into swarm behaviour in any gas.

6. RESULTS OF ANALYSIS AND DISCUSSION

| 10^{13} E/N | 10^4 Wd | D/u | Dr | Dl | Av. Energy |
|---------------|-----------|--------|--------------|--------------|------------|
| $V \cdot m^2$ | ms^{-1} | V | $m^2 s^{-1}$ | $m^2 s^{-1}$ | eV |
| 0.4 | 1.57 | 0.0435 | 17.1 | 50.7 | 0.0560 |
| 0.8 | 4.63 | 0.0793 | 45.9 | 137.5 | 0.0995 |
| 1.0 | 5.98 | 0.0701 | 41.9 | 114.5 | 0.192 |
| 1.5 | 7.80 | 0.114 | 59.5 | 76.3 | 0.180 |
| 2.0 | 8.89 | 0.127 | 56.2 | 69.0 | 0.223 |
| 3.0 | 10.0 | 0.192 | 64.3 | 36.4 | 0.318 |
| 3.25 | 10.2 | 0.222 | 69.7 | 35.0 | 0.349 |
| 3.75 | 10.2 | 0.227 | 65.9 | 32.9 | 0.363 |
| 4.0 | 10.4 | 0.251 | 65.2 | 27.0 | 0.409 |
| 5.0 | 10.1 | 0.335 | 67.7 | 20.8 | 0.513 |
| 6.0 | 9.48 | 0.394 | 62.2 | 17.6 | 0.608 |
| 7.0 | 8.99 | 0.484 | 62.2 | 15.9 | 0.733 |
| 8.0 | 8.70 | 0.535 | 58.2 | 15.2 | 0.852 |
| 9.0 | 8.06 | 0.677 | 60.6 | 13.0 | 0.995 |
| 10.0 | 7.68 | 0.748 | 57.4 | 11.6 | 1.14 |

T6.1. Swarm Parameters Using Refined Cross Section - CH₄

| 10^{13} E/N | 10^4 Wd | D/u | Dr | Dl | Av. Energy |
|---------------|-----------|--------|--------------|--------------|------------|
| $V \cdot m^2$ | ms^{-1} | V | $m^2 s^{-1}$ | $m^2 s^{-1}$ | eV |
| 0.4 | 1.38 | 0.0472 | 16.3 | 41.9 | 0.0556 |
| 0.8 | 4.51 | 0.0629 | 35.5 | 127.1 | 0.115 |
| 1.0 | 5.25 | 0.0703 | 36.9 | 127.2 | 0.127 |
| 1.5 | 7.81 | 0.151 | 78.5 | 82.6 | 0.233 |
| 2.0 | 8.36 | 0.182 | 76.3 | 48.5 | 0.312 |
| 2.5 | 8.73 | 0.267 | 93.2 | 44.6 | 0.429 |
| 3.0 | 8.35 | 0.277 | 77.3 | 39.7 | 0.515 |
| 3.5 | 8.25 | 0.397 | 93.7 | 33.9 | 0.659 |
| 4.0 | 7.72 | 0.451 | 86.9 | 27.0 | 0.769 |
| 5.0 | 7.21 | 0.651 | 93.9 | 18.1 | 1.07 |
| 6.0 | 6.30 | 0.939 | 98.6 | 14.5 | 1.20 |
| 7.0 | 5.59 | 0.902 | 72.1 | 20.3 | 1.53 |
| 8.0 | 5.17 | 1.35 | 87.4 | 14.8 | 1.60 |
| 9.0 | 5.08 | 1.42 | 79.9 | 17.0 | 1.96 |
| 10.0 | 4.66 | 1.51 | 70.3 | 15.1 | 2.31 |

T6.2. Swarm Parameters Using First Trial Cross Sections - CD₄

6. RESULTS OF ANALYSIS AND DISCUSSION

| 10^{13} E/N | 10^4 Wd | D/u | Dr | Dl | Av. Energy |
|---------------|-----------|--------|--------------|--------------|------------|
| $V \cdot m^2$ | ms^{-1} | V | $m^2 s^{-1}$ | $m^2 s^{-1}$ | eV |
| 0.4 | 0.505 | 0.0199 | 2.52 | 2.60 | 0.0443 |
| 0.8 | 0.676 | 0.0286 | 2.41 | 2.88 | 0.0414 |
| 1.0 | 0.887 | 0.0350 | 3.10 | 2.22 | 0.0447 |
| 1.5 | 1.39 | 0.0362 | 3.36 | 3.48 | 0.0475 |
| 2.0 | 1.82 | 0.0441 | 4.02 | 2.80 | 0.0496 |
| 3.0 | 2.75 | 0.0396 | 3.63 | 4.69 | 0.0561 |
| 4.0 | 3.71 | 0.0341 | 3.16 | 3.52 | 0.0622 |
| 5.0 | 4.61 | 0.0384 | 3.54 | 3.84 | 0.0693 |
| 6.0 | 5.32 | 0.0330 | 2.92 | 4.75 | 0.0762 |
| 7.0 | 6.09 | 0.0422 | 3.67 | 4.76 | 0.0853 |
| 8.0 | 6.81 | 0.0478 | 4.07 | 3.79 | 0.0957 |

T6.3. Swarm Parameters Using Boltzmann Cross Sections - SiH_4

| 10^{13} E/N | 10^4 Wd | D/u | Dr | Dl | Av. Energy |
|---------------|-----------|--------|--------------|--------------|------------|
| $V \cdot m^2$ | ms^{-1} | V | $m^2 s^{-1}$ | $m^2 s^{-1}$ | eV |
| 0.4 | 0.372 | 0.0235 | 2.18 | 2.27 | 0.0307 |
| 0.8 | 0.760 | 0.0245 | 2.33 | 2.08 | 0.0323 |
| 1.0 | 0.957 | 0.0269 | 2.58 | 2.91 | 0.0350 |
| 1.5 | 1.37 | 0.0244 | 2.23 | 2.45 | 0.0358 |
| 2.0 | 1.84 | 0.0305 | 2.81 | 2.38 | 0.0385 |
| 3.0 | 2.74 | 0.0229 | 2.09 | 2.25 | 0.0419 |
| 4.0 | 3.71 | 0.0299 | 2.77 | 3.28 | 0.0473 |
| 5.0 | 4.47 | 0.0224 | 2.00 | 4.18 | 0.0533 |
| 6.0 | 5.36 | 0.0335 | 2.99 | 2.77 | 0.0623 |
| 7.0 | 6.30 | 0.0346 | 3.11 | 2.35 | 0.0755 |
| 8.0 | 7.01 | 0.0404 | 3.54 | 4.41 | 0.0882 |

T6.4. Swarm Parameters Using Boltzmann Cross Sections - SiD_4

6. RESULTS OF ANALYSIS AND DISCUSSION

Cross Sections Used In The Analysis

T6.5. Boltzmann Output - CH4

| Energy eV | 10^{20} Q(el.) m^2 | 10^{20} Q(inel. 1) m^2 | 10^{20} Q(inel. 2) m^2 |
|--------------|---------------------------|-------------------------------|-------------------------------|
| 0.01 | 90.6 | | |
| 0.013 | 5.54 | | |
| 0.015 | 5.03 | | |
| 0.021 | 3.70 | | |
| 0.031 | 1.38 | | |
| 0.042 | 1.47 | | |
| 0.050 | 1.60 | | |
| 0.061 | 1.95 | | |
| 0.071 | 1.75 | | |
| 0.082 | 1.60 | | |
| 0.090 | 1.50 | | |
| 0.10 | 1.41 | | |
| 0.11 | 1.34 | | |
| 0.12 | 1.28 | | |
| 0.16 | 1.17 | ONSET | |
| 0.18 | 0.60 | 0.52 | |
| 0.20 | 0.58 | 0.52 | |
| 0.25 | 0.40 | 0.66 | |
| 0.30 | 0.43 | 0.63 | |
| 0.35 | 0.59 | 0.59 | |
| 0.36 | 0.61 | 0.58 | ONSET |
| 0.40 | 0.66 | 0.56 | 0.22 |
| 0.50 | 0.59 | 0.55 | 0.19 |
| 0.60 | 0.89 | 0.54 | 0.19 |
| 0.70 | 1.55 | 0.54 | 0.19 |
| 0.80 | 3.45 | 0.54 | 0.19 |
| 0.90 | 3.28 | 0.54 | 0.19 |
| 1.00 | 2.98 | 0.54 | 0.19 |
| 1.51 | 2.08 | 0.54 | 0.19 |
| 2.00 | 1.63 | 0.54 | 0.19 |

6. RESULTS OF ANALYSIS AND DISCUSSION

T6.6. Refined Monte Carlo Input - CH4

| Energy | 10^{20} Q(el.) | 10^{20} Q(inel. 1) | 10^{20} Q(inel. 2) |
|--------|------------------|----------------------|----------------------|
| eV | m^2 | m^2 | m^2 |
| 0.01 | 67.0 | | |
| 0.05 | 40.0 | | |
| 0.07 | 8.24 | | |
| 0.08 | 4.41 | | |
| 0.09 | 2.97 | | |
| 0.10 | 1.55 | | |
| 0.12 | 1.28 | | |
| 0.16 | 0.30 | ONSET | |
| 0.20 | 0.19 | | |
| 0.22 | | 0.15 | |
| 0.225 | | 0.54 | |
| 0.23 | | 0.54 | |
| 0.24 | | 0.36 | |
| 0.25 | 0.10 | | |
| 0.30 | 0.21 | | |
| 0.35 | 0.35 | | |
| 0.36 | | | ONSET |
| 0.40 | 0.48 | | |
| 0.42 | | | 0.15 |
| 0.425 | | | 0.38 |
| 0.43 | | | 0.38 |
| 0.44 | | | 0.36 |
| 0.50 | 0.59 | | |
| 0.60 | 0.89 | | |
| 0.70 | 1.55 | | |
| 1.00 | 2.30 | | |
| 1.25 | | 0.30 | 0.30 |
| 1.50 | 3.00 | | |
| 2.00 | 4.60 | | |
| 2.25 | | 0.17 | 0.17 |
| 2.75 | | 0.17 | 0.17 |
| 3.00 | 6.60 | 0.27 | 0.27 |
| 10.0 | 25.0 | 0.27 | 0.27 |

6. RESULTS OF ANALYSIS AND DISCUSSION

T6.7. Boltzmann Output - CD4

| Energy | 10^{20} Q(el.) | 10^{20} Q(inel.) |
|--------|------------------|--------------------|
| eV | m^2 | m^2 |
| 0.05 | 5.22 | |
| 0.06 | 3.54 | |
| 0.07 | 2.67 | |
| 0.08 | 1.61 | |
| 0.09 | 1.34 | |
| 0.10 | 1.35 | |
| 0.12 | 1.41 | |
| 0.123 | 0.80 | ONSET |
| 0.16 | 0.21 | 0.83 |
| 0.18 | 0.18 | 0.86 |
| 0.20 | 0.23 | 0.82 |
| 0.25 | 0.30 | 0.81 |
| 0.30 | 0.37 | 0.76 |
| 0.35 | 0.53 | 0.73 |
| 0.40 | 0.62 | 0.71 |
| 0.50 | 0.79 | 0.72 |
| 0.60 | 1.13 | 0.63 |
| 0.70 | 1.36 | 0.60 |
| 0.80 | 1.63 | 0.59 |
| 0.90 | 1.96 | 0.59 |
| 1.00 | 2.52 | 0.61 |
| 1.50 | 3.59 | 0.62 |
| 2.00 | 3.90 | 0.53 |
| 2.50 | 4.27 | 0.50 |
| 3.50 | 7.26 | 0.61 |
| 4.00 | 8.05 | 0.84 |
| 6.00 | 8.90 | 0.84 |

6. RESULTS OF ANALYSIS AND DISCUSSION

T6.8. Boltzmann Output - SiH4

| Energy | 10^{20} Q(Mom Tr.) | 10^{20} Q(inel.) |
|--------|----------------------|--------------------|
| eV | m^2 | m^2 |
| 0.05 | 19.0 | |
| 0.06 | 16.5 | |
| 0.07 | 13.2 | |
| 0.08 | 11.3 | |
| 0.09 | 11.3 | |
| 0.10 | 11.2 | |
| 0.11 | 11.1 | |
| 0.12 | 6.49 | ONSET |
| 0.16 | 6.02 | 7.61 |
| 0.18 | 5.95 | 7.71 |
| 0.20 | 5.89 | 8.08 |
| 0.25 | 5.80 | 8.53 |
| 0.30 | 5.40 | 8.72 |
| 0.35 | 5.42 | 8.99 |
| 0.40 | 5.50 | 6.26 |
| 0.50 | 5.71 | 6.39 |
| 0.60 | 6.57 | 6.72 |
| 0.70 | 7.89 | 6.63 |
| 0.80 | 10.0 | 6.77 |
| 0.90 | 14.8 | 7.68 |
| 1.00 | 19.3 | 9.69 |
| 1.50 | 63.8 | 23.8 |
| 2.00 | 66.9 | 24.6 |
| 2.50 | 66.9 | 25.4 |

6. RESULTS OF ANALYSIS AND DISCUSSION

T6.9. Boltzmann Output - SiD4

| Energy eV | 10^{20} Q(Mom Tr.) m^2 | 10^{20} Q(inel.) m^2 |
|--------------|-------------------------------|-----------------------------|
| 0.06 | 19.8 | |
| 0.07 | 12.4 | |
| 0.08 | 9.98 | |
| 0.09 | 7.36 | |
| 0.10 | 7.03 | ONSET |
| 0.11 | 6.96 | 2.85 |
| 0.12 | 6.84 | 6.22 |
| 0.16 | 7.10 | 7.59 |
| 0.18 | 6.69 | 8.38 |
| 0.20 | 6.24 | 9.22 |
| 0.25 | 5.54 | 10.4 |
| 0.30 | 5.35 | 6.21 |
| 0.35 | 5.14 | 5.82 |
| 0.40 | 5.14 | 5.40 |
| 0.50 | 5.34 | 5.07 |
| 0.60 | 5.90 | 4.62 |
| 0.70 | 6.79 | 4.82 |
| 0.80 | 8.48 | 5.79 |
| 0.90 | 10.5 | 5.36 |
| 1.00 | 12.1 | 4.88 |
| 1.50 | 17.0 | 6.36 |
| 2.00 | 23.1 | 8.36 |
| 2.50 | 49.0 | 13.4 |
| 3.00 | 65.0 | 13.6 |
| 3.50 | 61.6 | 13.7 |
| 4.00 | 62.0 | 13.8 |
| 5.00 | 62.3 | 14.0 |

6. RESULTS OF ANALYSIS AND DISCUSSION

T6.10. Boltzmann Output - PH3

| Energy eV | 10^{20} Q(Mom Tr.) m^2 | 10^{20} Q(inel.) m^2 |
|--------------|----------------------------------|--------------------------------|
| 0.05 | 189 | |
| 0.06 | 142 | |
| 0.07 | 107 | |
| 0.08 | 60.3 | |
| 0.09 | 52.1 | |
| 0.10 | 51.4 | |
| 0.11 | 37.2 | |
| 0.12 | 42.8 | |
| 0.123 | | ONSET |
| 0.16 | 59.7 | 1.78 |
| 0.18 | 52.1 | 1.89 |
| 0.20 | 43.2 | 1.95 |
| 0.25 | 23.2 | 2.11 |
| 0.30 | 11.5 | 2.27 |
| 0.35 | 8.76 | 2.51 |
| 0.40 | 7.59 | 2.69 |
| 0.50 | 6.49 | 3.00 |
| 0.60 | 6.29 | 2.65 |
| 0.70 | 6.24 | 2.60 |
| 0.80 | 6.70 | 2.68 |
| 0.90 | 7.24 | 2.79 |
| 1.00 | 7.83 | 3.06 |
| 1.50 | 15.6 | 8.75 |
| 2.00 | 51.0 | 19.3 |
| 2.50 | 37.5 | 24.4 |
| 3.00 | 32.3 | 24.7 |

Appendix I - Data Logger.

This is a brief description of the microcomputer based data logging system designed and developed as part of this research project. Further technical details are provided in the Data Logging Handbook (this Author, 1981).

A1.1/. Overview.

The Pet-Solartron Data Logging System was designed to enable rapid collection and treatment of multi-channel data. It consists of three major components, a Solartron LM1426 Digital Voltmeter (DVM), a Commodore CBM3016 Microcomputer (CBM), and a custom built interface. It treats data at about 25 times the rate of the old system, with less feedback disturbance of the sensitive electrical measurements being made.

The DVM supplies data in the 8421 Binary Coded Decimal (BCD) format, via a fan-out amplifier using -12V as a logical 1. A given block of data output from the DVM consists of 24 separate bits.

Each DVM decade (Units, tens etc.) - 4 bits

Range Information - 6 bits

Digit 5 - 1 bit

Sign Information - 1 bit

This 24 bit data is requested from the DVM by the CBM and is converted to 21 bit TTL (via level shift and then encoding of the range data) by the interface. This is stored as 3 bytes of CBM memory and is checked for stability. Once accepted (by the CBM) as valid data, it is converted into decimal format (four figure

Appendix I - Data Logger.

integer, with sign) and is manipulated by the software (either rejected (run abort) or stored in an array for statistical analysis). The detailed description of the hardware and software which facilitate this process is given in the user's handbook. A program listing for the system is included in Appendix III.

Appendix II - Cathode Making

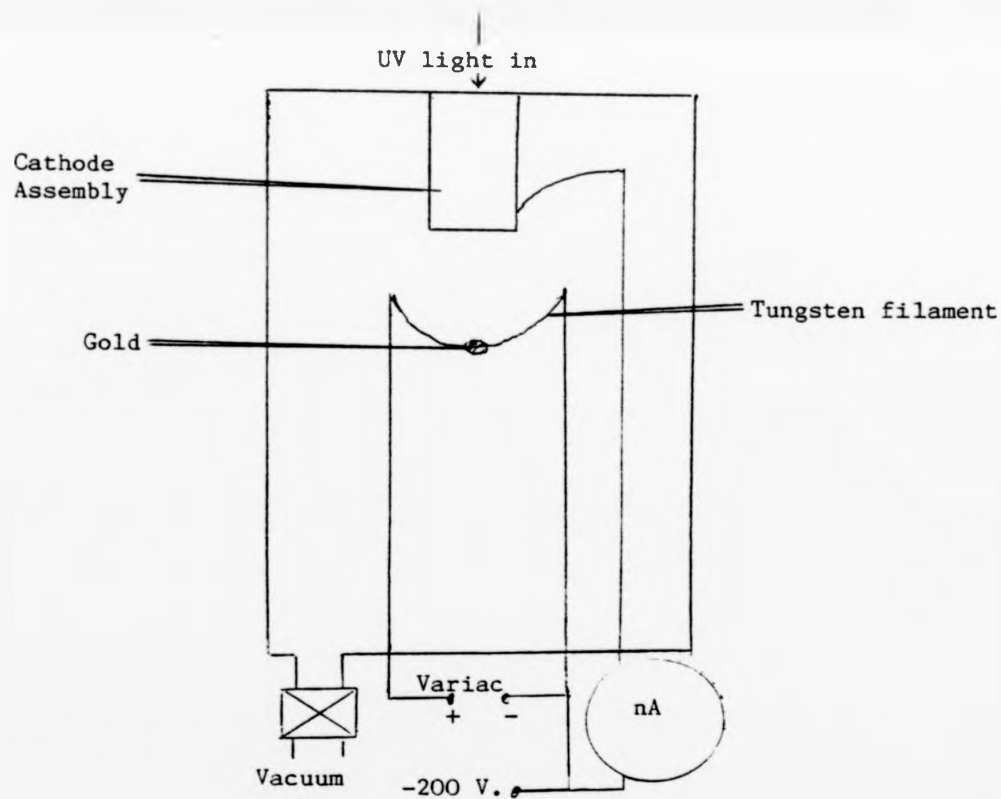
Aside from the limitations on photocurrent imposed by the gas under study (p. 55) the other serious problem in producing measurable currents is deterioration of the cathode. It is useful to have a reproducible method for producing good quality cathodes. In the course of this study, the following technique was found to produce good results.

Firstly, a thick conducting aluminium ring must be evaporated onto the cathode face. This is done in a large vacuum evaporation chamber by evaporating kitchen foil from a tungsten filament onto the masked face of the cathode at low pressure (not greater than 10 torr). The next stage is to evaporate on the gold film. The circuit is set up as shown and the evaporation chamber taken down to 10 torr. Gold wire is melted onto the tungsten filament at moderate temperature, until it rests as a ball in the centre. The temperature is increased until the gold shimmers, and then is reduced. The photocurrent under these conditions is measured by the nanoammeter, the true photocurrent being found by subtraction of the dark current. Note that the nanoammeter should be off during heating as thermal electron current is much larger than the photocurrent. This process of heating, shimmering and cooling is repeated. As this is done a gradual build up of the photocurrent is produced. The aim is to catch this current at its maximum, before it begins to diminish with increasing film thickness. As a guide, a current (at reduced pressure) of 20 nA is respectable, but this should increase substantially with a slight

Appendix II - Cathode Making

rise in pressure.

After evaporation, the cathode should be left to cool (half an hour) under vacuum, then transferred as soon as possible to the drift chamber which should then be evacuated and the photocurrent checked (10 A at 10 torr is respectable). Cathodes deteriorate rapidly on exposure to atmosphere. If an old cathode is to be reused, the old gold film should be removed by careful wiping with cotton wool or very soft tissue and the process taken from first evaporation of the gold film.



Schematic of Evaporation Chamber

(a). Monte Carlo Program

```

1000 REM ( * * * * M O N T E C A R L O P R O G R A M * * * * )
1010 REM -----

1030 REM THIS IS THE GENERALISED MONTE CARLO PROGRAM OF THE ELECTRON
1040 REM MOLECULE COLLISIONS GROUP, CHEMISTRY DEPARTMENT, UNIVERSITY
1050 REM OF STIRLING, SCOTLAND.

1070 REM GIVEN A GRID OF CROSS SECTION POINTS, IT SIMULATES THE MOTION
1080 REM OF AN ELECTRON SURM THROUGH A GAS, CALCULATING TRANSPORT
1090 REM COEFFICIENTS FOR THAT GAS.

1100 REM ( * * * * I N I T I A L I S A T I O N * * * * )

1110 DIM VSTORE(497000), ESTORE(497000), DSTORE(5000), RSTORE(5000)
1120 DIM ZSTORE(5000), DIS(100,10), OES(100), EIS(100,10), EES(100)

1130 OPEN "MDAT.DAT" AS FILE #12
1135 OPEN "MGRS.DAT" FOR OUTPUT AS FILE #22
1140 INPUT#12, REYZ, C, MHAAS, EM, NEPZ, #12, GAS#
1141 PRINT#22, "MONTE CARLO RESULTS IN ";GAS#
1142 PRINT#22, "MOLECULAR MASS ";MHAAS
1143 PRINT#22 \ PRINT#22, "INELASTIC PROCESSES"
1144 PRINT#22, "PROCESS", "ONSET", "LOSS"
1150 FOR I = 1 TO NEPZ \ INPUT#12, FES(I), OES(I)
1160 EES(I) = FES(I) * 1.60219E-19 \ OES(I) = OES(I) * 1E-20 \ NEXT I

```

(a). Monte Carlo Program

```

1170 REM READ IN INPUT PARAMETERS:
1180 REM
1190 REM
1200 REM
1210 REM
1220 REM
1230 REM
1240 REM
1250 REM
      NIPZ ----- NUMBER OF REAL COLLISIONS
      C ----- HULL COLLISION CONSTANT ( C = 0E / V )
      MWMSS ----- MOLECULAR MASS (IN AMU)
      EN ----- E/N (IN TOUNSEBDS)
      NIPZ ----- NUMBER OF POINTS GIVEN FOR ELASTIC CROSS SECTION
      NIZ ----- NUMBER OF INELASTIC PROCESSES
      EFS(I) ----- ENERGY ABSCISSA FOR ELASTIC CROSS SECTION (IN ELECTRON VOLTS)
      RES(I) ----- ELASTIC CROSS SECTION POINTS (IN ANGSTROMS ^2)

1260 FOR I = 1 TO NIZ \ INPUTNIZ, NIPZ(I) \ NEXT I
1270 FOR J = 1 TO NIZ \ FOR I = 1 TO NIPZ(I)
1280 INPUTNIZ, FIS(I,J), DIS(I,J)
1290 EIS(I,J) = EIS(I,J) + 1.60219E-19 \ DIS(I,J) + 1E-20
1300 NEXT J
1310 INPUTNIZ, EOI(J), ELI(J)
1312 PRINTNIZ, J, EOI(J), ELI(J)
1315 EOL(J) = EOI(J) + 1.60219E-19 \ ELI(J) = ELI(J) + 1.60219E-19
1320 NEXT J
1325 CLOSE 1

1330 REM READ IN INELASTIC CROSS SECTIONS:
1340 REM
1350 REM
1360 REM
1370 REM
      EIS(I,J) ---- ENERGY ABSCISSA FOR I' TH POINT OF J' TH INELASTIC PROCESS
      DIS(I,J) ---- INELASTIC CROSS SECTION FOR J' TH PROCESS AT I' TH ENERGY VALUE
      EOI(J) ----- ONSET ENERGY OF J' TH PROCESS
      ELI(J) ----- ENERGY LOSS FOR COLLISION OF TYPE J

1380 MWMSS = MWMSS + 1E-26 / 6.0231
1390 EMSS = 9.10056E-31 \ MWMSS = MWMSS + EMSS
1400 SMT = 19 / ( C + 1E23 )
1410 PRINTNIZ \ PRINTNIZ, "E/N = "; EN: "T.D."
1420 PRINTNIZ, "SAMPLE TIME " : SMT
1430 PRINTNIZ, "HULL X-SECTION CONSTANT " : C
1440 E = EN + 100 \ ACCN = E + 1.7588E11
1450 PIE = 3.1415926

```

Appendix III - Computer Listings.

(a). Monte Carlo Program

```

1450 REM ----- TIME LIMIT FOR SAMPLING
1460 REM E ----- FIELD STRENGTH (V/M), NUMBER DENSITY OF GAS FIXED AT 10^23 M^-3
1470 REM ACCN ----- ACCELERATION OF ELECTRON DUE TO FIELD

1480 OPEN "MOCAR.DAT" FOR OUTPUT AS FILE%Z
1490 PRINT%: "COUNTER", "ENERGY", "(R+Z)", "(Z3-Z2)", "WD."
1500 RANDOMIZE
1510 TOT = 0
1520 TOT = TOT + 1 \ IF TOT < 2000 THEN GOTO 2000
1530 GOSUB 5000
1540 TOT = 0 \ FLAG = 1
1550 TOT = TOT + 1 \ IF TOT < 1000 THEN GOTO 2000

1560 REM PRINT HEADINGS FOR RUN - TIME OUTPUT FILE
1570 REM SEND ELECTRON THROUGH PREDEFIN, THEN ZERO COORDINATES ETC, FOR START OF TRUE DRIFT REGION.

1580 PRINT%: "RESULTS OF SIMULATION"
1590 PRINT%: "-----"
1600 PRINT%: "NUMBERS OF COLLISIONS"
1610 PRINT%: "RUI", RI
1620 PRINT%: "ELASTIC", EL
1630 FOR I = 1 TO NIZ \ PRINT%: "INELASTIC":I, IL(I) \ ILT = ILT + IL(I) \ NEXT I
1640 PRINT%: "TOTAL REAL", EL + ILT
1650 PRINT%: "PRINT%Z"
1660 WD = Z / TOTIME \ ZBAR = WD * SMT + 200
1670 PRINT%: "DRIFT VELOCITY", WD; "M/S"
1680 IR = FSUM / USA / N / SMT / 200
1690 PRINT%: "EAD, DIFF. COEFF", DR; "M^2/S"
1700 FOR I = 1 TO USA \ USSTORE(I) = ( USSTORE(I) - ZBAR ) + Z
1710 ISTORE = ISTORE + USSTORE(I) \ NEXT I
1720 MI = ISTORE / USA / 2 / SMT / 200
1730 PRINT%: "LOGG. DIFF. COEFF.", MI; "M^2/S"
1740 PRINT%: "R0/A", " ", DR + E / WD; "VOLTS"
1750 PRINT%: "D1/D", " ", MI + E / WD; "VOLTS"
1760 EBAR = FSUM / US3
1770 PRINT%: "AVERAGE ENERGY", EBAR; "ELECTRON VOLTS"
1780 VE = EMAX + 1.60219E-19
1790 GOSUB 4800
1800 PRINT%: "X-SECTIONS AT HIGHEST ENERGY"
1810 PRINT%: "ENERGY", "0-PADDED"
1820 PRINT%: "EAX, SIGOR + 1E23, 01 + 1E20"
1830 PRINT%: "VALUE FOR RUI X-SECTION CONSTANT SHOULD BE > "; SIGOR * SOR ( 2 * KE / EMAX )
1840 CLOSE 2, 3, 4
1850 GOTO 7000

```


(a). Monte Carlo Program

```

2050 REM ( * * * * * H A T H P E R O G R A M * * * * * )
2060 PROB = RND \ T = - LOG ( 1 - PROB ) / ( C * 1E23 ) \ TOTALTIME = TOTALTIME + T
2070 SUNT = SUNT + T \ IF SUNT > SART THEN GOSUB 4000
2080 REM CALCULATE TIME TO NEXT COLLISION, IF PAST SAMPLE TIME
2090 REM THEN GO TO SAMPLING ROUTINE
2100 X = X + YVEL * T \ Y = Y + YVEL * T
2110 Z = Z + ZVEL * T + 0.5 * ACCN * T ^ 2
2120 ZVEL = ZVEL + ACCN * T
2130 IF Z < 0 AND FLAG = 1 THEN GOSUB 5000 \ GOTO 1520
2140 IF Z < 0 AND FLAG = 0 THEN GOSUB 5000 \ GOTO 1490
2150 TRUVEL = SQR ( XVEL * XVEL + YVEL * YVEL + ZVEL * ZVEL )
2160 VE = 0.5 * FRASS * TRUVEL + TRUVEL
2170 REM UPDATE ELECTRON POSITION, VELOCITY, CHECK FOR -VE Z.
2180 REM IF Z < 0 THEN ELECTRON HAS "CRASHED", START AGAIN.
2190 GOSUB 6000
2200 REM FIND CROSS SECTIONS AT THIS ENERGY.
2210 EP = RND \ PROBR = SIGOR / OT \ IF EP > PROBR THEN COL# = "N" \ HI = 0 + 1 \ GOTO 2030
2220 RP = RND \ PROBE = OE / SIGOR \ IF EP < PROBE THEN COL# = "E" \ EI = EI + 1 \ GOTO 2160
2230 COL# = "I" \ OIT = SIGOR - OE
2240 FOR I = 1 TO NIZ \ PROBIT1 = OI(1) / OIT \ OI(1) = 0 \ NEXT I
2250 RP = RND \ COZ = 0 \ SIGP = 0 \ COL#Z = 0
2260 COZ = COZ + 1 \ SIGP = SIGP + PROBIT(COZ)
2270 IF EP < SIGP THEN I(COZ) = I(COZ) + 1 \ COL#Z = COZ \ GOTO 2160
2280 IF COZ < NIZ THEN 2290
2290 REM DETERMINE TYPE OF COLLISION, IF NULL THEN BACK FOR UPDATE
2300 REM OF ELECTRON POSITION, VELOCITY.

```

(a). Monte Carlo Program

```

2360 IF YVEL = 0 OR YVEL = 0 OR ZVEL = 0 THEN 2380
2370 CX = XVEL / TRUEVEL \ CY = YVEL / TRUEVEL \ CZ = ZVEL / TRUEVEL
2380 PHI = ERB + 2 * PIF \ BLAH = 2 * ( RND - 0.5 )
2390 CALL ARCOS ( BLAH, THETA ) \ TA = THETA
2400 CX2 = SIN / TA \ COS ( PHI )
2410 CY2 = SIN ( TA ) \ SIN ( PHI )
2420 CZ2 = COS ( TA )
2430 BLAH = ( CX + CX2 + CY + CY2 + CZ + CZ2 )
2450 LOSS = 1 - 2 * ( EHASS / HHASS ) * ( 1 - BLAH )
2460 IF COUNT = "N" THEN KE = KE * LOSS
2465 IF COUNT = "I" THEN KE = KE - FI(COUNT)
2450 CY = CY2 \ CX = CX2 \ CZ = CZ2 \ TRUEVEL = SQR ( 2 * KE / EHASS )
2500 YVEL = TRUEVEL * CX \ YVEL = TRUEVEL * CY \ ZVEL = TRUEVEL * CZ
2510 IF FLAG = 0 THEN GOTO 1540
2515 IF FLAG = 1 THEN GOTO 1540

2520 REM COLLIDE ELECTRON. DEVELOP NEW DIRECTION COSINES, SCATTERING
2530 REM ANGLE. SUBTRACT ENERGY LOSSES ACCORDING TO TYPE OF COLLISION

2810 REM ( * * * S U B R O U T I N E L I B R A R Y * * * )

2910 REM 1/. POSITION AND ENERGY SAMPLING SUBROUTINE

4400 T5AH = SINT + T \ T = SUNT - SINT \ SHRT = T
4410 Y3 = X + YVEL + T5AH \ Y3 = Y + YVEL * T5AH \ Z3 = Z + ZVEL * T5AH + 0.5 * ACCN * T5AH + T5AH
4420 ZVEL = ZVEL + T5AH \ TRUEVEL = SQR ( XVEL * XVEL + YVEL * YVEL + ZVEL * ZVEL )
4430 US3 = US3 + 1 \ ESTORE(US3) = 0.5 * EHASS + TRUEVEL / 1.60219E-19
4440 ESHH = FSHH + ESTORE(US3) \ VSTORE(US3) = TRUEVEL
4450 IF ESTORE(US3) > FRAY THEN EMAY = ESTORE(US3)
4455 US2 = US2 + 1 \ IF US2 < 200 THEN X = X3 \ Y = Y3 \ Z = Z3 \ RETURN
4460 US4 = US4 + 1 \ RSTORE(US4) = ( X3 - X2 ) * 2 + ( Y3 - Y2 ) * 2
4470 RSHH = RSHH + RSTORE(US4) \ VSTORE(US4) = Z3 - Z2 \ USUM = USUM + VSTORE(US4)
4480 Z4 = Z3 \ ZSTORE(US4) = ( Z3 - Z2 ) / SINT / 200 \ X2 = X3 \ Y2 = Y3 \ Z2 = Z3
4490 PRINT 37, US4, FSHH/US3, RSTORE(US4), VSTORE(US4), ZSTORE(US4) \ US2 = 0
4495 X = X3 \ Y = Y3 \ Z = Z3 \ RETURN

```

Appendix III - Computer Listings.

(a). Monte Carlo Program

123

```

5910 3/1. START NEW SUBROUTINE
5920 TOTAL TIME = 0 \ SUPT = 0 \ USA = 0 \ Y = 0 \ Y = 0 \ 7 = 0 \ US2 = 0
5930 USUM = 0 \ RSUM = 0 \ DSUM = 0 \ Y2 = 0 \ Y3 = 0 \ Y4 = 0
5940 Y2 = 0 \ Y3 = 0 \ Y4 = 0 \ 72 = 0 \ 73 = 0 \ 74 = 0 \ ESUM = 0
5950 FOR AZ = 1 TO NTZ \ T(AZ) = 0 \ NEXT AZ \ EL = 0 \ HL = 0
5960 RETURN

5970 3/2. CROSS SECTION INTERPOLATION SUBROUTINE
6070 FOR I = 1 TO NTZ \ DT(I) = 0 \ NEXT I \ DE = 0 \ FOR AZ = 1 TO NPTZ
6080 IF NE < EFS(AZ) THEN GRAB = ( DES(AZ) - DES(AZ-1) ) / ( EFS(AZ) - EFS(AZ-1) ) \ DE = GRAB * ( NE - EFS(AZ - 1) ) + DES(AZ-1)
6090 NEXT AZ
6100 FOR J = 1 TO NTZ
6110 IF NE < FIS(I,J) THEN DT(I) = 0 \ GOTO 6070
6120 FOR I = 1 TO NPTZ(I)
6130 IF NE < FIS(I,J) THEN GRAB = ( DIS(I,J) - DIS(I-1,J) ) / ( FIS(I,J) - FIS(I-1,J) ) \ DT(I) = GRAB * ( NE - FIS(I-1, J) ) + DIS(I-1, J)
6140 NEXT I
6150 GRAB = 0 \ NEXT J
6160 DT = 0 \ TRNVEI \ SIGOR = 0
6170 FOR I = 1 TO NTZ \ SIGOR = SIGOR + DT(I) \ NEXT I
6180 SIGOR = SIGOR + DE
6190 DT = DT \ SIGOR
6200 RETURN
7000 END

```

Appendix III - Computer Listings.

(b). Data Logger Program

```

80 OPEN129,4
100 DIMVS(13),B(3),FS(2,2),FC(2),S9$(2)
110 VS(8)=.035:VS(9)=.04:VS(10)=.05:VS(11)=.06:VS(12)=.07:VS(13)=.08
120 B(1)=.2511:B(2)=.5004:B(3)=1.0005:H=10.073
130 VS(1)=.01:VS(2)=.012:VS(3)=.014:VS(4)=.017:VS(5)=.02:VS(6)=.025:VS(7)=.03
140 S9$(1)="MODE":S9$(2)="NUMBER OF SCANS"
200 PRINT"DATA LOGGING PROGRAM."
210 PRINT:PRINT:PRINT:POKE59468,14
220 PRINT" THIS PROGRAM CONTROLS THE PET - DVM
230 PRINT"INTERFACE. GIVEN CERTAIN INFORMATION"
240 PRINT"ABOUT THE EXPERIMENTAL CONDITIONS, IT"
250 PRINT"WILL LOG DARK AND PHOTOCURRENTS, AND"
260 PRINT"USE THESE TO CALCULATE D/U."
270 PRINT:PRINT:PRINT
280 PRINT" YOU WILL BE PRESENTED WITH A MENU"
290 PRINT"OF CHOICES. IF THE CURSOR FLASHES THUS;"
300 PRINT:PRINT"ENTER YOUR ANSWER, THEN PRESS RETURN"
310 PRINT:PRINT"IF THERE IS NO CURSOR THE ANSWER IS A"
320 PRINT"ONE LETTER INPUT, NO NEED TO PRESS"
330 PRINT" RETURN"
335 PRINT:PRINT"PRESS SPACE BAR TO CONTINUE"
340 PRINT" ";
350 FORC1=1TO200:NEXTC1
360 PRINT" "
380 FORC1=1TO200:NEXTC1
390 GETS1$:IFS1$<>" "THEN340
400 POKE59468,12
1000 PRINT" TODAY'S MENU."
1010 PRINT" #####"
1020 PRINT:PRINT"TYPE IN THE LETTER ACCORDING TO YOUR"
1030 PRINT" CHOICE"
1040 PRINT:PRINT:PRINT
1050 PRINT"ENTER OR CHANGE PARAMETERS ----- C"
1060 PRINT:PRINT"LOG DARK CURRENT ----- D"
1070 PRINT:PRINT"LOG PHOTOCURRENT ----- P"
1075 PRINT:PRINT:PRINT" TODAY'S SPECIAL"
1076 PRINT:PRINT"BACON, EGG, BEANS & BANGERS --- Z"
1077 IF F6%>0THENPRINT:PRINT"N.B. I SUGGEST YOU LOG ONE SCAN"
1078 IFF6%>0THENPRINT"AS YOU HAVE CHANGED ":S9$(F6%):
1080 GETS2$:IFS2$=""THEN1080
1090 IFS2$<>"C"ANDS2$<>"D"ANDS2$<>"P"THEN1000
1100 IFS2$="F"THENF1%=1:GOSUB3000:F1%=0
1110 IFS2$="D"THENF1%=2:GOSUB3000:F1%=0
1120 IFS2$="Z"THENGOSUB2000
1130 GOTO1000
2000 PRINT" PARAMETER CHANGE MENU."
2005 PRINT" #####"
2010 PRINT:PRINT" TYPE IN THE LETTER ACCORDING TO THE"
2020 PRINT" CHANGE YOU WISH TO MAKE."
2030 PRINT:PRINT:PRINT" ENTER ALL PARAMETERS >>>> E"
2040 PRINT:PRINT" CHANGE PRESSURE >>>> >>>> P"
2050 PRINT:PRINT" CHANGE VOLTAGE >>>>>>>>>> V"
2060 PRINT:PRINT" CHANGE MODE >>>>>>>>>>>>> M"
2070 PRINT:PRINT" CHANGE NUMBER OF SCANS >>>> N"
2080 PRINT:PRINT" CHANGE TEMPERATURE >>>>>>> T"
2190 GETS3$:IFS3$=""THEN2190
2200 IFS3$="E"ORS3$="P"ORS3$="V"ORS3$="M"ORS3$="N"ORS3$="G"THEN2200

```

Appendix III - Computer Listings.

(b). Data Logger Program

```

2210 S3$="":GOTO2000
2220 IFS3$="E"THENF4%=1
2240 IFS3$="V"ORF4%=1THENINPUT"ENTER VOLTAGE";V:E=V*.0745
2250 IFS3$="M"ORF4%=1THENINPUT"ENTER MODE";M:A=B(M):F6%=1
2260 IFS3$="T"ORF4%=1THENINPUT"ENTER TEMPERATURE (CELSIUS)";T:T=T+273
2265 IFS3$="N"ORF4%=1THENINPUT"NUMBER OF SCANS";NS:F6%=2
2270 IFS3$="G"ORF4%=1THENINPUT"ENTER NAME OF GAS";G$
2275 IFS3$="F"ORF4%=1THENGOSUB4000
2280 F4%=0:S3$="":RETURN
3000 REM
3010 REM * * * DATA LOGGING ROUTINE * * *
3020 REM
3030 IFF1%=1THENPRINT"      LOGGING PHOTOCURRENT"
3040 IFF1%=2THENPRINT"      LOGGING DARK CURRENT"
3045 FS(F1%,1)=0:FS(F1%,2)=0
3050 PRINT"SCAN", "  1", "  2"
3060 FORC1=1TONS:FORC2=1TO2
3070 REM
3080 REM  C1 --> SCAN COUNTER  C2 --> DATA CHANNEL COUNTER
3090 REM
3100 POKE59470,127:POKE59467,0:POKE16390,C2:POKE16388,1
3110 POKE59468,PEEK(59468)OR1
3120 REM
3130 REM  SET VIA FLAGS TO 0,  WAIT FOR DVM SAMPLE PULSE
3140 REM
3150 F3%=PEEK(59469):IF(F3%AND2)=0THEN3150
3160 WS(1)=999:WS(2)=999:WS(3)=999
3170 FORC3=1TO3
3180 DS(C3)=PEEK(16383+C3)
3190 NEXTC3
3200 FORC3=1TO3
3210 IFS(C3)=DS(C3)THENNEXTC3:GOTO3225
3220 FORC4=1TO3:WS(C4)=DS(C4):NEXTC4:GOTO3170
3225 POKE16388,0:POKE16390,0
3226 T%=(DS(1)AND15)+(DS(1)AND240)*.625+(DS(2)AND15)*.001
3230 IFT%=9999THENFORC4=1TO500:NEXTC4:GOTO3100
3240 IFS(C4)AND32)=C2THENT%=T%+1
3245 IFC2=1THENT%=T%
3250 FS(F1%,C2)=FS(F1%,C2)+T%
3260 GETS4$:IF$4$=" "THENFS(F1%,C2)=0:GOTO3030
3270 NEXTC2
3280 PRINTC1,T1%,T%:NEXTC1
3290 IFF1%=2THENPRINT$128,CHR$(7):GOTO3600
3300 FORC6=1TO2
3310 PC(C6)=FS(1,C6)-FS(2,C6)
3312 IFFC(C6) THENNEXTC6:GOTO3360
3315 PRINT"SORRY!"
3316 PRINT:PRINT"NOT ENOUGH PHOTOCURRENT ON HEAD";C6
3317 PRINT"DDDDDDDDDDDDDDDDDDDDDDDDDDDDDDDDDDDDDDDDDDDDDDDDDDDDDDDD"
3318 PRINT:PRINT"TYPE P TO LOG PHOTOCURRENT,"
3319 PRINT:PRINT"      M TO RETURN TO MENU"
3320 GETS4$:IF$4$=" "THEN3320
3330 IFS4$="M"THEN3600
3340 IFS4$="P"THEN3030
3350 GOTO3315

```

Appendix III - Computer Listings.

(b). Data Logger Program

```

3360 RA=PC(1)/(PC(1)+PC(2))
3365 D=SOR(H^2+A^2)
3367 EF=E/P:EN=EP*1.035E-2*I
3370 DM=-(D-H)*E/(2*LOG((1-RA)*D/H))
3380 PRINT"                                RESULTS"
3385 D=SOR(H^2+A^2)
3390 PRINT:PRINT:PRINTTAB(5):"VOLTS",V
3400 PRINT:PRINTTAB(5):"MODE ",M
3410 PRINT:PRINTTAB(5):"RATIO",RA
3420 PRINT:PRINT:PRINT:PRINTTAB(5):"E/P",EP
3430 PRINT:PRINTTAB(5):"E/N",EN
3440 PRINT:PRINTTAB(5):"D/U",DM
3450 PRINT:PRINT:PRINT"PRESS SPACE BAR FOR HARD COPY"
3460 PRINT:PRINT"          F TO LOG PHOTOCURRENT"
3470 PRINT:PRINT"          M TO RETURN TO MENU"
3480 GETS5$:IFS5$=""THEN3480
3490 IFS5$="M"THEN3600
3500 IFS5$="P"THEN3040
3510 IFS5$=" "THENPRINT£128,M:TAB(3):RA:TAB(12-LEN(STR$(RA))):EP;
3515 IFS5$=" "THENPRINT£128,TAB(12-LEN(STR$(EP))):EN;
3520 IFS5$=" "THENPRINT£128,TAB(12-LEN(STR$(EN))):DM:GOTO3600
3530 S5$="":GOTO3380
3600 RETURN
4000 PRINT"      PRESSURE MEASUREMENT
4010 PRINT:PRINT:PRINT"THESE ARE YOUR CHOICES:"
4020 PRINT:PRINT"ENTER LARGE MANOMETER HEIGHTS  UNMM M
4030 PRINT:PRINT"ENTER PRESSURE DIRECTLY  NMMNMMNMMNMM
4035 PRINT:PRINT:PRINT:PRINT
4040 GETS6$:IFS6$=""THEN4040
4050 IFS6$="D"THENINPUT"OK, WHAT IS THE PRESSURE?";P
4060 IFS6$="M"THEN4000
4065 PRINT"          1          2
4070 PRINT"          *%          *%
4080 PRINT"          R1%U1%          %
4090 PRINT"          *££%R2          *%
4100 PRINT"          *%          *%
4110 PRINT"          *%          *%
4120 PRINT"          *%          *%
4130 PRINT"          *%          *%
4140 PRINT"          *%          *%
4150 PRINT"          *#####*%
4160 PRINT"          M          *%
4170 PRINT"          #####*%
4180 PRINT:PRINT:PRINT"HEIGHT OF MENISCUS BASE, ARM 1 (R1) (U1) (P) (X1)
4190 PRINT"HEIGHT OF MENISCUS BASE, ARM 2 (R2) (U2) (P) (X2)
4200 PRINT"HEIGHT OF MENISCUS BASE, ARM 2 (R2) (U2) (P) (X3)
4210 PRINT"HEIGHT OF MENISCUS BASE, ARM 2 (R2) (U2) (P) (X4)
4220 P=5*((X1-X3)+(X2-X4))
4230 PRINT:PRINT"PRESSURE IS";P
4500 GOSUB5000
4510 RETURN

```

Appendix III - Computer Listings.

(b). Data Logger Program

```
5000 PRINT#128,"AT PRESSURE ";P;" TORR, THE FOLLOWING E/N VALUES WERE:"
5005 EP=E/P;EN=EP*1.035E-12
5010 FORCB=1TO4:PRINT#128;NEXTCB
5020 FORCB=1TO4:PRINT#128,TAB(12);"E/N";TAB(10);"V";NEXTCB:PRINT#128
5030 FORCB=1TO13
5040 PRINT#128,TAB(10);VS(CB);TAB(11-LEN(STR$(VS(CB))));V*VS(CB)/EN*1E;
5050 PRINT#128,TAB(13-LEN(STR$(V*VS(CB)/EN)));VS(CB)*10;
5060 PRINT#128,TAB(11-LEN(STR$(VS(CB)*10)));V*VS(CB)/EN*10;
5070 PRINT#128,TAB(13-LEN(STR$(V*VS(CB)/EN*10)));VS(CB)*100;
5080 PRINT#128,TAB(11-LEN(STR$(VS(CB)*100)));V*VS(CB)/EN*100;
5090 PRINT#128,TAB(12-LEN(STR$(V*VS(CB)/EN*100)));VS(CB)*1000;
5100 PRINT#128,TAB(10-LEN(STR$(VS(CB)*1000)));V*VS(CB)/EN*1000
5110 NEXTCB
5120 FORCB=1TO29:PRINT#128;NEXTCB
5140 PRINT#128,"GAS UNDER STUDY ";G*;" AT PRESSURE ";P
5150 PRINT#128:PRINT#128
5160 PRINT#128,"MODE";TAB(3);"RATIO";TAB(12);"E/P";TAB(12);"E/N";TAB(12);"D/U"
5170 PRINT#128
5200 RETURN
```

Appendix III - Computer Listings.

(b). Data Logger Program

```
5000 PRINT#128,"AT PRESSURE ";P;" TORR, THE FOLLOWING E/N VALUES APPLY"  
5005 EP=E/P:EN=EP*1.035E-2*1  
5010 FORCB=1T04:PRINT#128:NE:TCB  
5020 FORCB=1T04:PRINT#128,TAB(12);"E/N";TAB(10);"V";:NEXTCB:PRINT#128  
5030 FORCB=1T013  
5040 PRINT#128,TAB(10);VS(CB);TAB(11-LEN(STR$(VS(CB)))));V*VS(CB)/EN*1E;  
5050 PRINT#128,TAB(13-LEN(STR$(V*VS(CB)/EN)));VS(CB)*10;  
5060 PRINT#128,TAB(11-LEN(STR$(VS(CB)*10)));V*VS(CB)/EN*10;  
5070 PRINT#128,TAB(13-LEN(STR$(V*VS(CB)/EN*10)));VS(CB)*100;  
5080 PRINT#128,TAB(11-LEN(STR$(VS(CB)*100)));V*VS(CB)/EN*100;  
5090 PRINT#128,TAB(12-LEN(STR$(V*VS(CB)/EN*100)));VS(CB)*1000;  
5100 PRINT#128,TAB(10-LEN(STR$(VS(CB)*1000)));V*VS(CB)/EN*1000  
5110 NEXTCB  
5120 FORCB=1T029:PRINT#128:NEXTCB  
5140 PRINT#128,"GAS UNDER STUDY ";G#;" AT PRESSURE ";P  
5150 PRINT#128:PRINT#128  
5160 PRINT#128,"MODE";TAB(3);"RATIO";TAB(12);"E/P";TAB(12);"E/N";TAB(12);"D/U"  
5170 PRINT#128  
5200 RETURN
```


REFERENCES

- Allan, M. *Helv. Chim. Act.*, 65, 2008, (1982)
 Altshuler, S. *Phys. Rev.* 107, 114, (1957)
 Azria, R., LeCoat, Y., Lefevre, G., & Simon, D.,
J. Phys. B., 12, 679 (1979)
- Bailey, V.A., *Phil. Mag.* 50, 825, (1925)
 Bailey, V.A., & Duncanson, W.E., *Phil. Mag.*, 10, 145, (1930)
 Barbarito, E., Basta, M., & Calicchio, M.,
J. Chem. Phys. 71, 54, (1979)
 Baudler, V.M., Standeke, H., & Dobbers, J.,
Z. fur Anorg. und Alg. Chem., 353, 122, (1967)
 Bowman, C.R., & Gordon, D.E., *J. Chem. Phys.*, 2, 835, (1934)
 Bradbury, N.E., & Nielsen, R.A., *Phys. Rev.* 49, 388, (1936)
 Bradbury, N.E., & Tatel, H.E., *J. Chem. Phys.* 2, 835, (1934)
 Braglia, G.L., *Physica (Utrecht)*. C92, 91, (1977)
 Brose, H.L., & Keyston, J.L., *Phil. Mag.*, 20, 902, (1935)
 Buckingham, R.A., Massey, H.S.W., & Tibbs, S.R.,
Proc. Roy. Soc. A178, 119, (1941)
 Bulos, B.R., & Phelps, A.V., *Phys. Rev. A*, 14, 615, (1976)
 Burke, P.G., in "Atomic and Molecular Collision Theory",
 Ed. Gianturco, F.A., Plenum, N.Y., (1982)
- Cavalleri, G., *Phys. Rev.* 179, 186, (1969)
 Cherrington, B.E., "Gaseous Electronics and Gas Lasers",
 Pergamon, Oxford, (1979)
 Christophoru, L.G., & Christodoulides, A.A.,
J. Phys. B., 2, 71, (1969)
 Christophoru, L.G., Carter, J.G., & Maxey, D.V.,
J. Chem. Phys. 76, 2653, (1982)
 Claydon, C.R., Segal, G.A., & Taylor, H.S.,
J. Chem. Phys., 52, 3387, (1970)
 Cochran, L.W., & Forrester, D.W., *Phys. Rev.*, 126, 1785, (1961)
 Cottrell, T.L., Pollock, W.J., & Walker, I.C.,
Trans. Far. Soc. 64, 2260, (1968)
 Cottrell, T.L., & Walker, I.C., *Trans. Far. Soc.* 61, 1585, (1965)
 Cottrell, T.L., & Walker, I.C., *Trans. Far. Soc.* 63, 549, (1967)
 Crawford, O.H., Dalgarno, A., & Hays, P.B.,
Molec. Phys., 13, 181, (1967)
 Crompton, R.W., Gibson, D.K., & McIntosh, A.I.,
Aust. J. Phys., 22, 715, (1969)
 Crompton, R.W., in "Quarterly Report of the Ion Diffusion Unit",
 A.N.U., Canberra, (April 1982)
 Crompton, R.W., Rees, J.A., & Jory, R.L.,
Aust. J. Phys., 18, 541, (1965)
- Duncan, C.W., & Walker, I.C.,
J. Chem. Soc. Far. Trans. II. 68, 1514, (1972)
 Duncan, C.W., Ph.D. Thesis. University of Stirling, (1971)
- Fox, K., & Turner, J.E., *Phys. Lett.*, 23, 547, (1966)

REFERENCES

- Gianturco, F.A., & Thompson, D.G., J. Phys. B. 9, L383, (1976)
 Gianturco, F.A., & Thompson, D.G., J. Phys. B., 13, 613, (1980)
 Golden, D.E., & Bandel, H.W., Phys. Rev. 138, A14, (1965)
- Hasted, J.B., "Physics of Atomic Collisions",
 2nd. Ed., Butterworths, London, (1974)
- Hatano, Y., & Shimamori, H., in "Electron and Ion Swarms",
 L.G. Christophoru (Ed.), Pergamon, N.Y., (1981)
- Herzberg, G., "I.R. and Raman Spectra of Polyatomic Molecules",
 Van Nostrand, Princeton, (1945)
- Holstein, T., Phys. Rev. 70, 367, (1946)
- Hurst, G.S., O'Kelly, L.B., Wagner, E.B., & Stockdale, J.A.,
 J. Chem. Phys. 39, 1314, (1963)
- Hurst, G.S., Stockdale, J.A., & O'Kelly, L.B.,
 J. Chem. Phys. 38, 2572, (1963)
- Huxley, L.G.H., & Crompton, R.W.,
 "Diffusion and Drift of Electrons in Gases",
 Wiley, London, (1974)
- Jain, A., & Thompson, D.G., J. Phys. B., 16, L347, (1983)
- Kitamori, K., Tagashira, H., & Sakai, Y., J. Phys. D. 11, 283, (1978)
- Kleban, P., & Davis, H.T., Phys. Rev. Lett. 39, 456, (1977)
- Kleban, P., & Davis, H.T., J. Chem. Phys. 68, 2999, (1978)
- Lakshminarasimha, C.S., & Lucas, J., J. Phys. D. 10, 313, (1977)
- Lane, N.F., Rev. Mod. Phys. 52, 29, (1980)
- Lehning, H., Phys. Lett., 29A, 719, (1969)
- Lowke, J.J., & Parker Jr., J.H., Phys. Rev., 181, 302, (1969)
- Lowke, J.J., & Rees, J.A., Aust. J. Phys., 16, 447, (1969)
- Massey, H.S.W., & Burhop, E.H.S.,
 "Electronic and Ionic Impact Phenomena" 2nd. Ed.
 OUP, Oxford, (1969)
- McIntosh, A.I., Aust. J. Phys. 27, 59, (1974)
- Naidu, M.S., & Prasad, A.N., J. Phys. D. 2, 1431, (1969)
- Nolan, J.F., & Phelps, A.V., Phys. Rev. 140, A792, (1965)
- Nielsen, R.A., & Bradbury, N.A., Phys. Rev., 51, 69, (1937)
- Pitchford, L.C., O'Neill, S.V., & Rumble Jr., J.R.,
 Phys. Rev. A. 23, 294, (1981)
- Pitchford, L.C., & Phelps, A.V., Phys. Rev. A. 25, 540, (1982)
- Pollock, W.J., Trans. Far. Soc. 64, 2919, (1968)
- Pack, J.L., Voshall, R.E., & Phelps, A.V.,
 Phys. Rev., 127, 2084, (1962)

REFERENCES

- Ramsauer, C., Ann. Der. Physik. 64, 513, (1921)
 Ramsauer, C., Ann. Der. Physik. 66, 546, (1921)
 Rohr, K., J. Phys. B. 11, 4109, (1979)
 Rohr, K., J. Phys. B. 13, 4897, (1980)
 Ryzko, H., Arkiv. Fysik., 32, 1, (1966)
- Sanche, L., & Schulz, G.J., J. Chem. Phys. 58, 479, (1972)
 Schulz, G.J., Phys. Rev. 112, 150, (1958)
 Skullerud, H.R., J. Phys. D. 1, 1567, (1968)
 Sobol, I.M., "The Monte Carlo Method"
 University of Chicago Press, Chicago, (1974)
- Sohn, W., Jung, K., & Ehrhardt, H., J. Phys. B. 16, 891, (1983)
 Stamatovitch, A., & Schulz, G.J., Phys. Rev., 188, 213, (1969)
 Storch, F., J. Am. Chem. Soc., 56, 374, (1934)
- Townsend, J.S., & Bailey, V.A., Phil. Mag. 43, 593, (1922)
 Turner, J.E., Phys. Rev. 141, 21, (1966)
 Thomas, A.M., & Cross, J.L., J. Vac. Sci. & Tech., 4, 1, (1966)
- Wagner, E.B., Davis, F.J., & Hurst, G.S.,
 J. Chem. Phys. 47, 3138, (1967)
 Walker, I.C., in Chem. Soc. Revs., 3, 467, (1974)

AuthorIndex

| | |
|---|--------------------------------|
| Allan, M. | 7 |
| Azria, R. | 45 |
| Altshuler, S. | 46, 103 |
| Bailey, V.A. | 43, 44 |
| Bailey, V.A., see Townsend, J.S. | 36 |
| Bandel, H.W., see Golden, D.E. | 6 |
| Barbarito, E. | 41, 85 |
| Basta, M., see Barabarito, E. | 41, 85 |
| Baudler, V.M. | 56 |
| Bowman, C.R. | 40 |
| Bradbury, N.E. | 8, 45 |
| Bradbury, N.E., see Nielsen, R.A. | 44 |
| Braglia, G.L. | 30 |
| Brose, H.L. | 41 |
| Buckingham, R.A. | 39 |
| Bulos, B.R. | 30 |
| Burhop, E.H.S., see Massey, H.S.W. | 6 |
| Burke, P.G. | 42, 43 |
| Calicchio, M., see Barbarito, E. | 41, 85 |
| Carter, J.G., see Christophoru, L.G. | 43 |
| Cavalleri, G. | 9 |
| Cherrington, B.E., | 39 |
| Christodoulides, A.A., see Christophoru, L.G. | 44, 103 |
| Christophoru, L.G., | 44, 103 |
| Claydon, C.R. | 77 |
| Cochran, L.W. | 41, 73 |
| Cottrell, T.L., | 40, 41, 44, 46, 73, 74, 103 |
| Crawford, O.H. | 103 |
| Crompton, R.W., see Huxley, L.G.H. | 10, 17 |
| Crompton, R.W. | 48, 49, 75, 76, 80 |
| Cross, J.L., see Thomas, A.M. | 52 |
| Dalgarno, A. see Crawford, O.H. | 103 |
| Davis, F.J., see Wagner, E.B. | 9, 40 |
| Davis, H.T., see Kleban, P. | 18, 42 |
| Dobbers, J., see Baudler, V.M. | 56 |
| Duncan, C.W. | 20, 40, 45, 47, 73, 74, 78, 84 |
| Duncanson, W.E., see Bailey, V.A. | 44, 49 |
| Ehrhardt, H., see Sohn, W. | 41, 85 |
| Fox, K. | 46 |
| Forrester, D.W., see Cochran, L.W. | 41, 73 |

AuthorIndex

| | |
|---------------------------------------|------------|
| Gianturco, F.A. | 42,46 |
| Gianturco, F.A. see Burke, P.G. | 42,43 |
| Gibson, D.K., see Crompton, R.W. | 48,75,80 |
| Golden, D.E. | 6 |
| Gordon, D.E., see Bowman, C.R. | 40 |
| Hasted, J.B. | 38 |
| Hatamo, Y. | 58 |
| Hays, P.B., see Crawford, O.H. | 103 |
| Herzberg, G. | 76 |
| Holstein, T. | 16 |
| Hurst, G.S. | 9,44,46 |
| Hurst, G.S., see Wagner, E.B. | 9,40 |
| Huxley, L.G.H. | 10,17 |
| Jain, A. | 42 |
| Jung, K., see Sohn, W. | 41,85 |
| Jory, R.L., see Crompton, R.W. | 44 |
| Kitamori, K. | 18,42 |
| Keyston, J.L., see Brose, H.L. | 41 |
| Kleban, P. | 18,42 |
| Lakshminarasimha, C.S. | 40,43 |
| Lane, N.F. | 43,46 |
| Lowke, J.J. | 44,45 |
| Lehning, H. | 40 |
| Lucas, J., see Lakshminarasimha, C.S. | 40,43 |
| Massey, H.S.W. | 6 |
| Massey, H.S.W., see Buckingham, R.A. | 39 |
| Maxey, D.V., see Christophoru, L.G. | 43 |
| McIntosh, A.I. | 21 |
| McIntosh, A.I., see Crompton, R.W. | 48,75,80 |
| Naidu, M.S. | 43 |
| Nielsen, R.A., see Bradbury, N.E. | 8 |
| Nolan, J.F. | 9 |
| Nielsen, R.A. | 44 |
| O'Kelly, L.B., see Hurst, G.S. | 9,44,46,49 |
| O'Neill, S.V., see Pitchford, L.C. | 18,19,30 |
| Pack, J.L. | 44 |
| Parker Jr., J.H., see Lowke, J.J. | 45 |
| Phelps, A.V., see Bulos, B.R. | 30 |
| Phelps, A.V., see Nolan, J.F. | 9 |
| Phelps, A.V., see Pack, J.L. | 44 |
| Phelps, A.V., see Pitchford, L.C. | 18 |
| Pitchford, L.C. | 18,19,30 |

Author Index

| | |
|---------------------------------------|-----------------------------|
| Pollock, W.J. | 40, 84, 86, 91, 96, 101 |
| Pollock, W.J., see Cottrell, T.L. | 44, 46, 103 |
| Prasad, A.N., see Naidu, M.S. | 43 |
| | |
| Ramsauer, C | 6, 36 |
| Rees, J.A., see Crompton, R.W. | 44 |
| Rees, J.A., see Lowke, J.A. | 44 |
| Rohr, K., | 41, 45, 84, 85 |
| Rumble Jr., J.R., see Pitchford, L.C. | 18, 19, 30 |
| Ryzko, H. | 44 |
| | |
| Sakai, Y., see Kitamori, K. | 20 |
| Sanche, L. | 45 |
| Schulz, G.J. | 6 |
| Schulz, G.J., see Sanche, L. | 45 |
| Schulz, G.J., see Stamatovic, A. | 77 |
| Segal, G.A., see Claydon, C.R. | 77 |
| Shimamori, H., see Hatano, Y. | 58 |
| Skullerud, H.R. | 24 |
| Sobol, I.M. | 21, 26 |
| Sohn, W. | 41, 85 |
| Stamatovic, A. | 77 |
| Standeke, H., see Baudler, V.M. | 56 |
| Stockdale, J.A., see Hurst, G.S. | 9, 45, 46, 49 |
| Storch, F. | 56 |
| | |
| Tagashira, H., see Kitamori, K. | 20 |
| Tatel, H.E., see Bradbury, N.E. | 45 |
| Taylor, H.S., see Claydon, C.R. | 77 |
| Thomas, A.M. | 52 |
| Thompson, D.G., see Gianturco, F.A. | 42, 46 |
| Thompson, D.G., see Jain | 42 |
| Tibbs, S.R., see Buckingham, R.A. | 39 |
| Townsend, J.S. | 36 |
| Turner, J.E. | 46 |
| Turner, J.E., see Fox, K. | 46 |
| | |
| Voshall, R.E., see Pack, J.L. | 44 |
| | |
| Wagner, E.B. | 9, 44 |
| Wagner, E.B., see Hurst, G.S. | 9, 44 |
| Walker, I.C. | 46 |
| Walker, I.C., see Duncan, C.W. | 40, 41, 73, 78 |
| Walker, I.C., see Cottrell, T.L. | 40, 41, 44, 73, 74, 84, 103 |

Acknowledgements.

Thanks are due to many for help given during this work. Particularly Dr. Isobel Walker for instigating and overseeing the project, the SERC for a maintenance grant and my wife for her patience. Discussions with co-workers Don Dance and Taher Abouain were often a source of help. Finally, Ken Matheson made important contributions to the Monte Carlo analysis and has since taken to wrestling the beast full time. He earns my thanks (and a modicum of sympathy).